Review | Received 22 September 2024; Accepted 16 November 2024; Published 29 November 2024
https://doi.org/10.55092/aimat20250001

Research progress on SiC_f/SiC composites and their cladding components

Liangliang Shen[1,2,†], Xiulun Li[2,3,†], Yi Zhang[1,2], Hongyin Li[1,2], Xinyu Fan[4], Zhongwei Yan[5] and Jian Xu[1,2,*]

[1] State Key Laboratory of Fine Chemicals, Liaoning High Performance Polymer Engineering Research Center, School of Chemical Engineering, Dalian University of Technology, Dalian, China
[2] Zhejiang Key Laboratory of Data-Driven High-Safety Energy Materials and Applications, Ningbo Key Laboratory of Special Energy Materials and Chemistry, Ningbo Institute of Materials Technology and Engineering, Chinese Academy of Sciences, Ningbo, China
[3] College of Materials Science and Engineering, Zhejiang University of Technology, Hangzhou, China
[4] Aviation Industry Corporation of China, Ltd., Beijing, China
[5] Avic Shenyang Aircraft Company Limited, Shenyang, China

† These two authors contributed equally.

* Correspondence author: Jian Xu; E-mail: xujian1028@dlut.edu.cn.

Abstract: Owing to their outstanding high-temperature resistance, oxidation resistance, radiation tolerance, and corrosion resistance, silicon carbide fiber-reinforced silicon carbide (SiC_f/SiC) composites have shown extensive potential in advanced applications, including aerospace and nuclear industries. SiC_f/SiC composites are considered among the most promising accident-tolerant fuel cladding materials, especially in the context of fourth-generation fission reactor development, owing to their stability under extreme conditions. However, the complex processing and structural characteristics of the material leave room for further research, especially with the emergence of new technologies like artificial intelligence (AI). Therefore, this work will provide a review of various processes, including chemical vapor infiltration (CVI), polymer infiltration and pyrolysis (PIP), nano impregnation and transient eutectic method (NITE), and reactive melt infiltration (RMI), focusing on improving material density, mechanical properties, and irradiation stability. Additionally, an in-depth review of the mechanical properties and microstructural changes of SiC_f/SiC composites and their cladding components under extreme conditions, such as high temperatures, irradiation, and corrosion, is provided, as these factors directly affect their long-term stability in nuclear reactors. Notably, numerical simulation technology has become a crucial tool for predicting the service performance of materials. Integrating advanced technologies like AI is expected to further promote the application of SiC_f/SiC composites in future high-temperature structural materials. In summary, significant progress has been made in the study of SiC_f/SiC composites as next-generation nuclear fuel cladding materials. However,

further research is needed in areas such as fabrication process optimization, interface modification, service behavior evaluation, and integration with AI to meet the higher performance demands of future nuclear energy systems.

Keywords: SiC_f/SiC composites; fabrication processes; mechanical properties; service conditions; artificial intelligence

1. Introduction

Silicon carbide fiber-reinforced silicon carbide (SiC_f/SiC) composites have shown great potential for applications in aerospace and nuclear industries due to their exceptional high-temperature resistance, outstanding oxidation resistance, irradiation tolerance, corrosion resistance, and high specific strength [1–4]. In the aerospace field, SiC_f/SiC composites have become ideal candidates for high-performance engine components, thermal protection systems, and structural parts due to their stable performance in extreme environments, meeting the stringent requirements for heat resistance and lightweight high strength in spacecraft [5]. With advancements in fourth-generation fission reactor technology, SiC_f/SiC composites have emerged as leading cladding materials, valued for their stability and resilience under extreme conditions [6,7].

After the Fukushima nuclear power plant accident in 2011, the limitations of traditional zirconium-based alloy cladding materials became fully exposed, prompting the global nuclear industry to seek safer and more reliable alternatives [8]. With advancements in nuclear technology, particularly reactor development, material demands in the nuclear industry have intensified. SiC_f/SiC composites, known for their exceptional high-temperature resistance and irradiation tolerance, are regarded as highly promising cladding materials for nuclear fuel. Next-generation nuclear reactors, such as the Sodium-cooled Fast Reactor (SFR) and the Molten Salt Reactor (MSR), require materials to maintain long-term stability in environments of ultra-high temperatures, intense irradiation, and corrosive coolants. Traditional zirconium-based alloy cladding is prone to oxidation, hydrogenation, and high-temperature creep under these conditions. In contrast, SiC_f/SiC composites, with their unique crystal structure and interface design, exhibit excellent oxidation resistance, corrosion resistance, and outstanding irradiation stability. However, SiC_f/SiC composites leverage their distinct crystal structure and interface design to effectively prevent lattice defect accumulation due to irradiation [9]. Furthermore, they maintain mechanical strength even above 1000 °C and show strong oxidation resistance in oxygen-rich conditions [10], unlike zirconium-based alloys, which quickly form oxide layers. Additionally, when exposed to corrosive coolants like molten salt or sodium, SiC_f/SiC composites show a slower corrosion rate than zirconium alloys, maintaining structural stability over long-term operation [11]. Their outstanding mechanical and chemical stability make them a top candidate for use in Accident Tolerant Fuel (ATF) technology.

Choosing and refining preparation processes are essential for improving the performance of SiC_f/SiC composites, as different methods uniquely contribute to enhancing material characteristics and fulfilling application needs. It can be prepared using a range of techniques, such as CVI, (as depicted in Figure 1d), PIP, NITE, and RMI [12,13]. Each process offers distinct advantages and limitations. Therefore, selecting the optimal process for specific applications and refining process parameters is essential for improving material performance.

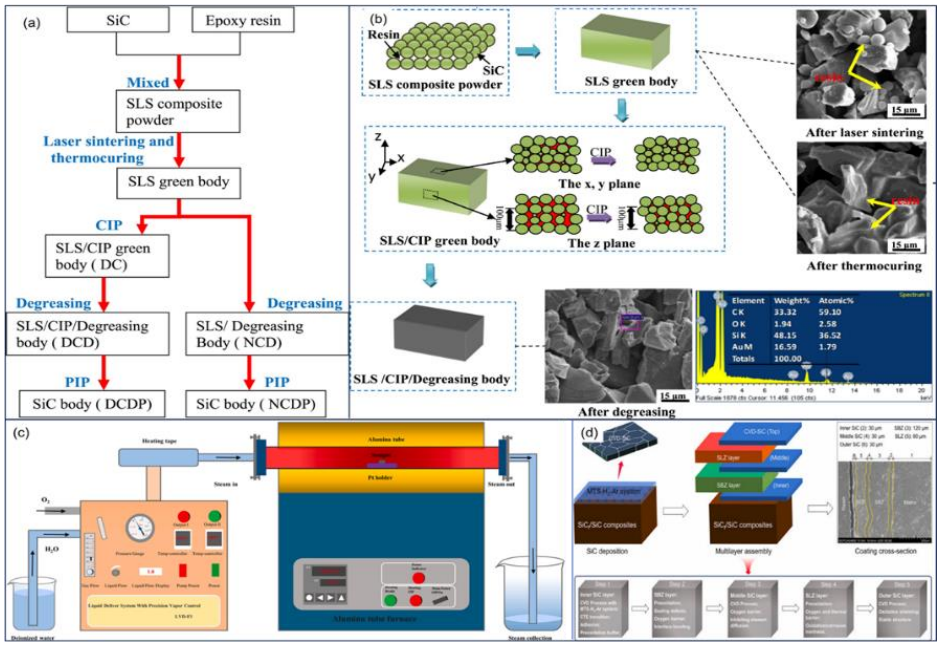

Figure 1. Preparation of silicon carbide composite materials: (a) SiC/SiC component fabrication process involving SLS, CIP, degreasing, and PIP [14]; Reprinted with permission. Copyright 2018, Elsevier. (b) Diagram of the SiC/SiC composite preparation sequence [14]; (c) Schematic of the water vapor corrosion testing setup [15]; Reprinted with permission. Copyright 2022, Elsevier. (d) Diagram of multilayer coating system fabrication [16]. Reprinted with permission. Copyright 2022, Elsevier.

In the subsequent discussion, the working principles and application scope of these processes are highlighted. CVI is widely used due to its ability to produce high-purity, dense SiC matrices at relatively low temperatures, though the process is complex and time-consuming. PIP is favored for its relatively lower cost and higher controllability, particularly demonstrating unique advantages in fabricating complex-shaped composites. NITE achieves efficient bonding between the fibers and the matrix at high temperatures, resulting in composites with excellent mechanical properties. However, this fabrication process requires advanced equipment. RMI rapidly forms a dense SiC matrix through the infiltration reaction of molten metal, making it suitable for large-scale production. However, it may face challenges related to matrix composition uniformity. The analysis of these processes places particular emphasis on the latest advancements in the optimization of SiC fiber preform structures, fiber interface modification, and matrix densification. These research findings not only further enhance the overall performance of SiCf/SiC composites but also provide crucial technical support for future material development.

The ability to perform in extreme environments is a key factor for SiC_f/SiC composites to excel in real-world applications, making the stability of their microstructure and mechanical properties under extreme conditions critically important. The changes in mechanical properties and microstructure under conditions like high temperature, irradiation, and corrosion are crucial to their practical feasibility in nuclear reactors [17,18]. Meanwhile, the low thermal expansion coefficient and high thermal conductivity of SiC_f/SiC composites under high-temperature conditions allow them to effectively reduce the temperature gradient of fuel elements in nuclear reactor accident scenarios, thereby decreasing thermal stress and enhancing reactor safety. Its remarkable irradiation resistance ensures that the material can maintain structural integrity and stable mechanical properties even under accumulated irradiation

damage. These properties make SiC_f/SiC composites not only suitable for fuel cladding in advanced nuclear reactors but also show broad application prospects in new nuclear energy systems, such as High-Temperature Gas-cooled Reactors (HTGR) and fusion reactors in future nuclear energy systems.

To effectively evaluate the application potential of SiC_f/SiC composites under real operating conditions, numerical simulation has become a vital tool for analyzing and improving material behavior. Through advanced numerical simulation methods, especially finite element numerical simulation techniques, a comprehensive analysis of the entire process of SiC_f/SiC composites from initial damage to final failure can be conducted. These numerical models not only provide solid theoretical support during the material design process but also offer valuable guidance for process optimization and cost control. Additionally, numerical simulation can be used to analyze the long-term service behavior of SiC_f/SiC composites in practical applications, aiding in the prediction of their long-term stability and reliability under extreme conditions such as those in nuclear reactors. With the continuous advancement of modern AI and its growing application in materials science, researchers are attempting to apply AI techniques, such as deep learning and image recognition, to SiC_f/SiC composites. However, there is still much to explore, especially in their application in cladding tubes.

In light of the significant application demands and current research status of SiC_f/SiC composites and their cladding components in the nuclear field and other high-tech areas, this paper will provide a detailed discussion on the application potential of SiC_f/SiC composites in aerospace and the nuclear industry, fabrication processes, performance under extreme environments, and the application of numerical simulation technology. This aims to provide further scientific basis and technical guidance for future research and application of these materials.

2. Fabrication processes

2.1. Continuous SiC fibers

Continuous SiC fibers are slender fibers composed of silicon carbide, existing in the form of continuous filaments, with advantages such as high-temperature resistance, oxidation resistance, wear resistance, and corrosion resistance, enhancing toughness in ceramic matrix composites [19]. Currently, the methods for preparing continuous SiC fibers in China include the precursor hot-press sintering method, precursor conversion method, chemical vapor deposition method, and reactive melt infiltration method [20]. The development history of SiC fibers (as shown in Figure 2) can be traced back to the 1970s. With continuous technological advancements, the performance of SiC fibers has significantly improved. The following sections will describe the three generations of fibers:

The development of the first generation of SiC fibers began in 1975 when the Yajima group at Tohoku University in Japan used polycarbosilane (PCS) as a precursor to produce continuous SiC fibers with a diameter of approximately 10 μm [21]. This process pioneered the precursor conversion method for preparing continuous SiC fibers. Subsequently, Nippon Carbon and Ube Industries in Japan advanced the engineering and commercialization of SiC fibers. Representative products of the first-generation SiC fibers include the Nicalon series fibers from Nippon Carbon [22] and the Tyranno Lox M fibers from Ube Industries [23]. These fibers have a high oxygen content (approximately 10 wt%) and a high carbon content (with a carbon-to-silicon ratio of about 1.3:1), and they are primarily in an amorphous state. In an oxygen-containing environment, these fibers maintain good thermal stability at 1050 °C. At

elevated temperatures, the strength of the fibers markedly declines as a result of the breakdown of the SiO_xC_y impurity phase and the accelerated growth of β-SiC grains [24,25].

The development of second-generation SiC fibers focused on reducing oxygen content and increasing the operating temperature. Nippon Carbon and Ube Industries adopted different technical approaches to successfully develop SiC fibers with low oxygen content. The typical representatives are Nippon Carbon's Hi-Nicalon fibers and Ube Industries' Tyranno ZE fibers. Hi-Nicalon fibers are manufactured through electron-beam irradiation crosslinking technology, maintaining an oxygen content below 1.2 wt% [25]. Tyranno ZE fibers are produced using an electron irradiation process, resulting in a further reduction in oxygen content [26]. The oxygen content of this generation of fibers is below 2 wt%, with a high carbon content (carbon-to-silicon ratio of approximately 1.3:1 to 1.4:1), and they exhibit good thermal stability in air at 1200 ℃ to 1300 ℃ [24,25]. Although these fibers have improved elastic modulus, high-temperature resistance, and creep resistance, their oxidation resistance remains suboptimal due to the presence of excess carbon, limiting the long-term use of second-generation SiC fibers at higher temperatures [17]. Additionally, the creep resistance of second-generation fibers remains limited under high-temperature stress, particularly under extreme conditions above 1200 ℃, where creep deformation may affect mechanical stability. Finally, the issue of increased brittleness after irradiation has yet to be fully resolved, potentially leading to crack propagation or fiber breakage during prolonged service, which could impact the durability of the composite. These limitations have driven the further optimization of third-generation SiC fibers to meet the higher demands of high-temperature and intense irradiation environments.

The third generation of SiC fibers further optimized their chemical composition and microstructure, significantly enhancing high-temperature resistance and oxidation resistance [17]. Nippon Carbon produced nearly stoichiometric Hi-Nicalon S fibers with a carbon-to-silicon ratio of 1.05:1 by removing excess carbon in a hydrogen atmosphere. Ube Industries used polyaluminocarbosilane (PACS) as a precursor to produce Tyranno SA fibers. The U.S. company Dow Corning (later COI Ceramics) used the CVD (Chemical Vapor Deposition) process to produce SiC fibers. This process involves placing a fiber substrate (such as carbon fiber) in a high-temperature reactor and introducing silicon-containing gases (such as $SiCl_4$) and carbon-containing gases (such as CH_4) to undergo deposition reactions at temperatures of 1200 ℃ to 1400 ℃ [27,28]. Hydrogen usually acts as a carrier gas, facilitating the decomposition of reactant gases on the substrate surface, forming a SiC layer. The deposition rate and thickness are controlled by adjusting the gas flow, reaction temperature, and reaction duration. After cooling, dense and high-purity SiC fibers are obtained, which are suitable for high-temperature oxidation-resistant and corrosion-resistant composite applications [29,30]. Later, using the Tyranno Lox-M fiber preparation process from Ube Corporation as a basis, a sintering aid B was incorporated to produce polycrystalline Sylramic fibers. Dow Corning later partnered with NASA Glenn Research Center to treat Sylramic fibers in high-temperature nitrogen, resulting in the development of Sylramic-iBN fibers [31]. The high-temperature nitrogen treatment has twofold benefits: it eliminates excess boron from the grain boundaries, facilitating grain growth and resulting in a cleaner and more stable grain boundary structure. This improved microstructure greatly boosts the fiber's creep resistance and electrical conductivity. Furthermore, the treatment forms a boron nitride (BN) layer on the fiber surface. The BN layer acts as a robust oxidation barrier, endowing the fibers with enhanced oxidation resistance in high-temperature and oxidative conditions. As a result, Sylramic-iBN fibers demonstrate

enhanced toughness and stability for mechanical applications, with prolonged durability and stability in high-temperature environments, making them well-suited for advanced ceramic matrix composites (CMC) and other challenging engineering applications. The third generation of SiC fibers features low oxygen content, near-stoichiometric composition, and a highly crystalline structure, exhibiting excellent high-temperature resistance and oxidation resistance. For example, Hi-Nicalon S fibers maintain a strength of 1.8 GPa after being treated at 1600 ℃ in an argon atmosphere for 10 hours. Tyranno SA fibers can withstand temperatures up to 2200 ℃ in an inert atmosphere, while Sylramic fibers retain a tensile strength of over 2.8 GPa after being treated at 1550 ℃ in an argon atmosphere for 10 hours [24,25]. The parameters of each generation of fibers can be found in Table 1.

The development history of the three generations of SiC fibers demonstrates continuous progress, from early fibers with high oxygen content and limited low-temperature performance to modern fibers with low oxygen content, high crystallinity, and excellent high-temperature performance. The first generation of SiC fibers laid the foundation for the precursor conversion method, but their high oxygen content limited their high-temperature applications. The second generation of SiC fibers significantly improved high-temperature performance by reducing oxygen content, yet they still faced issues with insufficient oxidation resistance. The third generation of SiC fibers achieved near-stoichiometric composition and a highly crystalline structure by optimizing chemical composition and introducing sintering aids, resulting in outstanding mechanical properties and oxidation resistance under extreme high-temperature conditions.

Although third-generation SiC fibers exhibit excellent performance in many aspects, particularly in terms of mechanical and oxidation resistance at extreme high temperatures, some unresolved challenges remain in practical applications [32]. These challenges relate not only to further optimization of the material itself but also to the complexity of application environments and the scalability and cost-effectiveness of production processes.

The long-term service stability, interfacial performance, and production cost are major challenges for third-generation SiC fibers in extreme applications. Although third-generation SiC fibers perform well in high-temperature environments, harsh conditions such as those in nuclear reactors can lead to microstructural degradation due to irradiation and high-temperature corrosion, particularly with issues such as stress concentration and crack propagation at the interface layer [33]. In-depth research on failure mechanisms under extreme conditions, development of efficient interfacial coating technologies, and optimization of fiber-matrix bonding could enhance their long-term stability. In terms of interfacial performance, although high-crystallinity SiC fibers have improved interfacial bonding, dynamic stress and thermal cycling can still cause interfacial failure, reducing the material's damage resistance [34]. Further optimization of interfacial coating design could effectively slow oxidation and crack propagation, enhancing interfacial bonding strength. On the production side, the high crystallinity and low oxygen content of SiC fibers make the manufacturing process complex and costly [35]. To enable wider applications, it is necessary to further simplify production processes, develop low-cost raw materials, and improve manufacturing efficiency.

Therefore, although third-generation SiC fibers have shown significant advantages in material performance, further optimization and improvements in long-term stability, interface performance, and production costs are required for their widespread application in high-temperature, nuclear, and

aerospace fields. Addressing these issues will greatly promote the application of SiC composites in extreme conditions and pave the way for large-scale industrial production.

Table 1. Properties of commercial available SiC fibers [36].

Properties	Nicalon NI-202	Tyranno Lox-M	Hi-Nicalon	Hi-Nicalon-S	Tyranno SA
Generation	First	First	Second	Third	Third
Si/%	56.6	54.0	62.4	68.9	67.8
C/%	31.7	31.6	37.1	30.9	31.3
O/%	11.7	12.4	0.5	0.2	0.3
Hetero-element%	-	2.0(Ti)	-	-	0.6(Al)
Fiber diameter/μm	14	8.5	14	12	10
Tensile strength/GPa	3.0	2.8	2.8	2.6	2.8
Tensile modulus/GPa	200	190	270	420	380
Elongation/%	1.1	1.4	1.0	1.0	0.7
Density/(g/cm^3)	2.55	2.37	2.74	3.10	3.10

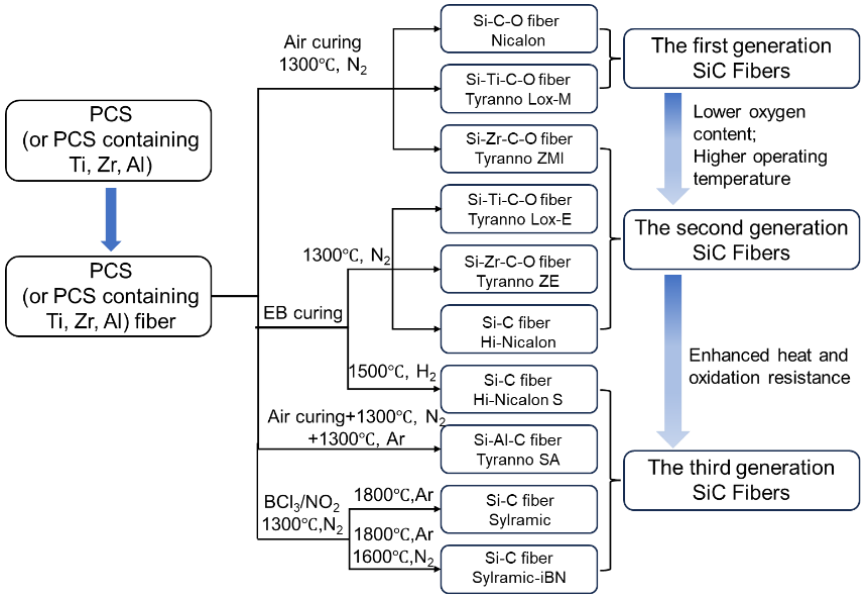

Figure 2. Development history of SiC fibers.

2.2. Forming methods

The nuclear fuel cladding tube is the first safety barrier of a nuclear reactor and must withstand harsh operating conditions, including high temperatures, high pressure, intense radiation, and severe corrosion [37]. Therefore, nuclear structural materials must possess the following characteristics: low neutron absorption cross-section, radiation damage resistance, high thermal conductivity, high thermal stability, and excellent chemical corrosion resistance [38]. Currently, the main methods for preparing SiC_f/SiC composites include CVI, PIP, RMI, NITE, and the combination of various processes. Each of these preparation

techniques comes with specific advantages and disadvantages, which will be examined in the subsequent sections.

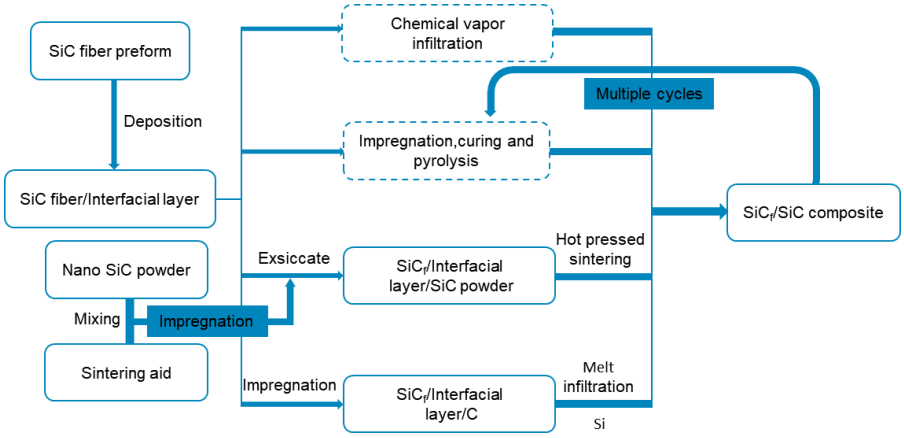

Figure 3. The process flow of CVI, PIP, RMI, and NITE.

2.2.1. Chemical vapor infiltration

The basic process of preparing SiC_f/SiC composites using the CVI method involves loading the SiC fiber preform into the CVI reactor, introducing gaseous precursors such as Methyltrichlorosilane (MTS, CH_3SiCl_3) [39] and Trichlorosilane ($HSiCl_3$) [40] to create a vapor environment necessary for SiC deposition. The gaseous precursors infiltrate through the pores of the fiber preform, decompose on the fiber surfaces, and through repeated infiltration and deposition, a high-purity SiC matrix is formed on the fiber surfaces.

The advantages of the CVI process include synthesizing the SiC matrix at relatively low temperatures (1000–1100 °C), which minimizes damage to the fibers and coatings [41]. The shape of the fiber preform has minimal impact on gas diffusion, making it suitable for fabricating complex-shaped components. By adjusting parameters like the gas flow rate, diffusion time, temperature, and pressure gradient, gradient materials with continuous variations in composition and properties can be produced. However, the CVI process also has some drawbacks: achieving a dense matrix often requires multiple deposition and polishing steps, resulting in a long preparation cycle and complex process. Gas diffusion into the interior of the preform can be obstructed, making it less effective for thick samples. The gaseous precursors are toxic, and the process generates corrosive gases, posing environmental pollution and safety risks. During deposition, SiC may clog pores and external channels, leading to a higher product porosity. Due to density non-uniformity, the material's thermal conductivity also varies along the thickness direction, causing thermal stress concentration in high-temperature environments, which accelerates thermal aging or early failure. Additionally, the presence of pores reduces the high-temperature resistance of the composite, impacting its dimensional stability under high-temperature conditions. Pores and density gradients may gradually affect the durability of the material under extreme conditions.

To overcome the challenges of the CVI process, such as slow infiltration rate, high porosity, and low densification, the Kim team at the Korea Atomic Energy Research Institute [42] introduced SiC whiskers. They employed *in situ* growth of SiC whiskers to bridge the large pores among fiber bundles, followed by filling the matrix to improve the density of the composites (Figure 4a). To further verify this, Hua *et*

al. [43] introduced two reinforcing phases, SiC whiskers and SiC particles, for comparison. They found that the fracture toughness and bending strength of the SiC whisker-reinforced composites (SiC_W/SiC) were higher than those of the SiC particle-reinforced composites (SiC_P/SiC). Both cases confirmed the advantages of SiC whiskers in toughening and strengthening.

To further enhance the strength and thermal stability of the bonding layer, researchers have improved the bonding technique for SiC ceramics by introducing SiC nanowires. Figure 4b shows the process of achieving SiC ceramic bonding using C-Si reaction bonding technology enhanced by SiC nanowires. The preparation process involves three main stages: slurry preparation and optimization, formation of a multi-component bonding layer, and growth of SiC nanowires. The introduction of nanowires significantly enhances the strength and thermal stability of the bonding layer, allowing SiC ceramics to maintain excellent structural integrity in high-temperature and extreme environments. Moreover, compared to traditional methods, the introduction of SiC nanowires significantly reduces interlayer delamination and porosity issues. Tao *et al.* [44] successfully fabricated a dense three-layer SiC cladding tube by introducing SiC nanowires onto a graphite rod, as shown in Figure 4c. Kang *et al.* [45] further discovered that incorporating silicon carbide nanowires can effectively enhance the matrix infiltration efficiency of SiC_f/SiC composites. As observed in Figure 4d, the composites coated with SiC nanowires achieved higher density in a shorter CVI time. Compared to traditional methods, the introduction of SiC nanowires significantly reduces interlayer delamination and porosity issues, enhancing the material's density and mechanical properties. This offers a novel method for the effective production of high-performance SiC cladding tubes.

In studies aimed at enhancing composite material performance, the thickness of the interface layer, in addition to the introduction of nanowires, has been shown to significantly impact the material's overall properties. The strengthening effect of nanowires is typically combined with interface layer optimization to improve the material's mechanical properties and irradiation stability. Therefore, investigating the effect of interface layer thickness helps to further understand the synergistic interaction between nanowires and the interface layer. In discussing the influence of the interface layer thickness on the performance of composites, studies by Liu *et al.* [46] and Sun *et al.* [47] have both investigated the effect of SiBN interface thickness on the tensile fracture behavior and strength distribution of silicon carbide fiber-reinforced silicon carbide matrix composites (SiC_f/SiC). Liu *et al.* [46] found that a thicker SiBN interface improved the fracture toughness and strength of the composite, with an average tensile strength of 450 MPa. For materials with thinner interfaces, tensile strength initially increased with interface thickness but then decreased, as shown in Figure 4f. Sun *et al.* [47] further indicated that the optimal BN interface thickness is approximately 670 nm, at which the BN interface effectively enhances the mechanical properties of SiC_f/SiC composites, with significant improvements in both tensile strength and fracture toughness, as shown in Figure 4g. Both studies emphasized the crucial role of the SiBN interface in enhancing the mechanical properties of SiC_f/SiC composites.

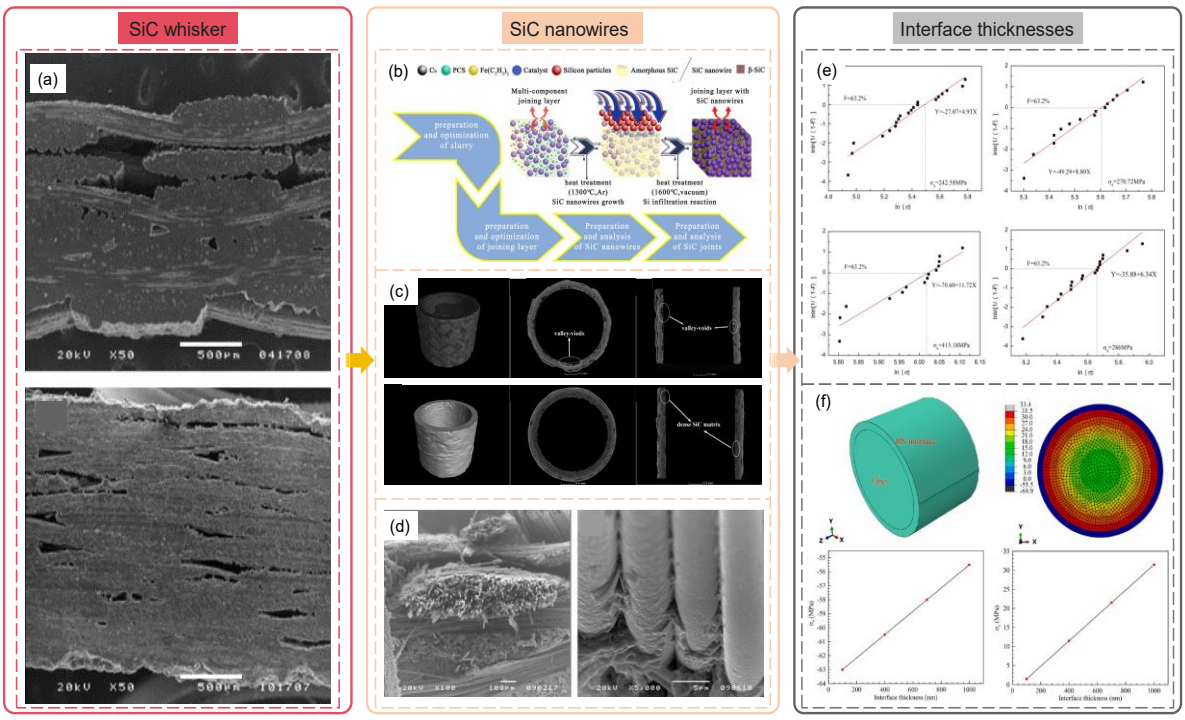

Figure 4. The influence of microstructure and interface layer thickness on the mechanical properties of SiC-based composites: (a) Cross-section SEM images after one and three whisker growth/matrix infiltration cycles [42]; Reprinted with permission. Copyright 2006, Elsevier. (b) SiC ceramics joined by SiC nanowire-reinforced C-Si bonding [48]; Reprinted with permission. Copyright 2021, Elsevier. (c) Morphology of three-layer SiC cladding tube [44]; Reprinted with permission. Copyright 2019, John Wiley and Sons. (d) NW-CVI with PyC-coated SiC nanowires [45]; Reprinted with permission. Copyright 2011, Elsevier. (e) Weibull distribution of SiC_f/SiC tensile strength by interface thickness [46]; Reprinted with permission. Copyright 2015, Elsevier. (f) Interface thickness *vs.* radial stress at SiC fiber surface [47]. Reprinted with permission. Copyright 2023, Elsevier.

Additionally, to further explore the impact of composite fabrication processes on material properties. Deck *et al.* [49] further optimized the CVI process parameters by combining experimental and modeling approaches. Compared to the non-optimized CVI process, the optimized CVI process resulted in SiC_f/SiC composites with a density of 3.1 g/cm^3 and a porosity of less than 5%. Meanwhile, the high-density composites exhibited a compressive strength of 700 MPa and a tensile strength of 500 MPa at 1500 ℃. The study also confirmed that density and porosity have a significant impact on the thermodynamic response of composites.

The CVI method can be used to produce composites with a high-purity SiC matrix, which is highly beneficial for enhancing the corrosion and irradiation resistance of cladding tubes. However, the raw materials and process conditions used in the CVI method differ significantly from those of SiC fibers and interface phases. This discrepancy can lead to a mismatch in the crystal structure and physicochemical properties between the matrix, interface phase, and fibers, resulting in mismatched physical and chemical properties at the interface. Therefore, to optimize the physicochemical properties at the interface and ensure the overall performance of the composites, further in-depth research into these differences is necessary.

2.2.2. Polymer infiltration and pyrolysis

The specific process for preparing SiC_f/SiC composites using the PIP method involves immersing the SiC fiber preform in a polymer solution containing SiC precursors [50,51]. The impregnated fiber preform is then cured under appropriate temperature and pressure, allowing the polymer precursor to distribute uniformly within the fiber preform and bond with the fibers to form a solid state. Finally, the cured preform is subjected to pyrolysis at high temperatures, where the polymer precursor decomposes and transforms into a SiC ceramic matrix, resulting in a continuous SiC ceramic matrix and fiber composite. To achieve the desired density and properties, it is often necessary to repeat the impregnation and pyrolysis processes multiple times.

Although the traditional PIP process is straightforward, the use of carbon-rich polycarbosilane as a precursor generates a significant amount of low molecular weight gaseous byproducts during the pyrolysis process, accompanied by substantial volumetric shrinkage. These factors result in a range of issues with SiC_f/SiC composites produced via the PIP process, such as high residual carbon content, low crystallinity of SiC grains, high porosity between fiber bundles, and low thermal conductivity. To address these issues, researchers both domestically and internationally have made several improvements to the PIP process by optimizing precursor composition and structure, as well as refining the pyrolysis technique. In terms of optimizing precursor composition and structure, researchers have utilized liquid polycarbosilane with a composition closer to stoichiometry, combined with low-temperature curing techniques, to successfully fabricate SiC matrices that exhibit higher density, lower porosity, and near-stoichiometric composition [52,53]. This enhancement considerably decreases volumetric shrinkage and the formation of gaseous byproducts during the pyrolysis process, thus improving the overall material performance. In terms of improvements in the pyrolysis process, researchers have employed third-generation SiC fibers that are more resistant to high temperatures and have effectively enhanced the crystallinity of the SiC matrix by increasing the pyrolysis temperature. These improvements enable the fabricated SiC_f/SiC composites to possess higher thermal conductivity and superior irradiation resistance [54,55]. Additionally, the introduction of a hot press process during the precursor pyrolysis can significantly enhance the density and mechanical properties of the composites while also reducing the fabrication cycle time [56]. With the ongoing advancements in these studies, the PIP process is expected to play an increasingly important role in the future of materials science and engineering.

Although the PIP process can effectively fill the ceramic precursors in the fiber preform, it often struggles to achieve a high degree of densification, especially with considerable voids potentially remaining between the fiber bundles. Electrophoretic deposition (EPD) can effectively address the densification issues of the PIP process. The specific procedure involves initially depositing nano-sized SiC particles onto the fiber preform using EPD technology to reduce the porosity between the fiber bundles. Then, the PIP process is used to fill the tiny voids with ceramic precursors, allowing for repeated pyrolysis and infiltration to produce high-density SiC_f/SiC composites. Li *et al.* [57] fabricated 3D4d woven SiC_f/SiC composites using EPD assisted PIP process. They incorporated 500 nm β-SiC particles to improve thermal conductivity and fill the voids between fiber bundles. As observed in the curve of Figure 5a, the EPD technique improved densification efficiency. Characterization showed that the composites created using this method exhibit a thermal conductivity of 6.60 W/(m·K), which is 2.3 times greater than that of the composites produced exclusively through the PIP process. The bending

strength is 647.08 ± 69.53 MPa, which represents a reduction of approximately one-third compared to the latter. Although this method improves thermal conductivity, it also leads to a reduction in the fiber volume fraction and can damage the interface coating and fibers due to the effects of the electric field. Yin *et al.* [58] also employed a hybrid technique of EPD and PIP to fabricate SiC_f/SiC composites. They used EPD to fill the large voids between fiber bundles and optimized the EPD parameters, as shown in Figure 5b. After seven PIP cycles, the composites achieved a relative density of 91.9%, exhibiting a high strength of 289 MPa and non-brittle fracture behavior, while also exploring the relationship between microstructure and mechanical response. Iveković *et al.* [59] found that after only six PIP cycles, the matrix density of the SiC samples reached approximately 86.5% TD (Theoretical Density), with an average pore size of about 90 nm. While EPD is effective in addressing densification issues in the PIP process, it also has certain limitations. Due to gas formation on the electrodes, EPD usually cannot use water as a medium and instead relies on costly, toxic, and flammable organic solvents, which pose environmental and health risks [60,61]. Additionally, achieving uniform deposition on non-conductive or complex-shaped substrates is challenging, which may lead to density inconsistencies in the composite [61]. Moreover, EPD requires complex control over thickness and quality, necessitating precise management of suspension stability, deposition time, and voltage, which increases the difficulty of process operations and may lead to inconsistencies in layer thickness and density [60,61].

Additionally, the gradient concentration polymer infiltration and pyrolysis method (GC-PIP) is an improved PIP process that gradually increases the concentration of the precursor solution in each infiltration cycle to progressively fill the voids between the fiber bundles, thereby enhancing the density of SiC_f/SiC composites, as shown in Figure 5c. This method effectively reduces the porosity of the material and significantly enhances its density and mechanical properties, while avoiding damage to the fibers and interface, demonstrating strong application potential. Zhang *et al.* [62] and Wei *et al.* [63] proposed and introduced an innovative process for fabricating SiC_f/SiC composites using the GC-PIP method. Zhang *et al.* [62]effectively filled the voids between fiber bundles by gradually increasing the concentration of the precursor solution in each PIP cycle, reducing the porosity of the composites to below 6% and significantly enhancing their density and mechanical properties, demonstrating excellent bending strength and toughness. Wei *et al.* [63] used multiple PIP cycles with a low-concentration PCS solution in the initial stages to form a continuous carbon layer with alternating carbon and SiC matrix layers (Figure 5d), followed by rapid densification using a high-concentration PCS solution to achieve a denser and more uniform matrix. The experimental results indicate that the composites fabricated using this method achieved bending strength and fracture toughness of 850.7 ± 52.6 MPa and 40.2 ± 8.7 $MPa \cdot m^{1/2}$, respectively, significantly outperforming those produced by the traditional PIP method and demonstrating broad application potential.

The PIP process faces limitations such as high residual carbon content, low SiC crystallinity, and low thermal conductivity, which hinder its broader application. These issues are closely related to the development of the ceramic conversion technology for polycarbosilane precursors. As the development of precursor materials with near-stoichiometric conversion characteristics continues to advance, the cost and performance advantages of SiC_f/SiC composites fabricated using the PIP process may gradually align with the application requirements of nuclear structural materials.

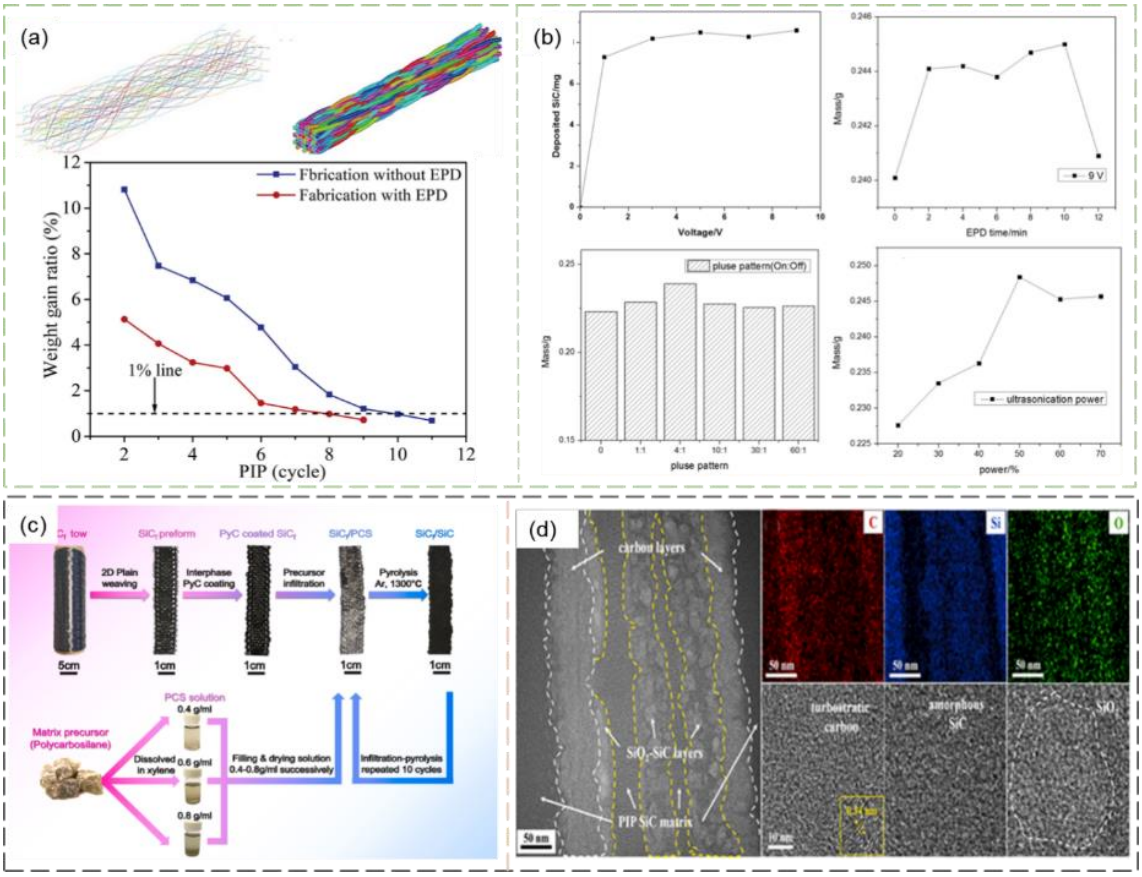

Figure 5. Optimization of the fabrication process for SiC_f/SiC composites: (a) Weight gain ratio of composites with/without EPD assistance [57]; Reprinted with permission. Copyright 2019, Elsevier. (b) EPD parameter optimization: effects of voltage, deposition time, pulse pattern, and ultrasonic power [58]; Reprinted with permission. Copyright 2016, Elsevier. (c) SiC_f/SiC composite fabrication via GC-PIP method [62]; (d) TEM images of carbon layer region [63]. Reprinted with permission. Copyright 2023, Elsevier.

2.2.3. Nano impregnation and transient eutectic method

In 2002, the NITE process was proposed by Japanese scientist Kohyama *et al.* [64]. In the NITE process, SiC nanoparticles are combined with sintering agents (Al_2O_3, Y_2O_3, and CaO) in an organic solvent to produce a slurry, which is subsequently dried and cured, followed by hot pressing and sintering to achieve a dense SiC matrix. SiC_f/SiC composites fabricated using the NITE process offer advantages such as high density, high crystallinity, high thermal conductivity, and short fabrication cycles. However, the high temperature and pressure conditions during the process can easily damage SiC fibers, and residual sintering aids in the matrix may contain neutron poisons.

In the application of the NITE process, although it can achieve densification of the material through pressure assistance, it also presents several challenges. However, the application of the process still requires some optimization requirements. For example, the type and amount of sintering aids, as well as factors such as sintering temperature and pressure, can significantly affect the density, microstructure, and properties of SiC_f/SiC composites [65]. To meet the requirements for nuclear applications, it is essential to explore a sintering aid system free of neutron poisons for SiC_f/SiC composites. Kohyama *et*

al. [66] used Y_2O_3-Al_2O_3 sintering aids to fabricate SiC_f/SiC composites and evaluated them under nuclear application conditions. The results showed that the permeability of He gas for the composites produced by this method was 2 to 6 orders of magnitude lower than that of composites made using other processes. Konishi *et al.* [67] studied the influence of sintering aids on the irradiation swelling behavior of SiC_f/SiC composites and found that the swelling rate of the Y_2O_3-Al_2O_3 system was approximately 0.2%, significantly lower than the 3.86% observed in the YAG system.

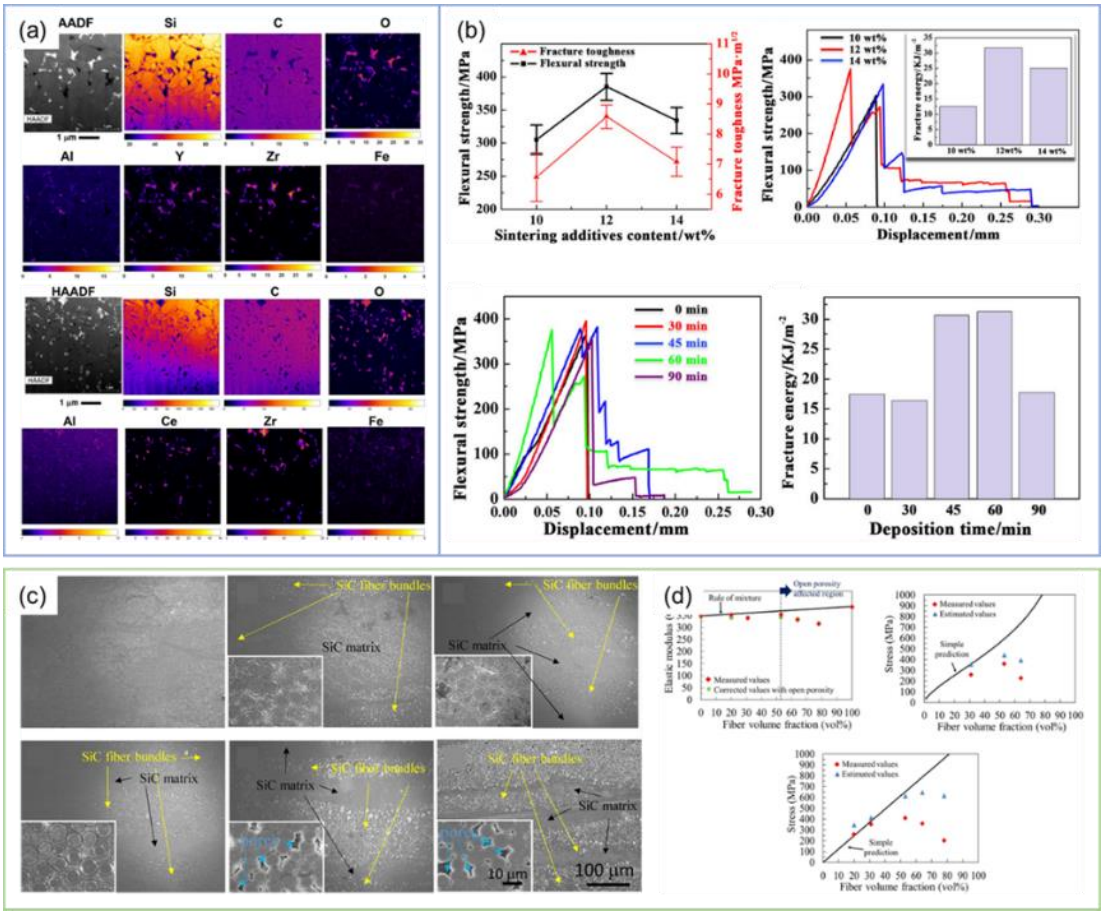

Figure 6. The influence of parameters on mechanical properties in the NITE process: (a) X-ray maps of uncorroded and corroded CZA-2-NITE regions at low magnification [68]; Reprinted with permission. Copyright 2017, Elsevier. (b) Mechanical properties of SiC_{nf}/SiC composites with various sintering additive contents, including strength-displacement curves and corresponding fracture energy [69]; Reprinted with permission. Copyright 2024, John Wiley and Sons. (c) Cross-sectional FE-SEM images of SiC_f/SiC-matrix composites with different fiber contents [71]; Reprinted with permission. Copyright 2021, Elsevier. (d) Influence of fiber volume fraction on mechanical properties of SiC_f/SiC-matrix composites [71].

Additionally, to investigate the impact of different sintering aid systems on material performance, Parish *et al.* [68] systematically analyzed the effects of three sintering aid systems (Y_2O_3-Al_2O_3, CeO_2-ZrO_2-Al_2O_3, and Y_2O_3-ZrO_2-Al_2O_3) on the hydrothermal corrosion resistance of SiC ceramics (Figure 6a). They found that the Y_2O_3-ZrO_2-Al_2O_3 system exhibited the best hydrothermal corrosion resistance. Chen *et al.* [69] optimized the content of 12 wt% Al_2O_3-Y_2O_3 sintering aids and a BN coating deposition

time of 60 minutes. From the curve in Figure 6c, it can be concluded that the mechanical properties of SiC_f/SiC composites produced by the NITE process were improved, achieving a bending strength of 385 MPa and a fracture toughness of 10.44 MPa·$m^{1/2}$, providing an effective strategy for the preparation of high-performance SiC_f/SiC composites (Figure 6b). Meanwhile, Lee *et al.* [70] and Shimoda *et al.* [71] further improved the density and performance of the composites by optimizing parameters. Lee *et al.* [70] found that a sintering temperature of 1780 ℃ could achieve a higher material density, with unidirectional fiber structures outperforming two-dimensional woven structures in terms of densification and mechanical properties. Shimoda *et al.* [71] discovered that as the fiber volume fraction increased, the mechanical properties of the composites gradually improved, reaching their peak at 53 vol%, demonstrating an ultimate tensile strength of 408 MPa and a proportional limit stress of 358 MPa, as shown in Figures 6c,d. However, when the fiber volume fraction exceeds 64 vol%, the material properties begin to decline due to fiber damage and increased porosity within the matrix. This study emphasizes the importance of optimizing the fiber volume fraction during the fabrication process to achieve optimal material performance.

It is evident that the NITE process requires pressure assistance for densification, which poses significant challenges for the fabrication and processing of special-shaped components, such as SiC_f/SiC composite cladding tubes for nuclear applications. The development of low neutron poison sintering aids may reduce the sintering temperature of the NITE process and enable pressureless sintering; however, it inevitably leads to the formation of high volume fractions of grain boundary phases, potentially increasing defects and cracks under neutron irradiation.

2.2.4. Reactive melt infiltration

The RMI process was initially applied to porous SiC and carbon preforms, serving as a technique for generating a dense SiC matrix through liquid silicon infiltration of a porous structure. The key to this process is that liquid silicon can wet SiC and easily fill the pores but does not wet carbon, thus requiring a reaction with carbon during infiltration to form β-SiC. During this reaction, the formed β-SiC gradually covers the carbon preform, further advancing the silicon front within the material. This mechanism enables the RMI process to effectively form a dense, high-temperature-resistant SiC matrix within porous materials [72–74].

However, a primary issue facing the RMI process is incomplete reactions, which often leave unreacted free silicon within the composite. Moreover, the content and impact of free silicon are closely related to several process parameters [75]. Higher temperatures can accelerate the reaction between silicon and carbon, thereby reducing unreacted silicon content, but may lead to abnormal SiC grain growth [76]. Appropriate pressure can improve silicon infiltration efficiency and reduce free silicon residue, though excessive pressure may introduce additional stress. Extending infiltration time allows for increased reaction time between silicon and carbon, helping to reduce free silicon, though time and cost need to be balanced. Therefore, to reduce or eliminate unreacted silicon residue, recent studies have explored using silicon alloys (such as silicon-aluminum and silicon-titanium alloys) as infiltration materials. These alloys improve silicon wettability during infiltration and provide greater uniformity in reaction with carbon, thereby reducing unreacted silicon residue and enhancing material density and overall performance [77,78].

Through this process improvement, RMI technology has shown increasing potential in high-temperature applications for composites, achieving significant progress, particularly in enhancing the mechanical stability, oxidation resistance, and thermal stability of SiC-based composites. These advancements have positioned the RMI process as an effective method for preparing high-temperature materials, opening new possibilities for producing high-performance SiC composites. In addition, the reaction thickness between silicon and carbon is approximately 10 μm; only an appropriate pore size distribution and porosity can ensure that the silicon infiltration reaches a sufficient thickness to produce high-performance SiC composites [79,80]. Hu *et al.* [81] investigated the microstructure and properties of high-density SiC_f/SiC composites fabricated using the RMI process. The results showed that the material had a density of 2.83 g/cm^3, with a porosity of only 1.6%. The size of the free silicon in the matrix was small, which enhanced the mechanical properties and high-temperature creep resistance of the material. The bending strength of the material at high temperatures (1200 ℃) is 576 MPa, demonstrating excellent mechanical stability and non-brittle fracture characteristics. Additionally, the thermal conductivity of the material is 41.7 W/(m·K) at room temperature, decreasing to 18.9 W/(m·K) at 1300 ℃, indicating high thermal stability. After 1000 hours of oxidation at 1200 ℃ in air, the bending strength of the material only decreased by 19%, showing good high-temperature oxidation resistance, making it suitable for hot-end components in aerospace engines.

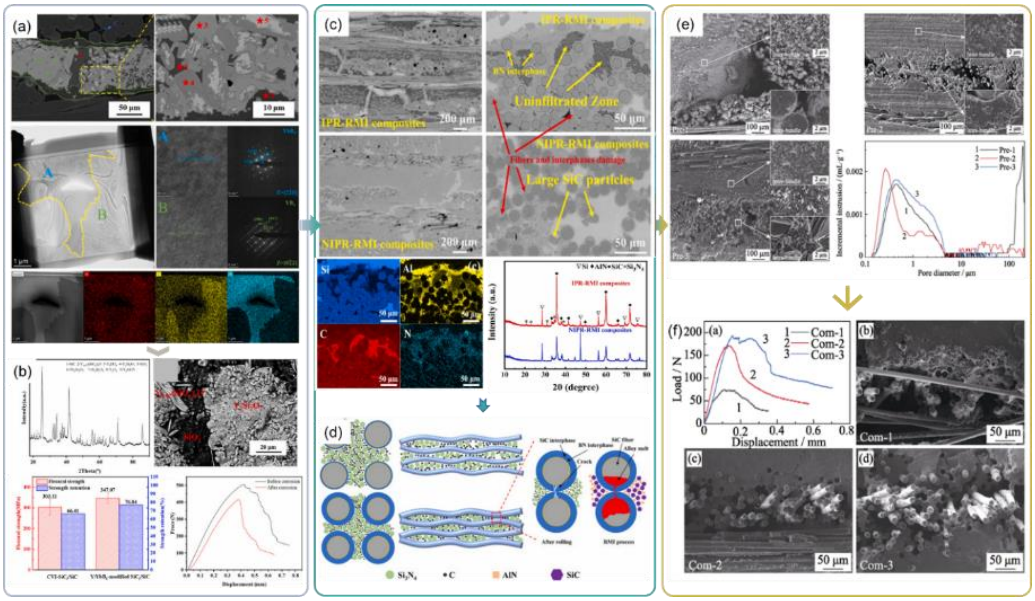

Figure 7. Characteristics of materials prepared by RMI: (a) Microstructure and EDS mapping analysis [82]; Reprinted with permission. Copyright 2023, Elsevier. (b) Flexural strength, strength retention rate, and force-displacement curves post-oxidation [82]; (c) SEM, EDS, and XRD results [83]; Reprinted with permission. Copyright 2024, Elsevier. (d) Schematic of erosion process [83]; (e) Cross-sectional SEM images [84]; (f) Bending load-displacement curves and fracture surface SEM images of composites [84].

Furthermore, scholars have explored the variations in the mechanical properties of the materials by examining the RMI process under various conditions. Wang *et al.* [82] fabricated Y/YbB4 modified

SiC_f/SiC composites using slurry infiltration (SI) and RMI methods, significantly reducing the open porosity of the material to 3.2 ± 0.4% and increasing the density to 2.67 ± 0.11 g/cm^3. After 100 hours of corrosion in a 1200 ℃ water-oxygen environment, the material retained 76.84% of its strength, reflecting a 15.71% improvement, which is attributed to the formation of rare earth silicate phases that enhanced the corrosion resistance of the material, as shown in Figures 7a,b. Sun *et al.* [83] investigated the effects of low-temperature RMI process on SiC_f/SiC-AlN composites and found that larger pore sizes and higher porosity facilitate the full infiltration of the alloy melt, resulting in a dense and uniform matrix. This led to a bending strength of 160.2 MPa for the composites, approximately 1.5 times that of materials with smaller pore sizes; however, the erosion of the fibers and interface by the Si-Al alloy melt negatively impacted the material properties, as shown in Figures 7c,d. Zhang *et al.* [84] focused on the influence of pore structure on the performance of SiC_f/SiC composites in the RMI process. They found that a uniform pore structure facilitates the full infiltration of the melt, reduces residual porosity, and enhances mechanical properties, resulting in excellent composites with a bending strength of 200.5 MPa and an elastic modulus of 79.19 GPa, as shown in Figure 7e,f.

The main challenge faced by the RMI process is that SiC_f/SiC composites often contain a significant amount of unreacted free silicon, with a volume fraction typically ranging from 12% to 18%.

Due to the melting point of silicon being 180 ℃, composites fabricated using the RMI process are typically suitable for use in environments below 1200 ℃. However, when the operating temperature exceeds 1300 ℃, the residual silicon in the matrix can accelerate diffusion, migrating along the SiC grain boundaries and eroding the SiC fibers and their coatings, thereby significantly degrading the performance of the composites [85]. Additionally, the RMI process may also result in residual unreacted carbon in the composite matrix, which can weaken the material's oxidation and corrosion resistance.

Given the extreme conditions of high temperature, strong corrosion, intense radiation, and strong oxidation in nuclear energy systems, the RMI process has not yet been applied to the fabrication of nuclear-grade composites. In the future, for both nuclear and non-nuclear applications, the RMI process will need to design reasonable reaction pathways and optimize process conditions to ensure that silicon and carbon can fully react and convert into near-stoichiometric SiC.

2.2.5. Combination of multiple processes

The combination of multiple processes leverages the advantages of various techniques in the fabrication of SiC_f/SiC composites while avoiding their disadvantages, thereby enhancing densification, optimizing microstructure, and improving the properties of the samples. Representative combined processes include PIP+CVI, CVI+RMI, and CVI+NITE.

The widely utilized hybrid method is the combination of PIP and CVI, which greatly enhances the properties of the materials. The National Aeronautics and Space Administration (NASA) employs a combination of PIP and CVI processes to fabricate SiC_f/SiC composites, first performing liquid precursor infiltration, followed by the infiltration of small molecular gaseous precursors using the CVI method, achieving a higher degree of densification. Liu *et al.* [86] demonstrated that a lower CVI deposition rate and an appropriate amount of SiC matrix deposition contribute to improving the mechanical properties of the composites, achieving performance levels that are twice those of the single PIP or CVI pathways. Mu *et al.* [87] investigated the effect of combining a PyC interlayer with Al_2O_3 filler on the mechanical and electromagnetic shielding properties of 2.5D KD-I SiC_f/SiC composites.

This combination, essentially a "hybrid method", utilizes different fillers and interlayer materials to significantly enhance the composite's flexural strength (313 MPa), fracture toughness (12.7 $MPa \cdot m^{1/2}$), and electromagnetic shielding effectiveness (SET of 30 dB and SEA of 20 dB). This approach demonstrates that using a mixed strategy with different components can tune multiple properties of composites. Wei *et al.* [88] proposed a new strategy of hybrid application of CVI and PIP to adjust interface stress in SiC_f/SiC composites. The study found that this hybrid method enhanced interface shear strength (139.8 MPa) and dynamic friction strength (44.2 MPa) by increasing interface compressive stress, resulting in a proportional limit stress of 729.8 MPa and a modulus of 288.0 GPa. This study clearly demonstrates the potential of the CVI-PIP hybrid strategy in improving mechanical properties. Zhang *et al.* [89] studied the effect of the hybrid CVI-PIP method on the long-term oxidation performance of SiC_f/SiC composites in static air at 1200 ℃. By comparing the microstructures of composites prepared using single PIP and hybrid CVI-PIP techniques before and after oxidation (Figure 8b), they found that materials made by the hybrid method retained strength better, maintaining 76% of their initial flexural strength after 200 hours of oxidation. This further validates the advantage of the hybrid method in enhancing the high-temperature oxidation resistance of composites. Combining CVI and PIP processes or introducing various fillers can significantly enhance the mechanical properties, oxidation resistance, and electromagnetic shielding performance of SiC_f/SiC composites. These methods provide effective pathways to optimize the application potential of composites in high-temperature and complex environments.

Meanwhile, other combinations of processes also demonstrate significant research value. Brennan [90] employed the CVI-RMI process, first depositing a BN transition layer and a SiC layer on the surface of SiC fibers using the CVI method. Subsequently, a SiC slurry was infiltrated into the woven SiC fibers, followed by infiltration with molten silicon, resulting in a denser composite that enhances the thermal conductivity. Li *et al.* [91] proposed a composite preparation technique that combines CVI with NITE. Initially, a short duration of CVI deposition is used to reinforce the SiC fiber preform structure, reserving infiltration pores for the ceramic slurry. Then, using nano SiC powder, sintering aids, and the ceramic precursor PCS as raw materials, a method combining vacuum infiltration and electrophoretic infiltration is employed to obtain a tightly structured composite. Finally, after undergoing hot isostatic pressing, SiC_f/SiC thin-walled tubular samples with a density of 2.77 g/cm^3 are produced, demonstrating application potential for the fabrication of long-sized SiC_f/SiC composite cladding tubes.

Further research also involves the exploration of other hybrid processes. Raju *et al.* [92] demonstrated a novel hybrid technique that successfully fabricated low-porosity SiC_f/SiC composites using CVI, EPD, and LSI (liquid silicon infiltration). The microstructure is illustrated in Figure 8d (left). Initially, a dual-layer coating of BN and SiC was applied to the SiC fabric using the CVI technique. Subsequently, the EPD technique was employed to infiltrate a ceramic matrix composed of SiC and carbon black nanoparticles into the fine pores of the fabric. Finally, the remaining small pores were filled through LSI, allowing silicon to react with carbon to form SiC, thereby achieving a dense microstructure. The experimental results indicate that the obtained composite has a density of 2.62 g/cm^3, with a porosity of only 0.55%, and a bending strength of 111 MPa at room temperature. Compared to SiC_f/SiC composites fabricated using traditional single processes, the materials produced through hybrid processes exhibit significant advantages in terms of density, porosity, and mechanical properties.

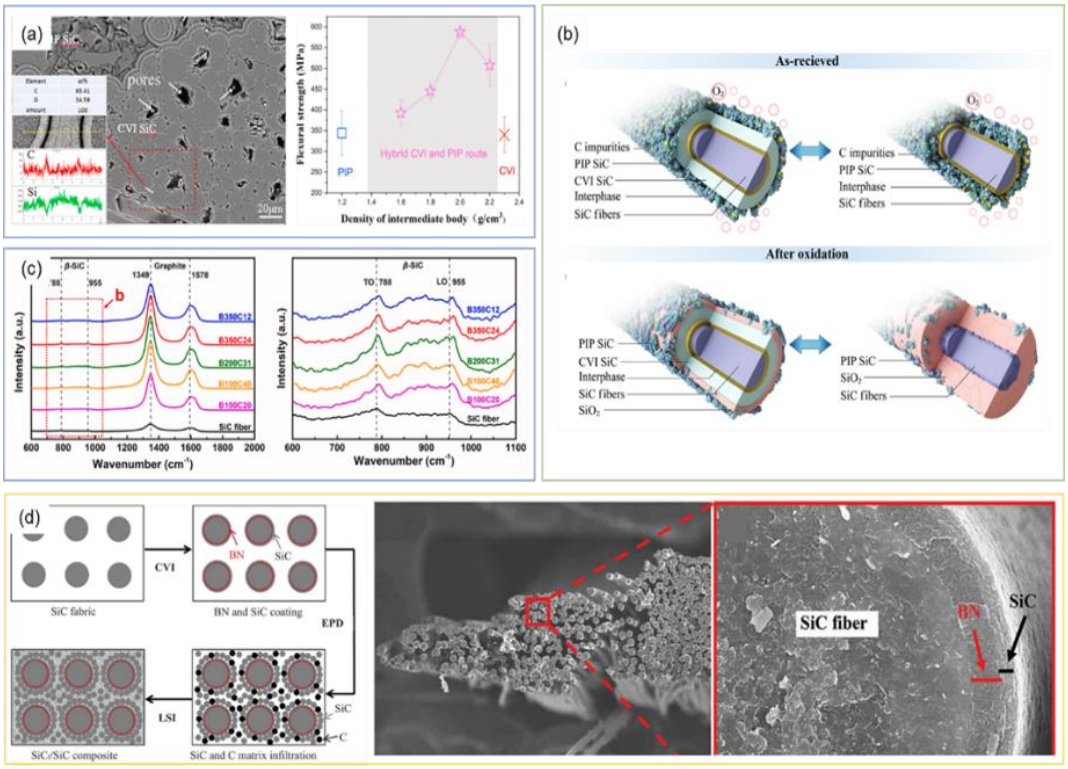

Figure 8. Schematic of the microstructure and properties of SiC_f/SiC composites prepared using combination of multiple processes: (a) SEM images of SiC_f/SiC composites fabricated via hybrid CVI and PIP routes, with a line scan inset of the CVI-derived SiC matrix showing two dark fringes [86]; Reprinted with permission. Copyright 2021, Elsevier. (b) Schematic of the SiC microstructure architecture [89]; Reprinted with permission. Copyright 2024, Elsevier. (c) Raman spectra of SiC fiber in various samples, with a magnified view of the β-SiC section [88]; (d) CVI, EPD, and LSI hybrid process flow and microstructure of a typical CVI dual-coated SiC fabric at two magnifications [92].

Table 2. The advantages and disadvantages of the preparation process.

Fabrication Method	Advantages	Disadvantages
CVI	1. Low-temperature synthesis. 2. Suitable for complex shapes. 3. Enables gradient material properties.	1. Slow process, high porosity. 2. Toxic gases, safety risks.
PIP	1. Simple and cost-effective. 2. Suitable for complex structures.	1. High residual carbon, low density. 2. Volume shrinkage issues.
RMI	1. Fast densification. 2. Cost-effective for large-scale production.	1. Residual silicon limits high-temp use.
NITE	1. High density, crystallinity, thermal conductivity. 2. Short processing time.	1. High-temp pressure can damage fibers. 2. Sintering aids may limit nuclear use.
EPD	1. Fills voids, improves density. 2. Boosts thermal conductivity.	1. Expensive, toxic solvents. 2. Complex quality control.
Hybrid Processes	1. Expensive, toxic solvents. 2. Complex quality control.	1. Complex coordination and cost.

In summary, it can be seen that whether it is the straightforward PIP process, the high crystallinity CVI process, the highly densified NITE process, or the low-cost RMI process, each has its advantages

and disadvantages, and none can simultaneously meet the nuclear application requirements for SiC_f/SiC composites in terms of high density, high purity, high crystallinity, and low cost. Future development requires the optimization and improvement of each process, and based on this, the comprehensive utilization of the advantages of various techniques to develop new multi-process hybrid technologies. New ceramic sintering mechanisms and processes may offer new opportunities for the advancement of nuclear-grade SiC_f/SiC composites.

3. Research on SiC_f/SiC composites in extreme environments

In recent years, silicon carbide composites reinforced with silicon carbide fibers have been extensively studied for various high-temperature, irradiation, and corrosion applications, the influence of high-temperature behavior, irradiation-induced damage, and corrosion resistance on the mechanical performance of SiC_f/SiC composites has emerged as a major focus of research.

3.1. Thermodynamics

During a loss-of-coolant accident (LCA) and a station blackout (SBO) event, the fuel assemblies may be exposed to high-temperature steam environments exceeding 700 ℃. For example, in a nuclear reactor, temperatures could potentially exceed 1800 ℃ [93]. Currently, nuclear power plants commonly use Zircaloy-4 (Zr-4) cladding and uranium dioxide fuel assemblies. Nonetheless, Zr-4 cladding may experience expansion and rupture at the relatively low temperature of 725 ℃ as a result of the interplay between internal pressure and steam, this results in a marked decrease in its strength [94,95]. In addition, during the reflow process of the fuel assemblies, due to the differences in geometric shrinkage rates, the cladding may endure additional axial loads [94]. In certain accident scenarios, the temperature of Zr-4 can rapidly rise to 1850 ℃, leading to the repositioning of the fuel, consequently further diminishing the fuel's cooling capacity. Thus, researching the mechanical performance of silicon carbide ceramic matrix composites under extreme temperatures has become increasingly critical.

In order to address the challenges mentioned above, in recent years, researchers have undertaken comprehensive investigations into silicon carbide composites. Shapovalov *et al.* [96] studied the mechanical properties of nuclear-grade silicon carbide composites under high-temperature conditions, the results indicate that the SiC coating maintain strengths close to room temperature at 1100 ℃ are shown in Figure 9a, this is of significant importance for the ATF program. Lu *et al.* [97] reported that the $SiC_f/BN/SiC$ composites prepared by chemical vapor deposition exhibited a maximum tensile strength of 365 MPa at 1000 ℃. However, when the temperature rises to 1500 ℃, the tensile strength decreases to 205.73 MPa, this indicates that the BN interfacial layer significantly enhances the high-temperature mechanical properties of the material. Ma *et al.* [98] found that, the $SiC_f/BN/SiC$ composites prepared by the CVI method exhibited significantly improved mechanical properties after heat treatment (1000 ℃ and 1300 ℃) following infiltration, the flexural strength increased from 366 MPa to 377 MPa. However, heat treatment before infiltration resulted in a decline in mechanical properties. Xu *et al.* [99] evaluated the residual strength of SiC_f/SiC composites after 100 thermal shock cycles at 1200 ℃. Additionally, the surface stress of the material was evaluated are shown in Figure 9d, the results indicate a significant decrease in the material's strength, However, by optimizing the interfacial treatment, this can mitigate the negative impact of thermal shock on the material's performance.

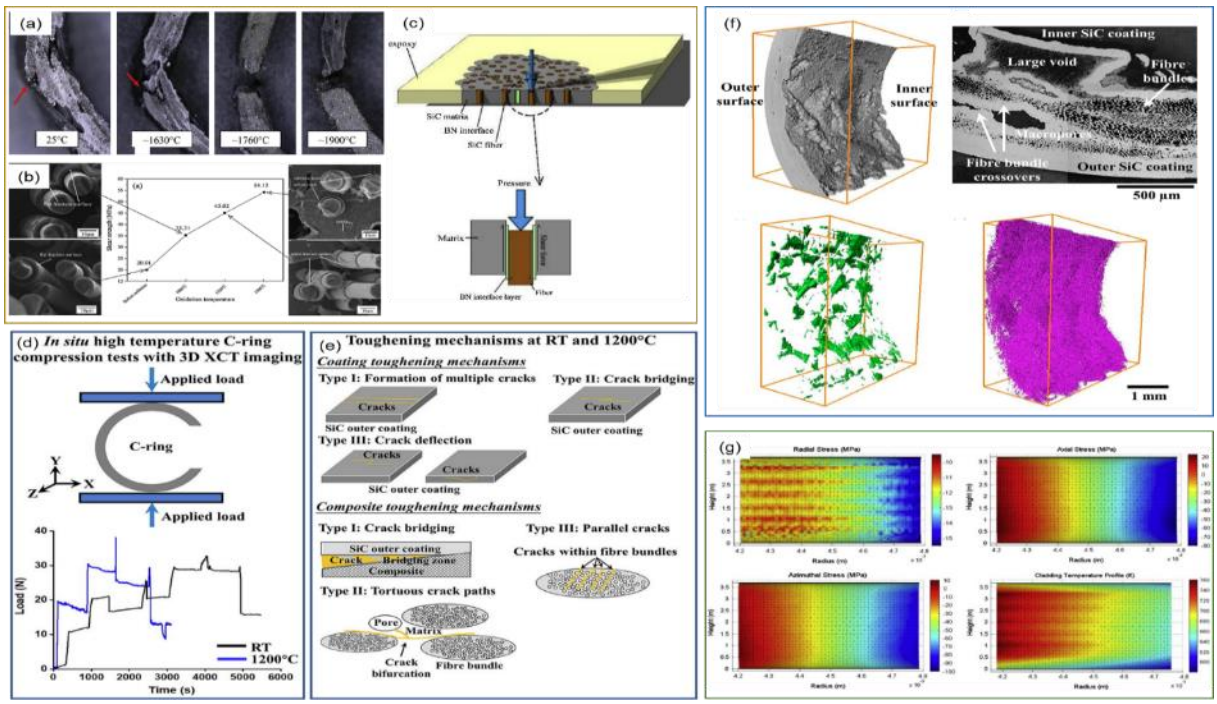

Figure 9. Schematic diagram of SiC_f/SiC composite microstructure at varying temperatures: (a) Fracture sites of c-rings tested in argon at various temperatures, with arrows indicating crack locations [96]; Reprinted with permission. Copyright 2019, Elsevier. (b) The schematic diagram of SiC_f/BN/SiC mini-composites for the fiber push-out test [97]; Reprinted with permission. Copyright 2020, Elsevier. (c) SEM images of flexural fracture surface morphologies for three composite types [97]; (d) In situ high temperature C-ring compression tests with 3D XCT imaging [100]; (e) Toughening mechanisms at RT and 1200 ℃ [100]; (f) As-received SiC_f-SiC_m cladding tube material [100]; (g) 2D stress and temperature profiles after 1 year of K_{11} rod irradiation with nonuniform power and coolant temperature profiles [101]. Reprinted with permission. Copyright 2014, Elsevier.

Simultaneously, a comprehensive analysis of the material's damage behavior in high-temperature environments is performed, contributing to a deeper understanding of its performance under extreme conditions. Jing *et al.* [102] examined the tensile creep behavior of 3D four-step woven SiC_f/SiC ceramic matrix composites in air at temperatures of 1100 ℃ and 1300 ℃. They discovered that the fibers significantly influence the creep deformation rate. Moreover, at 1300 ℃, creep predominantly occurs during the primary creep stage. Yuan *et al.* [100] utilized *in situ* high-temperature 3D imaging technology to analyze the damage behavior of SiC_f/SiC composites in high-temperature environments are shown in Figure 9f, the study found that it primarily manifested as debonding at the interface between the matrix and fibers, as well as fiber fracture, particularly at 1200 ℃, The fracture stress of the fibers significantly decreases. Cluzel *et al.* [103] studied the behavior of self-healing ceramic matrix composites under high temperatures and mechanical loads, the results indicate that the material exhibits excellent self-healing capability during thermal-mechanical cycling at 1000 ℃, its tensile strength and flexural strength remain above 200 MPa and 300 MPa, respectively. Ben-Belgacem *et al.* [101] analyzed the thermodynamic behavior of SiC_f/SiC composites after one year of irradiation under light water reactor (LWR) conditions, as shown in Figure 9g. The study found that under conditions of 300

°C and 15 MPa, the material exhibits excellent mechanical properties, the tensile strength is 250 MPa, the compressive strength is 350 MPa. This demonstrates a promising application potential in LWR environments.

Using composites in high-temperature and extreme environments requires further enhancement of their structure and properties to ensure long-term stability. At high temperatures, SiC and BN interlayers provide effective oxidation protection, preventing oxidation and interface reactions between fiber and matrix, thereby enhancing the composite's creep resistance and maintaining strength and toughness under extreme conditions. Additionally, fibers play a crucial role in controlling creep behavior by slowing primary creep rates and reducing deformation accumulation at high temperatures, further enhancing the overall stability of the material. Moreover, self-healing ceramic matrix composites exhibit damage recovery capabilities during high-temperature thermal cycling, and developing self-healing interface coatings or matrix materials can significantly enhance their reliability under extreme conditions. These mechanisms provide key directions for the design and optimization of future composites.

3.2. Irradiation damage

In advanced nuclear energy systems, under high-temperature and strong neutron irradiation conditions, the irradiation damage of SiC_f/SiC composites and its impact on mechanical properties is one of the key areas of current research. The Oak Ridge National Laboratory in the United States has conducted a series of neutron irradiation damage studies on SiC_f/SiC composites. The Ozawa team [104–106] investigated composites that combine the third-generation silicon carbide fiber Tyranno-SA with the second-generation silicon carbide fiber Hi-Nicalon-S, along with SiC matrices prepared using different processes. The results demonstrate that the ultimate tensile strength of both SiC fiber-reinforced composites exhibits minimal variation following irradiation. Silicon carbide ceramic matrix composites prepared using the CVI process at 750 °C, under irradiation conditions with a neutron flux of 12×10^{25} n/m², the slip stress between the interface and the matrix significantly decreases [104]. Under irradiation conditions of 800 °C and a neutron flux of 5.9×10^{25} n/m², the crack propagation resistance of the composites shows no significant decrease [105]. The energy release rate of silicon carbide ceramic matrix composites prepared by the hot pressing sintering method (NITE) shows little variation before and after irradiation, indicating good damage tolerance [106].

To further investigate the relationships between the fibers, matrix, and interface, Koyanagi *et al.* [107] evaluated the conditions following neutron irradiation at approximately 100 dpa, examining the mechanical properties and microstructural changes of CVI-SiC matrix composites at temperatures of 319 °C and 629 °C, as depicted in Figure 10b. The study revealed that the composites displayed brittle fracture behavior after irradiation at 319 °C, which is closely associated with the loss of interfacial functionality. However, the samples irradiated at 629 °C experienced partial debonding between the fibers and the matrix, exhibiting a higher apparent fracture strain. Nogami *et al.* [108] implanted helium gas into the composites through experiments, the study shows that neutron irradiation without helium pre-implantation results in a decrease in the flexural strength, elastic modulus, and proportional limit stress of the composites. However, after helium pre-implantation, neutron irradiation results in a significant increase in the hardness and elastic modulus of Hi-Nicalon fibers. Additionally, the number of layers in the PyC interface phase significantly affects the material properties. Nozawa *et al.* [109] investigated the impact of neutron irradiation on the interfacial shear strength of CVI-SiC_f/SiC

composites featuring single-layer pyrolytic carbon (PyC) and $(PyC/SiC)_n$ interfaces, utilizing a monofilament push-out method. The results indicate that following neutron irradiation, the reduction in interfacial shear strength of the $(PyC/SiC)_n$ interface is more significant than that of the single-layer PyC. However, the strength retention rate of the corresponding composites remains relatively high. Research by Katoh and Perez-Bergquist *et al.* [110–112] found that, under high-dose neutron irradiation, the interface of SiC_f/SiC composites undergoes degradation, resulting in a significant reduction in shear strength and interfacial friction stress. Consequently, this leads to a decrease in the macroscopic tensile strength of the material. Therefore, from the perspective of the interfacial phase, the interfacial phase system containing PyC may struggle to meet the long-term service requirements of SiC_f/SiC in nuclear environments.

In the field of ion irradiation, researchers have also investigated its effects on the microstructure and mechanical properties of SiC_f/SiC composites. The study by Chai *et al.* [113] indicates that 3 MeV silicon ion irradiation significantly reduced the interfacial shear strength of SiC_f/SiC composites, it decreased from 146.42 MPa in the unirradiated state to 75.04 MPa at 1 dpa and 73.31 MPa at 5 dpa. Irradiation caused disordering of the carbon phase, additionally, microcracks were found at the fiber-matrix interface. The overall mechanical properties of the material were impacted, as illustrated in Figure 10f. In a similar manner, the influence of hydrogen-helium ion irradiation on SiC_f/SiC composites with Ti_3SiC_2 interfacial phases or coatings was studied by Yang *et al.* [114]. The research results indicate that irradiation-induced lattice expansion and the formation of voids negatively impact the interfacial bonding strength. This further weakened the radiation resistance of the composites (Figure 10g). Furthermore, the impact of C and He ion irradiation on the microstructure of SiC_f/SiC composites was investigated by Liu *et al.* [115]. Irradiation was found to induce the formation of nanocrystals within the SiC fibers and matrix, additionally, microcracks and bubbles were observed at the interface, as illustrated in Figure 10h. These microstructural changes may significantly affect the overall mechanical properties of the composites.

Not only does irradiation influence interfacial properties, but it also has a significant effect on the microstructure of the matrix and fibers. Koyanagi *et al.* [116] found through 5 MeV Si^{2+} ion irradiation that the SiC matrix exhibits a greater expansion rate compared to the fibers, this leads to a reduction in the residual stress of the matrix and an increase in the yield strength, this phenomenon indicates that irradiation-induced microstructural changes may lead to degradation of the material properties. In a 300 keV silicon ion irradiation experiment conducted at 300 °C, Zhao *et al.* [117] observed severe crystal structure damage to the fibers and matrix. The matrix exhibited expansion, while the fibers and interfacial layer contracted axially, leading to a sharp decrease in hardness. Xu *et al.* [118] found that under 300 keV silicon ion irradiation, irradiation caused the PyC interface, fibers, and matrix to expand, resulting in reduced hardness and Young's modulus. These microstructural changes may significantly affect the mechanical properties and service life of the material.

The creation of defects, including bubbles and voids, during irradiation is a critical factor affecting the properties of materials. Research by Taguchi *et al.* [119,120] indicates that after dual ion irradiation, He bubbles were generated in the SiC matrix, with bubble size increasing as the irradiation dose rose. This phenomenon may lead to a decline in the mechanical properties of the material. Li *et al.* [121] studied the effects of helium ion irradiation on SiC_f/SiC composites and found that as the irradiation temperature increased, the bubble density rose, leading to a decrease in tensile strength and hardness by approximately 20% and 15%, respectively. These changes further weaken the mechanical properties of

the material. Ye *et al.* [122] observed that during triple ion beam irradiation experiments, cracks and bubbles developed between the PyC interface phase and the multilayer SiC coating, particularly the formation of He bubbles leads to material expansion and degradation of physical properties. Nogami *et al.* [123] discovered through He and C dual ion beam irradiation that while the SiC matrix showed good stability towards helium and no voids or dislocation loops were observed, dimensional changes occurred in the fibers and graphite layers, suggesting that these size alterations due to irradiation could impact the material's overall stability. Xu *et al.* [124] explored the collaborative effects of helium and krypton ion irradiation on the evolution of bubbles in SiC_f/SiC composites, discovering that this evolution is affected by the concentration ratio of vacancies to helium atoms. This research provided the first *in situ* observation of the competition between irradiation-assisted bubble growth and re-dissolution in the SiC matrix, offering new perspectives for controlling bubble density. Ye *et al.* [125] discovered that irradiation with 6 MeV gold ions resulted in a notable increase in the hardness of SiC fibers, which is mainly attributed to the pinning effects of point defects and small defect clusters.

Figure 10. Microscopic failure morphology of SiC_f/SiC composites under irradiation damage: (a)

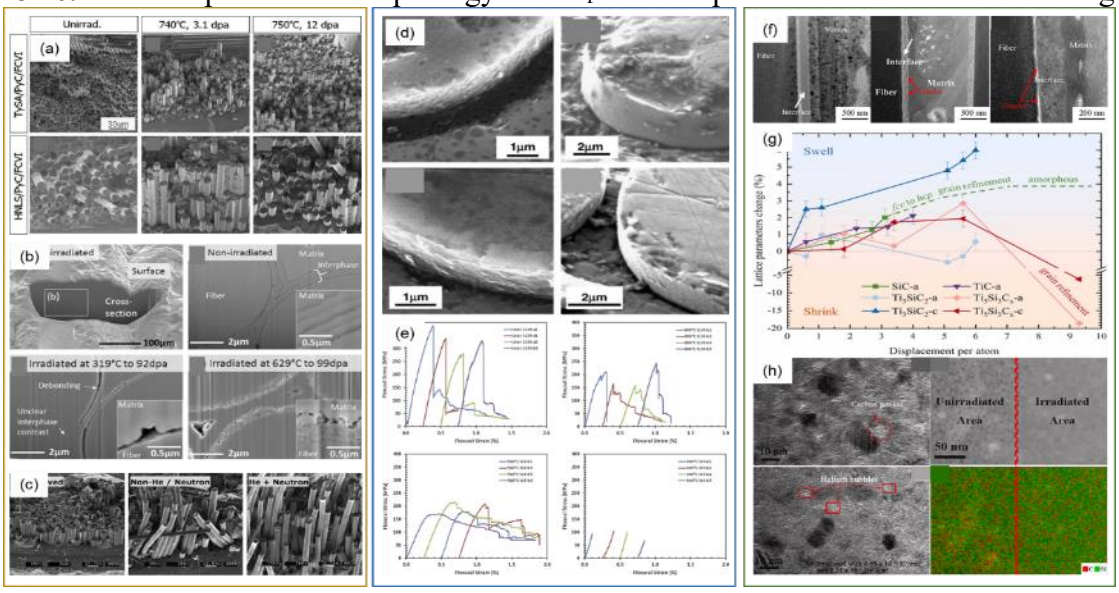

Fracture surfaces of unirradiated and neutron-irradiated tensile specimens [104]; Reprinted with permission. Copyright 2007, Elsevier. (b) Secondary electron micrographs of CVI SiC_f/SiC composite cross-sections [107]; Reprinted with permission. Copyright 2018, Elsevier. (c) SEM fracture surface observations for as-received, non-He-implanted and neutron-irradiated (Non-He/Neutron), and He-implanted and neutron-irradiated (He + Neutron) composites [108]; Reprinted with permission. Copyright 2004, Elsevier. (d) Typical pushed-out fiber surfaces [109]; Reprinted with permission. Copyright 2007, Elsevier. (e) Flexural stress–strain properties of Hi-Nicalon Type S, CVI-SiC-matrix composites in unirradiated condition [111]; Reprinted with permission. Copyright 2015, Elsevier. (f) TEM images of SiC_f/SiC composites pre- and post-Si ion irradiation [113]; Reprinted with permission. Copyright 2018, Elsevier. (g) Relationship between irradiation damage and lattice parameter changes [114]; Reprinted with permission. Copyright 2024, Elsevier. (h) Bright-field TEM images showing morphologies of unirradiated and irradiated SiC fibers [115]. Reprinted with permission. Copyright 2021, Elsevier.

To enhance the stability of SiC_f/SiC composites in irradiated environments, the design of multilayer structures is particularly important. Research conducted by Katoh *et al.* [126] and Kishimoto *et al.* [127,128] demonstrates that multilayer CVI-SiC_f/SiC composites maintain excellent dimensional stability when subjected to dual ion irradiation at doses up to 100 dpa and temperatures of 1000 °C. This multilayer interface introduces silicon carbide (SiC) or carbon (PyC) coatings between the fibers and matrix via chemical vapor infiltration (CVI), effectively reducing irradiation-induced defect diffusion and improving radiation resistance by lowering stress concentration at the interface. By carefully controlling the number and thickness of layers, the mechanical properties of the interface are optimized, allowing the material to maintain structural integrity and dimensional stability under high-temperature and high-irradiation conditions.

Overall, the evolution of microstructure and mechanical property changes in SiC_f/SiC composites under conditions of high-temperature strong neutron and ion irradiation demonstrate considerable complexity. Studies have shown that irradiation significantly affects material interfacial performance, the microstructure of the matrix and fibers, the formation of bubbles and voids, and the stability of multilayer structures. Particularly in the context of neutron and ion irradiation, the decline in interfacial slip stress, along with the formation and growth of bubbles and crystal damage to both fibers and the matrix, contributes to a reduction in the material's strength and toughness. The design of multilayer interfaces and the application of high-crystallinity SiC fibers contribute to enhancing the irradiation resistance of the material. Nevertheless, additional studies are required to explore the performance of these materials under elevated irradiation doses and prolonged exposure conditions, ensuring their reliability and safety in advanced nuclear energy systems.

3.3. Corrosion

In research on nuclear cladding materials, interactions with coolant and corrosive environments are vital in assessing the safety and durability of these materials. In order to improve the corrosion resistance and longevity of nuclear cladding materials, extensive investigations have been conducted on their behavior in hydrothermal environments, oxidative conditions, and corrosive media, with the goal of optimizing corrosion performance by refining manufacturing processes and implementing environmental barrier coatings. The focus of this paper is on the microstructural evolution, interfacial behavior, and application of coating technologies in these studies. Through a summary of pertinent research results, we aim to enhance our understanding and evaluation of nuclear cladding materials' performance under extreme conditions, offering theoretical insights for future material design and engineering applications.

In recent years, SiC_f/SiC composites have attracted considerable interest from scholars worldwide as a promising option for nuclear fuel cladding materials. To enhance the safety and cost-effectiveness of commercial reactors, there is growing advocacy for the application of SiC_f/SiC composites in commercial LWRs. Nevertheless, there is a scarcity of studies on the stability of SiC_f/SiC composites in high-temperature and high-pressure cooling water, especially concerning the corrosion resistance of these materials, which has seldom been addressed. In a high-temperature oxidative environment, SiC reacts with oxygen to produce a SiO_2 oxide layer, which thickens over time and with elevated temperatures, resulting in a deterioration of the mechanical properties of SiC_f/SiC composites. Especially in high-temperature vapor environments, the oxidized SiO_2 layer can form a liquid or amorphous structure that fills the gaps left by the oxidation of the pyrolytic carbon interface, resulting

in fiber breakage and total degradation of the composite, further intensifying corrosion (see Figure 11a). SiC may react with water to generate $Si(OH)_4$, resulting in the dissolution of the material and loss of mass. Additionally, the oxidation of SiC at different temperatures produces various gaseous products: primarily CO_2 at temperatures below 700 ℃, mainly CO above 850 ℃, and both CO and CO_2 within the temperature range of 700 ℃ to 850 ℃. Terrani *et al.* [129] explored the process by which SiC interacts with H_2O to form SiO_2, suggesting several potential reaction pathways (refer to Reaction Equations (1)–(4)).

$$SiC(s) + 2H_2O(aq) = SiO_2(s) + CH_4(g) \quad (1)$$

$$SiC(s) + 2H_2O(aq) = SiO_2(s) + 2H_2(g) + C(s) \quad (2)$$

$$SiC(s) + 3H_2O(aq) = SiO_2(s) + 3H_2(g) + CO(g) \quad (3)$$

$$SiC(s) + 4H_2O(aq) = SiO_2(s) + 4H_2(g) + CO_2(g) \quad (4)$$

The preparation methods and environmental conditions of SiC_f/SiC composites, such as temperature, pressure, dissolved oxygen, dissolved hydrogen, and pH, significantly influence the corrosion rate of SiC [130]. Additional studies have shown that SiC produced through CVD techniques demonstrates superior corrosion resistance. Park *et al.* [131] and Qin *et al.* [132] discovered that SiC produced via CVD demonstrates outstanding corrosion resistance. This is because the CVD process can produce a high-density, low-porosity SiC structure, effectively reducing the pathways for corrosive substances to penetrate and thereby significantly decreasing the corrosion rate. Additionally, Park *et al.* [131] compared the behaviors of SiC produced via CVD and NITE processes under high-temperature and high-oxygen conditions. The experimental results indicate that CVD-SiC effectively reduces oxidation-induced weight loss, whereas NITE-SiC shows a significant weight loss rate, attributed to active oxidation at the PyC interface produced by NITE. Berdoyes *et al.* [133] studied the corrosion behavior of differently oriented CVD-SiC in contact with molten silicon at high temperatures. The experimental results indicate that the <111> oriented SiC coating has a dense microstructure, which can further enhance the material's stability in harsh environments.

The incorporation of an interfacial layer into the material can markedly improve its resistance to oxidation. Nasiri *et al.* [134] investigated the oxidation behavior of SiC/SiC ceramic matrix composites in air at temperatures between 1200 and 1400 ℃, discovering that the thickness of the oxide layer (SiO_2) increases progressively with rising temperature and duration. At 1400 ℃, the oxide layer thickness reached a maximum of about 8 μm after 48 hours. The addition of a BN interface to SiC demonstrates superior oxidation resistance at 1400 ℃ when compared to pure SiC. The BN interface initially acts as an oxidation barrier in dry environments, enhancing the durability of the composite. However, in high-temperature and humid environments, it transforms into a fragile glassy phase, weakening fiber strength and further accelerating composite degradation under cyclic stress. Zok *et al.* [135] observed that the BN interface reacts with steam in high-temperature vapor environments, and energy-dispersive X-ray spectroscopy (EDS) mapping showed elliptical characteristics at the interface (refer to Figure 11d). The absence of significant EDS signals for this feature confirms it as a pore. The resulting borate, in conjunction with silica on the fibers, forms a non-protective molten glass, which reduces fiber strength and accelerates the material's overall degradation. Guo *et al.* [136] investigated the transition from BN-SiC interface/fiber separation mode to BN-SiC interface/matrix separation mode at high temperatures. In the BN-SiC interface/fiber separation mode, cracks propagate between the interface and fiber, causing stress to act directly on the fiber. In the SiC interface/matrix separation mode, cracks propagate along

the BN-SiC interface and matrix, and the difference between the two separation modes can be seen directly in Figure 11e.

Cui *et al.* [137] conducted further research on the BN/SiC multilayer interface, revealing that microstructural changes induced by oxidation have a considerable effect on the damage process of the composites, especially at elevated temperatures (1100 °C and 1400 °C). The deterioration of the BN interface causes a delay in fiber fracture, and the bending strength and modulus are temperature-sensitive, decreasing as oxidation temperature increases (Figure 11f). Wang *et al.* [138] investigated the oxidation behavior of multilayer PyC interface composites, finding that the PyC interface is fully consumed at higher temperatures, leading to a decline in mechanical performance. Nevertheless, at a temperature of 900 °C, the material displays self-healing properties, as the thin PyC layer is rapidly closed off by a growing silicon layer at high temperatures, which restricts oxidation damage. This self-healing effect, however, is limited to areas near the outer surface.

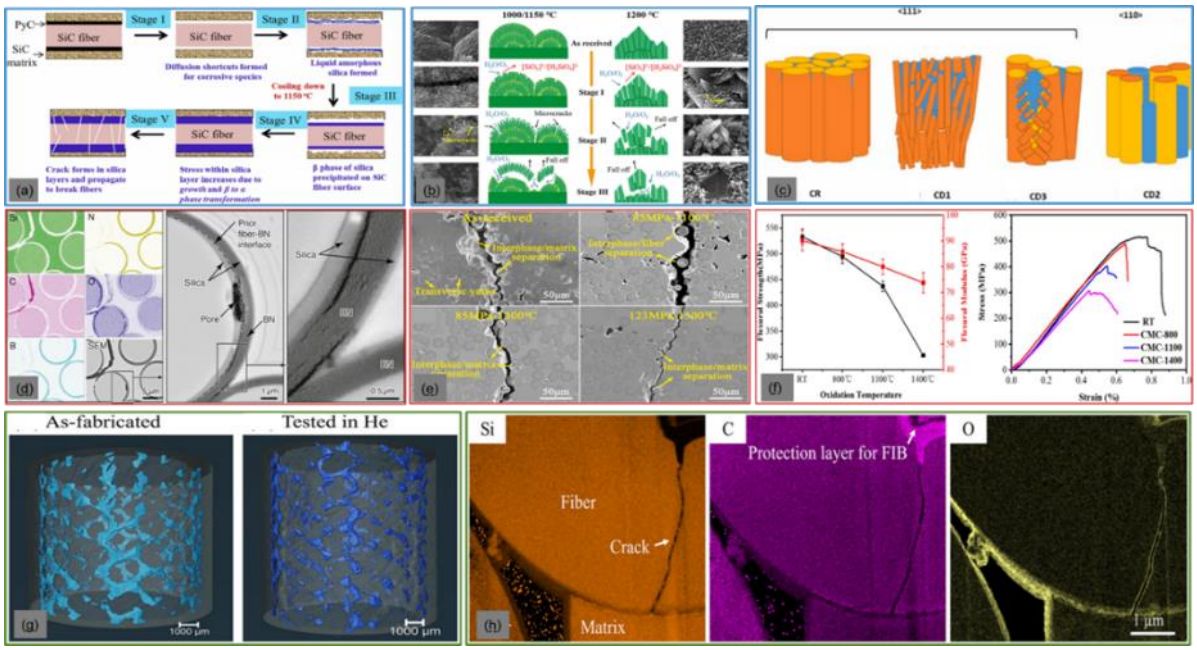

Figure 11. Analysis of structural degradation and surface morphology in high-temperature corrosion environments: (a) Schematic of SiC_f/SiC composite degradation mechanism under mixed water vapor and oxygen corrosion at 1300 °C [139]; Reprinted with permission. Copyright 2022, Elsevier. (b) Corrosion mechanisms of SiC coatings deposited at various temperatures over corrosion time [132]; Reprinted with permission. Copyright 2021, Elsevier. (c) Lattice structure of cubic SiC and corrosion mechanism [133]; Reprinted with permission. Copyright 2024, Elsevier. (d) EDS mapping confirms silica scales on fibers and matrix, and pores at the fiber-BN interface [135]; Reprinted with permission. Copyright 2019, John Wiley and Sons. (e) Crack morphology of untreated SiC_f/SiC [136]; Reprinted with permission. Copyright 2024, Elsevier. (f) Crack morphology of untreated SiC_f/SiC [137]; Reprinted with permission. Copyright 2021, Elsevier. (g) X-ray computed tomography of SiC_f/SiC composite tubes [140]; Reprinted with permission. Copyright 2022, John Wiley and Sons. (h) STEM-EDS maps of SiC_f/SiC composite tube tested in steam [140].

Luan *et al.* [141] incorporated polymer-derived SiBCN ceramics (PDC SiBCN) as a self-repairing component into SiC fiber-reinforced SiC, discovering that it effectively protects the fibers and interfaces

from oxidative damage in humid oxygen conditions. Koyanagi *et al.* [140] reported the experimental results of SiC_f/SiC composite tubes undergoing stress rupture tests in a steam environment at 1000 ℃. Experimental results indicated that the rupture time of the composite materials in a steam environment was between 400 and 1300 seconds, whereas in an inert gas environment, 75% of the samples did not rupture for more than 8500 seconds. Analysis of the microstructure reveals that the cracking of fiber bundle areas and fiber pullout due to the steam environment are the main factors leading to the failure of the composite materials in high-temperature conditions. These experimental findings are crucial for assessing the cladding performance of SiC_f/SiC composite materials in the context of nuclear reactor accident scenarios.

In the research on corrosion resistance of SiCf/SiC composites, Westinghouse and Oak Ridge National Laboratory in the United States jointly carried out the research on high-performance fuel cladding materials for the fourth generation nuclear energy system, and developed a multi-layer SiCf/SiC composite cladding tube, providing a new design scheme for improving its performance in extreme environments [142].

Koyanagi *et al.* [143] investigated the critical degradation mechanisms of multilayer SiC fiber-reinforced SiC matrix composites in environments associated with loss-of-coolant accidents in light water reactors. The experiment involved mechanical testing of SiC composite tubes in steam and inert environments at 1000 ℃. It was found that exposure to the steam environment caused embrittlement of the SiC composite tubes when subjected to lower tensile loads. Furthermore, Kim and Terrani *et al.* [129,144] explored the hydrothermal corrosion characteristics of multilayer SiC composite tubes under various microstructural conditions in a simulated pressurized water reactor (PWR) environment. According to Kim *et al.* [144], the Tyranno SA3 SiC fibers and single-crystal SiC deposited at 1200 ℃ demonstrated superior corrosion resistance owing to their well-defined crystal structure. In contrast, the SiC phase deposited at 1000 ℃ underwent significant dissolution in water, particularly at the grain boundaries where an amorphous SiC phase developed. The presence of dissolved hydrogen did not notably enhance the hydrothermal corrosion resistance of the SiC phase containing amorphous SiC in the CVI process, leading to substantial weight loss and a reduction in the hoop strength of the multilayer SiC composite tubes following corrosion. In the course of corrosion, defects in the crystal structure and the presence of impurity elements in SiC have a substantial impact on its corrosion resistance. The research by Terrani *et al.* [129] indicated that, as seen in the curve of Figure 12e, the samples suffered substantial weight loss in static water, showing a linear trend. The dissolution of SiC's grain boundaries occurred preferentially, resulting in a characteristic columnar structure, while the corrosion products, SiC_xO_y and SiO_2, were found to be amorphous and readily soluble in water, which ultimately caused a decrease in sample mass.

In relation to this oxidation behavior, Tan *et al.* [145] categorized the process into the following three stages: (I) Oxygen quickly interacts with the surface of the material, leading to the formation of a continuous oxide layer and an increase in the material's weight. (II) With the increasing thickness of the oxide layer, the diffusion of oxygen becomes restricted, causing some volatile substances to directly enter the atmosphere, which leads to a reduction in the material's weight. (III) Oxygen continues to diffuse through the oxide layer, reacting with materials close to the surface, leading to the ongoing volatilization of substances and a logarithmic correlation in the weight variation of the material.

At present, enhancing SiC's corrosion resistance can be achieved through two primary methods: first, by optimizing conventional fabrication techniques to improve the density, crystallinity, and purity

of SiC; second, by applying environmental barrier coatings onto the surface of SiC. Studies indicate that the stability and corrosion resistance of SiC_f/SiC composite materials in harsh environments are significantly influenced by the design and implementation of environmental barrier coatings (EBCs). Among the systems for protecting SiC from oxidation, iridium (Ir) is the most effective, as Ir coatings exhibit exceptional oxidation resistance in high-temperature oxidative environments [146]. Li *et al.* conducted a series of studies [15,147,148] to examine the protective effects of a three-layer EBC applied via plasma spraying on SiC_f/SiC composite materials. The schematic diagram of the EBC is shown in Figure 12b. They found that at the LMA-YbMS interface of Yb_2SiO_5 and $LaMgAl_{11}O_{19}$ coatings in a 1300 ℃ high-temperature steam environment, atomic interdiffusion leads to the formation of a new $Yb_3Al_5O_{12}$ layer, as shown in Figure 12c. Nonetheless, the failure of these coatings is mainly due to thermal mismatch stresses and the development of thermally grown oxide (TGO), as illustrated in Figure 12d. To address these issues, Garcia *et al.* [149] developed a $Yb_2Si_2O_7$-Yb_2SiO_5 composite EBC using plasma spraying, which exhibited strong crack healing capabilities and thermal mechanical stability at 1200 ℃, indicating that the coating can effectively maintain gas impermeability in high-temperature environments.

In optimizing the coating structure and interface materials, the research by Mainzer *et al.* [150] demonstrates that the combination of Si-BN/SiC/PyC fiber coatings and LSI processes significantly improves the flexural strength and damage resistance of the composite materials. Simultaneously, Hu *et al.* [151] investigated the oxidation resistance of annealed SiC_f/SiC composites under LMA/YbDS T/EBCs coatings, finding that the coated system after annealing exhibited a higher strength retention rate after oxidation at 1350 ℃, demonstrating superior high-temperature protection. However, despite significant advances in coating design and material optimization for improving the performance of SiC_f/SiC composites, the failure mechanisms of the coatings remain a key area of research. This finding underscores the importance of the hydrothermal corrosion model proposed by Seshadri *et al.* [152], which experimentally incorporates more influencing factors such as flow rate, resistivity, pH, and surface roughness, suggesting a bilayer metal coating as a mitigation strategy and validating its protective effect against SiC dissolution.

Additionally, the stability of coatings in extreme environments should not be overlooked. Zhong *et al.* [153] conducted a study on three-layer coatings applied to SiC-based composites using atmospheric plasma spraying technology, finding that these coatings retained excellent adhesion and crack resistance after 40–50 thermal shock cycles at 1350 ℃. The extensive plastic deformation of $Yb_2Si_2O_7$ coating, such as twinning and dislocations, significantly enhances the crack propagation resistance of the coating. Finally, Wang *et al.* [154] investigated the performance of BSAS-based environmental barrier coatings in gas environments, demonstrating that this coating can effectively protect the SiC matrix at 1200 ℃, significantly enhancing the oxidation and corrosion resistance of the composite material, showcasing its great potential for applications in extreme environments. These investigations offer essential data backing for the advancement of high-performance SiC_f/SiC composites, establishing a robust basis for their use in nuclear reactors, aerospace, and related domains.

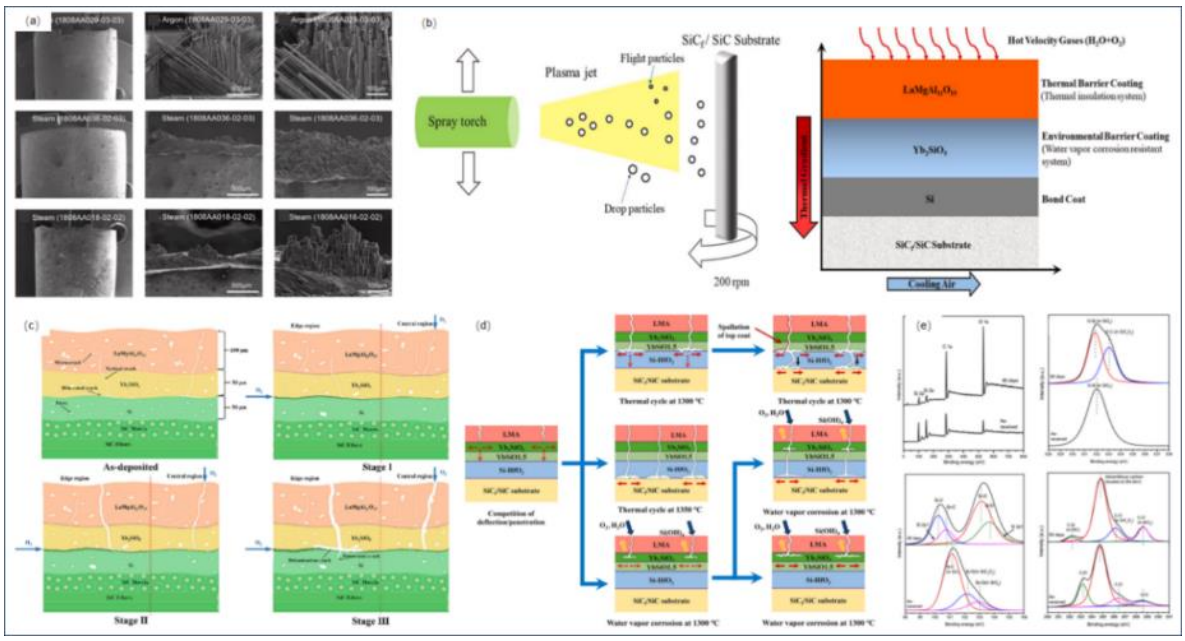

Figure 12. Environmental Barrier Coating: (a) Secondary electron micrographs of fractured SiC_f/SiC composite pipes in a steam environment [143]; Reprinted with permission. Copyright 2024, Elsevier. (b) Deposition process for plasma-sprayed coating and schematic of tri-layer Si/Yb_2SiO_5/$LaMgAl_{11}O_{19}$ on SiC_f/SiC substrate [15]; (c) Schematic of crack development in tri-layer Si/YbMS/LMA under as-deposited and isothermal oxidation at 1300 °C [147]; Reprinted with permission. Copyright 2023, Elsevier. (d) Evolution schematic of failure mechanisms for multi-layer HfO_2-Si/$YbSi_{1.5}$/Yb_2SiO_5/LMA EBCs under high-temperature testing [148]; Reprinted with permission. Copyright 2022, Elsevier. (e) XPS analysis of SiC_f/SiC composite surfaces, as-received and post-60-day corrosion [130]. Reprinted with permission. Copyright 2018, Elsevier.

4. Numerical simulation

To overcome the economic challenges in the design and manufacturing of SiC_f/SiC composites, it is crucial to develop finite element numerical models capable of accurately predicting their mechanical behavior. Such models can simulate the entire process from initial damage to final failure of the composite and validate their accuracy through experimental comparison, thereby optimizing manufacturing processes and reducing costs. In recent years, advances in micromechanical testing techniques have facilitated progress in studying the micrometric parameters of SiC_f/SiC [155]. However, some critical parameters remain challenging to obtain using current methods, affecting the precise calculation of macroscopic mechanical properties [156–158]. Therefore, reliable numerical models have become essential to compensate for the limitations of micro-parameter data in predicting overall mechanical performance.

With the increasing demand for automation, complex forming processes such as weaving and winding have been widely applied in the fabrication of SiC_f/SiC composites. Especially under complex loading conditions, the components produced by these processes exhibit significant differences in mechanical properties compared to traditional laminated structures due to their unique mesostructure. In advanced nuclear energy systems, the forming processes for SiC_f/SiC composite cladding tubular

preforms are mainly divided into winding and weaving, as shown in Figures 13a,b. Factors influencing the macroscopic performance of the final components include, but are not limited to, the intrinsic properties of the matrix and fibers, interfacial bonding strength [159], fiber orientation, fiber volume fraction [160], fiber spatial distribution, porosity [161], and the overlap patterns of the fibers.

The complex interplay of these factors determines the performance of SiC_f/SiC composites in practical applications, thus necessitating in-depth research to optimize their design and manufacturing processes.

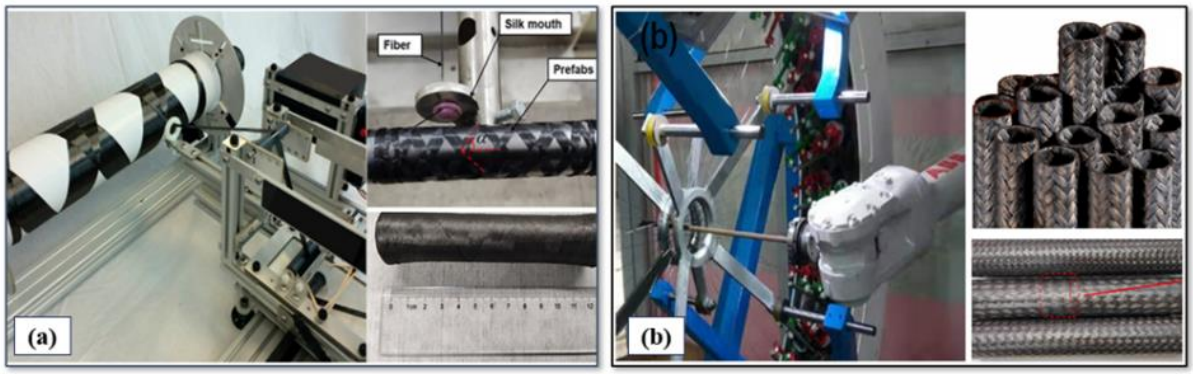

Figure 13. Forming processes for SiC_f/SiC composite cladding tubular preforms: (a) winding equipment and wound tube [162]; (b) weaving equipment and woven tube [163].

4.1. Multiscale simulation

In recent years, a multiscale mechanical analysis method aimed at acquiring micromechanical parameters has provided a reference for the finite element computational analysis of composite components influenced by complex microstructures. This method assumes that the matrix is homogeneous and isotropic, while the fiber tows are anisotropic, with micromechanical parameters obtained through micro RVE modeling [164,165], as shown in Figure 14a. This method uses the single-layer mechanical properties obtained from the micro RVE model as input parameters for macromechanical performance simulation, thereby enabling the multiscale finite element numerical simulation where parameters are transferred from the micro to meso and finally to the macro level. To further investigate the multiscale nonlinear mechanical properties and damage failure behavior of the composites, three-dimensional RVE models [166] and RVE RVC models that consider pore defects have been further developed [167,168], as shown in Figure 14b,c.

Based on the representative volume element (RVE) model, many researchers have conducted in-depth multiscale studies on SiC_f/SiC materials. Gao *et al.* [169] simulated the micro-scale crack propagation and deflection in SiC_f/SiC composites with weak interfaces using a phase field method combined with a single fiber RVE model, revealing the toughening mechanisms of crack propagation in SiC_f/SiC ceramic composites, including fiber pull-out, crack deflection, and interfacial debonding. Wang *et al.* [170] developed an RVE model featuring cracks, grounded in a multicomponent damage constitutive model for two-dimensional SiC_f/SiC composites. They predicted the impact of factors such as SiC fiber volume fraction, porosity, and SiC matrix microcrack density on the deformation and

damage behavior of these composites. Utilizing the failure envelopes derived from these micro-meso features, they constructed a data-driven failure model for ceramic composites.

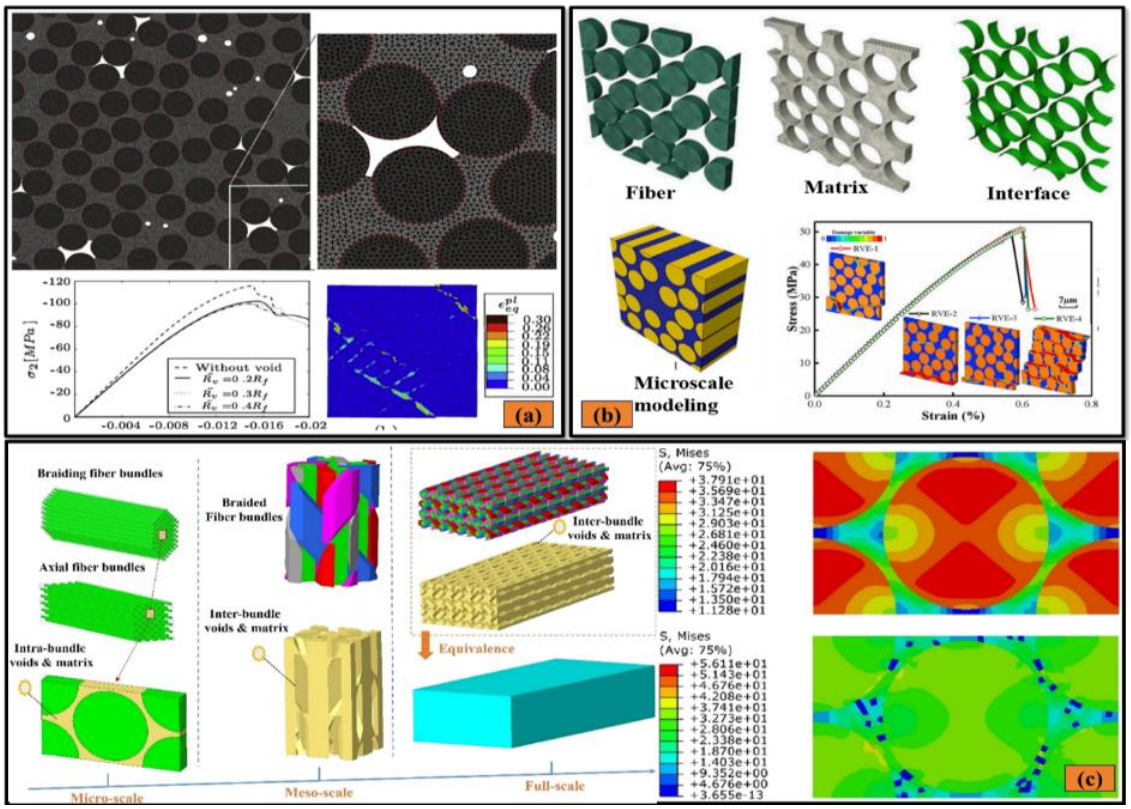

Figure 14. Microscopic Models: (a) 2D RVE [164]; Reprinted with permission. Copyright 2014, Elsevier. (b) 3D RVE [166]; Reprinted with permission. Copyright 2019, Elsevier. (c) RVE and RVC models [168]. Reprinted with permission. Copyright 2020, Elsevier.

To accurately describe the mechanical and damage behavior of SiC_f/SiC composites at the micro, meso, and macro scales, Shi *et al.* [171] constructed a piecewise damage model through a multilevel experimental approach. The model can accurately predict the mechanical properties, deformation, and stress field distribution of SiC_f/SiC composites under different loading conditions, and effectively simulate their damage evolution process. Zhang *et al.* [172] constructed macro and mesoscopic finite element models for the damage process and mechanisms of Mo-SiC_f/SiC heterogeneous composite tubes, discovering that microcracks originate from pores on the outer side of the SiC_f/SiC layer and propagate along the fiber bundle boundaries. Simultaneously, due to the periodic pore distribution, the SiC_f/SiC layer exhibited "bamboo joint" damage during the C-ring tests. The research indicates that before the formation of major cracks in the SiC_f/SiC layer, the Mo layer remains intact, suggesting that the Mo-SiC_f/SiC cladding can maintain gas tightness and structural integrity until complete failure of the sample, with the damage process divided into five stages.

While the application of the RVE model provides an effective tool for predicting the performance of SiC_f/SiC composite cladding at the microscale, achieving cross-scale research from micro to macro still requires precise and efficient macroscopic three-dimensional models. To perform accurate numerical analysis of the mechanical behavior of SiC_f/SiC composite cladding tubes, it is essential to establish a numerical analysis model that aligns with actual conditions. However, due to the complex geometric

positioning of the woven and wound fibers within the ceramic matrix, accurately modeling the matrix is quite challenging. Even with continuous modeling, the quality of subsequent mesh generation is often suboptimal. Considering the computational time costs, existing analytical models frequently utilize laminated plate models for mechanical performance analysis; however, these models typically do not account for the impact of the actual mesostructure (such as fiber weaving and winding) on the macromechanical performance of the components. Compared to fiber-resin system composites, the material property design standards for SiC_f/SiC composites are not yet mature and lack reliable micromechanical analysis methods validated by extensive computational data comparisons [173], indicating that the standards for assessing their mechanical properties require further refinement.

To address these issues, many researchers have made significant efforts in constructing accurate and realistic macroscopic three-dimensional models. In the modeling of woven composites, Feng *et al.* [163] proposed a multiscale modeling method for SiC_f/SiC nuclear fuel cladding tubes based on finite element simulations of the weaving process. By integrating the matrix mesh and fiber mesh through embedded region constraints, they successfully avoided the difficulties associated with mesh generation, as shown in Figure 15a. Subsequently, mechanical parameters from the microscale RVE model were used for multiscale finite element simulations, ensuring morphological consistency from the micro to macro scale. The response curves under complex loading conditions (tensile and torsional) were highly consistent with experimental data, validating the model's accuracy in multiscale prediction. Wu *et al.* [174] built an axially graded woven composite model, which demonstrated high consistency with the actual material in both morphology and physical property inputs. The simulated load-displacement curves and failure morphology showed strong agreement with experimental results, confirming the model's reliability. Additionally, the researchers investigated the tensile failure evolution patterns by constructing a three-dimensional woven tubular model with pores [175], as shown in Figure 15c. For the failure behavior of the 2.5D SiC_f/SiC thickened dovetail joint structure under tensile loading [176], the researchers constructed a joint model that reflects its true structure, as shown in Figure 15e. Tang *et al.* [162] developed a three-dimensional yarn path modeling method based on computational geometry, constructing the model according to the actual fabrication process of the material. This approach ensured high consistency in morphology from the macro to the meso scale with actual SiC_f/SiC composites. The model's input parameters were directly derived from the material's real properties, and comparisons between the simulation results and experimental data validated its accuracy in predicting mechanical behavior. Additionally, this model overcomes the drawback of traditional laminated models that ignore yarn overlapping effects, as shown in Figure 15b. Based on the three-dimensional winding model, Pu *et al.* [177] investigated the effect of winding angle on the axial tensile damage of SiC_f/SiC cladding tubes, while Yan *et al.*[178] studied the failure modes and crack initiation mechanisms of SiC_f/SiC cladding tubes under radial loading, as shown in Figure 15d. Additionally, some studies have constructed a realistic three-dimensional finite element model of SiC_f/SiC materials using experimental CT scans and computer tomography images, utilizing CT images to investigate the initiation of damage and crack propagation [179,180], as shown in Figure 15f.

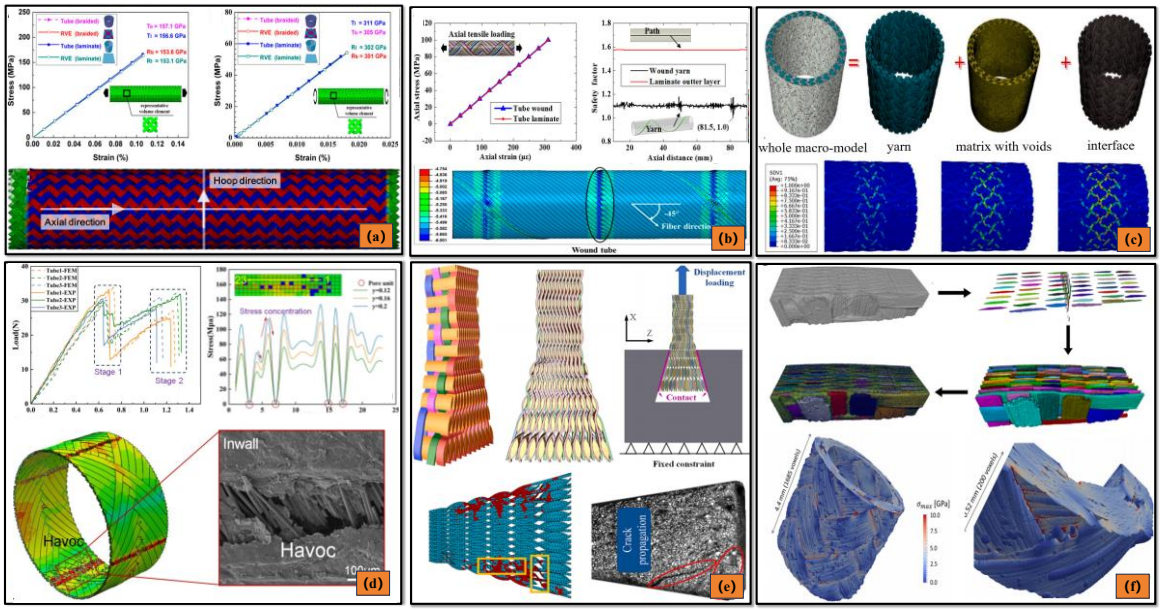

Figure 15. The models of SiC_f/SiC composites: (a) Stress-strain curves and macroscopic models [163]; (b) Axial stress-strain curves and macroscopic braiding models [162]; (c) Macroscopic model with cracks [175]; Reprinted with permission. Copyright 2023, Elsevier. (d) Damage evolution mechanism [178]; (e) Dovetail joint structure model [176]; Reprinted with permission. Copyright 2024, Elsevier. (f) CT image scanning [179,180]. [179] Reprinted with permission. Copyright 2019, Elsevier. [180] Reprinted with permission. Copyright 2017, Elsevier.

Finite element simulation is an effective tool for reducing the manufacturing costs of SiC_f/SiC composites and shortening the development cycle. The key to achieving effective finite element simulation lies in considering the impact of micromechanical parameters on macromechanical performance. Employing a multiscale numerical analysis approach, linking micro parameters with macromechanical performance, enhances the accuracy and reliability of the calculations. However, the current system for evaluating the mechanical performance of SiC_f/SiC composite components using finite element numerical simulations is still not well-developed, requiring further exploration by more researchers to establish a complete and unified set of evaluation standards. While it is true that multiscale FEA models that incorporate irradiation defect evolution are still under development, FEA for nuclear applications is an active research area.

There are various types of interphases in SiC/SiC composites, among which the pyrolytic carbon (PyC) interphase is considered the optimal interphase material for SiC/SiC composites. This is because PyC not only possesses excellent anisotropic mechanical properties and microstructure but also effectively protects the fibers during processing [181]. Currently, research on SiC/SiC interphase materials primarily focuses on experimental methods [182–188]. Due to the high cost of materials and time in experiments, molecular dynamics (MD) simulations are gradually becoming an important approach for studying the behavior of SiC/SiC interfaces.

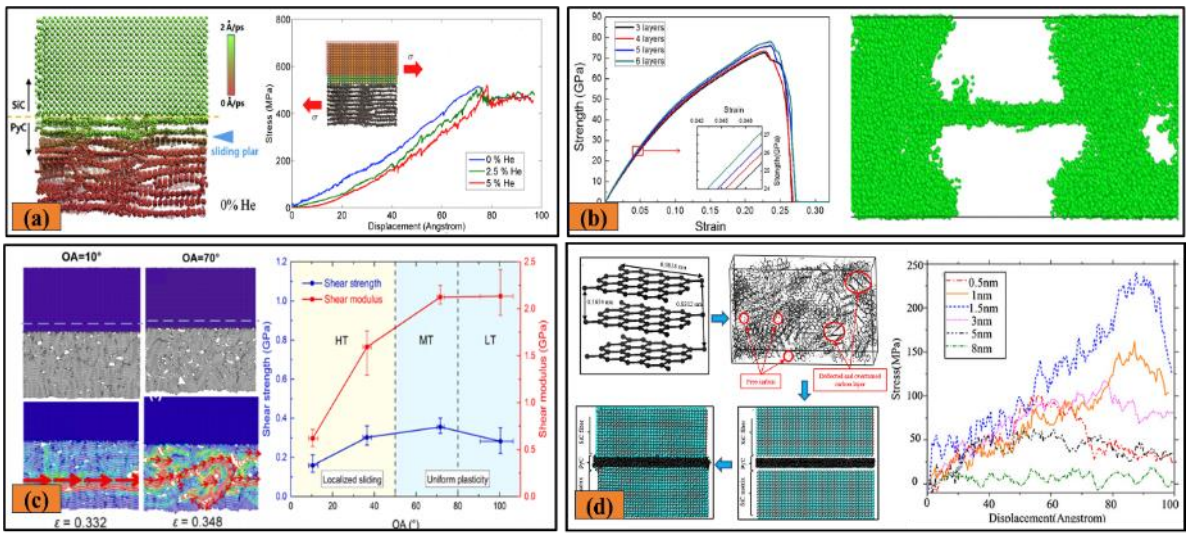

Figure 16. Molecular Dynamics Simulations: (a) Study of temperature and interfacial strength of SiC composites [189]; Reprinted with permission. Copyright 2016, Elsevier. (b) SiC/Graphene simulation [190]; Reprinted with permission. Copyright 2017, Elsevier. (c) OA modeling method [191]; Reprinted with permission. Copyright 2023, Elsevier. (d) SiC/PyC/SiC interface simulation [192].

Jin *et al.* [189] employed molecular dynamics (MD) simulations to investigate the relationship between temperature and interfacial strength in SiC composites, as illustrated in Figure 16a. However, these models are based on two-dimensional structures observed via transmission electron microscopy (TEM) and fail to capture the three-dimensional disordered structure of the PyC interphase. Zhan *et al.* [190] simulated the tensile behavior of SiC/Graphene composites using LAMMPS software and discovered that when graphene sheets are in contact with the SiC (1 1 1) surface, interfacial interactions are enhanced, inhibiting tensile deformation, as shown in Figure 16b. Wang *et al.* [193] evaluated the damage behavior of cracked SiC/PyC interfaces using MD simulations and validated the findings through a multiscale finite element model. The results indicate that the disordered structure of the PyC interface exhibits a complex shear mechanism during the shearing process, including relative sliding of carbon layers, collision and compression, and bending or folding deformation. These mechanisms enhance the overall shear strength of the structure. To further investigate the intrinsic mechanisms of the SiC/PyC interface under shear load, Wang *et al.* [191] adopted a new OA (Orientation Angle) directional modeling method, as shown in Figure 16c. The study found that the characteristic mass of PyC is closely related to shear strength. As the OA increases, the interfacial shear deformation behavior shifts from localized penetration sliding to large-scale uniform plasticity. Additionally, the mechanism behind the reduced shear resistance of PyC was revealed by incorporating amorphous carbon (a-C) components into PyC. Niu *et al.* [192] discovered through molecular dynamics simulations that due to the disordered structure of the PyC interface, the carbon layers undergo non-planar shearing, overlapping, flipping, and deflection during the shearing process, which increases the shear strength of the composite. The study indicates that when the strength of the PyC interface is less than the bonding strength between the fiber and the matrix, failure is primarily caused by internal damage within the PyC interface. However, when the PyC interface strength exceeds the bonding strength with the fiber or matrix, failure occurs due to debonding between the PyC interface and the fiber or matrix, as shown in Figure 16d.

4.2. Artificial intelligence

As global attention to the nuclear power industry continues to grow, there is particular focus on key aspects such as the lifespan and operational efficiency of existing nuclear reactors [194]. SiC_f/SiC composites, as the primary candidate material for fuel cladding containers, have garnered significant attention due to their outstanding mechanical properties, thermal performance, and resistance to corrosion and radiation. Under harsh conditions such as high temperatures, severe corrosion, and high-flux neutron irradiation, SiC_f/SiC composites demonstrate excellent stability and reliability. They effectively prevent the escape of fission products, protect the fuel pellets from coolant corrosion, and ensure the timely conduction of fission heat. Therefore, SiC_f/SiC composites are regarded as a crucial barrier to ensuring the safe operation of reactors, playing a key role in enhancing the safety and efficiency of nuclear reactors.

However, despite the promising prospects of SiC_f/SiC composites as nuclear fuel cladding, their complex fiber/matrix/interface interactions present numerous challenges. Issues such as material densification, pipe forming technologies, and interface performance optimization still require further breakthroughs. Meanwhile, with the rapid advancement of technology, AI techniques such as deep learning, image recognition, and data-driven approaches are being increasingly applied across various disciplines. Particularly in the field of materials research and applications, these technologies are gaining significant importance. In response to this trend, the U.S. Nuclear Regulatory Commission (NRC) advocates the introduction of Digital Twin (DT) technology in the nuclear field as an important direction for future research. According to NRC studies, the digital transformation of nuclear power plants is expected to bring various benefits, including improved operational efficiency, enhanced safety and reliability, reduced human errors, faster information transfer, and increased predictive capabilities. However, Digital Twin technology remains a novel concept in the nuclear field, and the current stage of development is primarily focused on defining objectives and identifying technical challenges that need to be addressed.

In recent years, various advanced technologies beyond DT have gained widespread attention from researchers, with machine learning (ML)-based data-driven approaches and precise segmentation and recognition techniques for large-scale images standing out in particular. The core of these technologies lies in combining advanced AI algorithms with multiscale research methods, while relying on microscopic structure images generated by high-precision morphology capture devices. This marks a significant turning point in materials science research, particularly in the field of resin-based composites. With the swift advancement of AI algorithms and the extensive accessibility of large databases, models based on artificial neural networks (ANN) have emerged as a significant research focus due to their outstanding capabilities in managing multi-parameter prediction and optimization in high-dimensional spaces [195,196]. However, many challenges remain when integrating these advanced algorithms with traditional multiscale modeling methods. For example, effectively integrating models at different scales in the context of large-scale datasets to form a comprehensive understanding of complex material behavior remains a bottleneck in current research (see Figure 17a).

As the application scope of ANN models (see Figure 17b,c) continues to expand, they have evolved from initially being used for performance prediction based on experimental data to employing data augmentation techniques as a substitute for traditional constitutive modeling, thereby accelerating the

multiscale modeling process [197]. This evolution has not only enhanced the predictive capabilities of models but also provided researchers with more efficient tools to explore the complex mechanical properties of materials. Nevertheless, these models may exhibit limitations in certain cases, such as in the study of woven composites. In particular, when the database sample size is relatively small, the predictive accuracy of the models is often unsatisfactory [198,199]. To address these challenges, Li *et al.* [200] proposed an ANN-based homogenization model in their study of woven composites. This model utilizes ANN to accurately predict the stress-strain behavior of materials under various loading conditions by analyzing the microstructure of the composite in detail (see Figure 17d–k). Specifically, the model's input features include key microstructural information such as fiber volume fraction, fiber orientation angle, matrix material properties, and loading conditions, selected based on an in-depth understanding of the composite's micromechanical behavior. During training, the ANN model captures the material's complex nonlinear response through a combination of multilayer network structures and nonlinear activation functions. Results indicate that this model not only accurately predicts the mechanical properties of composites with varying fiber volume fractions and orientations but also surpasses traditional finite element methods in computational efficiency and accuracy. This superiority mainly stems from the ANN model's efficient exploration and fitting capability within the parameter space, allowing it to achieve high prediction accuracy even with small datasets, thus avoiding the large computational costs and lengthy processing times associated with traditional finite element methods. Additionally, the flexibility of the ANN model makes it applicable to various material design and performance optimization scenarios, enabling quick adaptation to different material structures and process conditions.

This finding opens new avenues for future composite research, particularly in the fields of material design and performance optimization, where the ANN model demonstrates great potential and application prospects. With further optimization of the neural network architecture and training strategy, this model is expected to be applied more broadly in composite applications, providing a reliable tool for efficient and accurate mechanical property prediction.

Over the past decade, researchers have devoted significant effort to characterizing the damage and fracture of CMCs. As a result, accurately identifying and quantifying the initiation and propagation of cracks during loading has become a critical research topic. This research demand has led to an urgent need for precise and efficient image segmentation methods [201]. With the rapid advancement of ML technologies, particularly the remarkable performance of its branch, deep learning, in image recognition, more and more studies have begun applying these techniques to the characterization and analysis of CMCs. Zhang *et al.* [202], using a deep learning-based image segmentation method (see Figure 18a–e), successfully identified matrix cracking and fiber pull-out phenomena in CMCs (see Figure 18f), which further enabled the exploration of the changes in the volume and volume fraction of transverse matrix cracks under different loading levels. This method provides a new approach to studying crack behavior, contributing to a deeper understanding of the damage mechanisms in materials. Additionally, Zhang *et al.* [203] applied the Deeplab v3+ neural network to track the evolution of microcracks in CMCs under high-temperature conditions, demonstrating the powerful potential of deep learning technology in analyzing material behavior in complex high-temperature environments. Similarly, Ai *et al.* [204] conducted a 3D reconstruction of plain-woven C/SiC composites (see Figure 18g), using a deep learning-based identification method to separate the fiber and matrix phases from CMC CT images.

They further explored the damage and failure characteristics of the material through image-driven finite element simulations (see Figure 18i–h). The above studies indicate that deep learning methods not only demonstrate outstanding application results in resin-based composites but also play a crucial role in the characterization and modeling of ceramic matrix composites. The application of this technology has provided new tools for materials science, greatly advancing the in-depth study of CMC damage and fracture behavior.

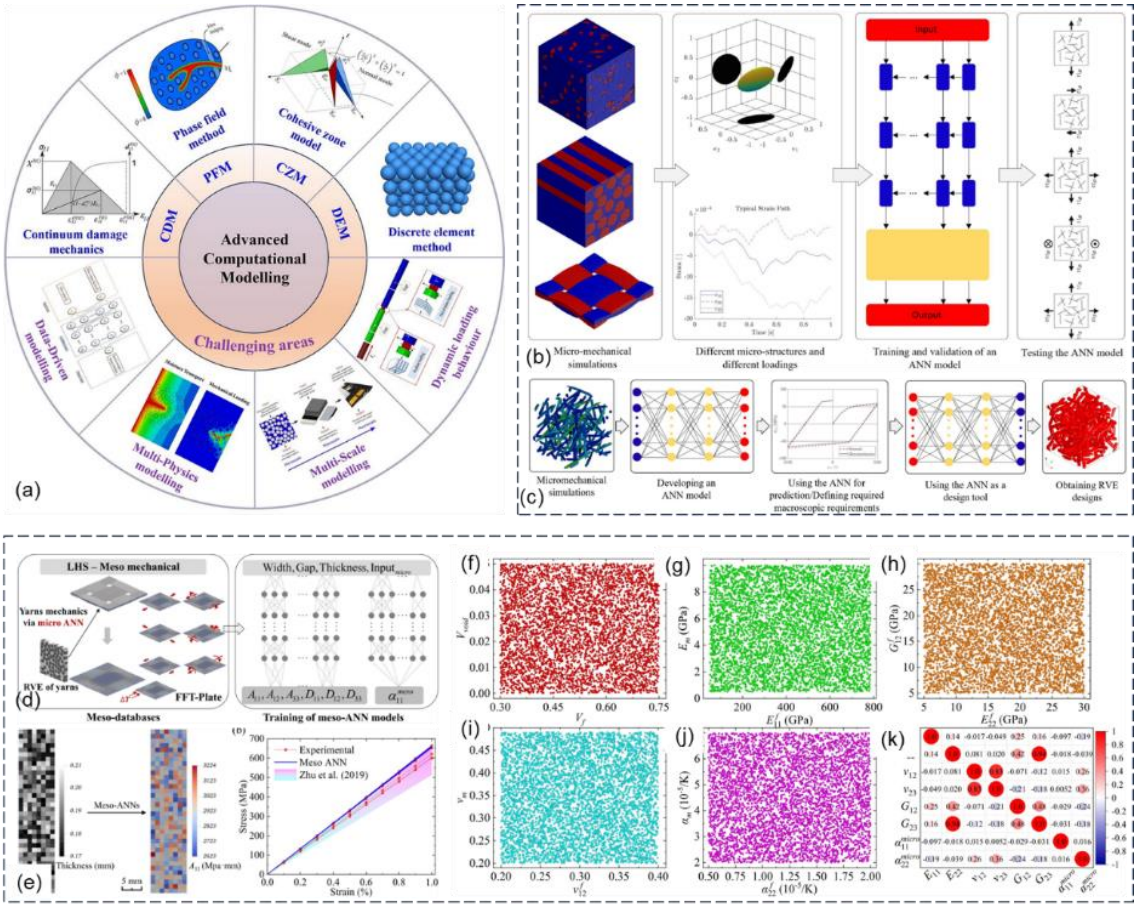

Figure 17. Applications of ANN models in fiber-reinforced composites: (a) The research model and multiscale evolution [195]; (b) Schematic of ANN model development for composites based on micromechanics [197]; (c) Schematic of composite design using ANN [197]; (d) Mesoscale homogenization ANN model [200]; Reprinted with permission. Copyright 2024, Elsevier. (e) Randomly distributed macrolaminate model and experimental validation [200]; (f–j) Data sampling distribution for the micro-homogenization ANN model [200]; (k) Pearson correlation coefficients of output features [200].

Deep learning has promising applications in CMC research, but it also faces certain limitations. First, model training relies on large amounts of labeled data, yet obtaining high-quality CMC image data is challenging. Secondly, the “black box” nature of deep learning models makes results difficult to interpret, which poses a challenge in the high-safety-requirement field of CMCs. Moreover, deep learning requires high computational power, and the cost of processing high-resolution images is considerable; further optimization is also needed for multi-scale damage feature extraction and

generalization to complex environments. These factors somewhat limit the comprehensive application of deep learning in the field of CMCs.

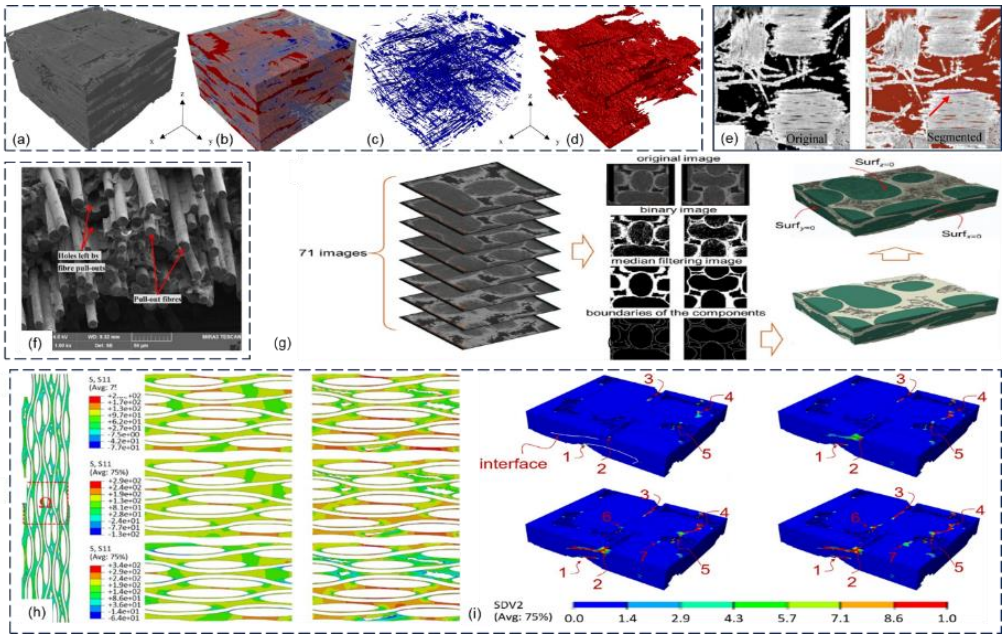

Figure 18. Applications of deep learning and image recognition in the field of CMCs: (a–d) Mesoscale structure of plain-woven SiC_f/SiC composites from CT image reconstruction and segmentation, showing micropores and voids [202]; Reprinted with permission. Copyright 2021, Elsevier. (e) Deep learning-based segmentation results [202]; (f) SEM of fractured fiber bundles [202]; (g) 3D reconstruction of plain-woven C/SiC composites [204]; Reprinted with permission. Copyright 2021, Elsevier. (h) S_{11} evolution in CVI-SiC matrix under load [204]; (i) Damage progression in 3D C/SiC composites under load [204].

In composite material research, failure morphologies such as damage and defects typically occur at the microscopic level, making them difficult to capture through conventional methods. To overcome this challenge, optical microscopy [205] and scanning electron microscopy (SEM) [206], with their high spatial resolution, have gradually become the preferred tools for researchers to observe damage and failures in composites. These microscopy techniques provide high-quality microscopic images, offering crucial support for materials science research. Meanwhile, to further address the complexities of internal damage in materials, X-ray micro-computed tomography (μ-CT) technology has been widely applied in the analysis of the microstructure of composites [207], as shown in Figure 19a.

X-ray CT technology performs layer-by-layer scanning of material samples to obtain 2D tomographic images, which are then used to reconstruct a 3D volume model, providing precise spatial information of the internal microstructure in a non-destructive manner. However, despite the increasingly widespread application of various X-ray CT techniques in carbon fiber-reinforced polymer (CFRP) composites, accurately characterizing damage in X-ray tomographic images is not always easy to achieve. This is mainly due to the similar X-ray absorption coefficients of carbon fibers and most polymer resins, making it difficult to produce clear phase-contrast imaging [208].

To address this issue, researchers have begun exploring deep learning-based image recognition methods to improve the accuracy of damage characterization in composites [209–211]. Especially with the rise of advanced in-situ experimental equipment (as shown in Figure 19b), researchers are now able to monitor the damage evolution process of materials in real-time during loading. Wang *et al.* [212] systematically characterized the damage evolution of fiber-reinforced composites using in-situ X-ray CT, deep learning, and digital volume correlation (DVC) techniques. During continuous loading, they used a U-Net image segmentation model to accurately identify the microstructure and damage of the material (as shown in Figure 19c), while DVC was employed to analyze the three-dimensional deformation field, providing a more comprehensive damage analysis (as shown in Figure 19d). These research findings demonstrate that combining advanced imaging techniques with deep learning methods not only overcomes the limitations of traditional approaches but also provides novel solutions for damage analysis in composites, further advancing research in this field.

In recent years, with the continuous advancement of modern observational equipment, scholars have conducted a series of in-depth studies on SiC ceramic matrix composites, particularly making significant progress in understanding internal microcracks and porosity characteristics [213–215]. To gain a more comprehensive understanding of microcrack evolution, researchers have built upon traditional image segmentation algorithms, such as grayscale thresholding and region growing, by utilizing advanced image segmentation tools to extract microcrack features and perform quantitative analysis [216,217]. The application of these methods has provided valuable data to uncover the internal damage mechanisms of materials.

DVC technology, as a three-dimensional extension of digital image correlation (DIC), is designed to measure the 3D deformation of materials and provide key evidence for the study of damage mechanisms. Notably, Mazars and Forna-Kreutzer *et al.* successfully achieved quantitative characterization of internal microcracks in CMCs through a segmentation procedure of DVC residuals [218,219]. This method not only captures the spatial distribution of microcracks but also provides a new perspective for studying crack propagation and interactions. Chen *et al.* [220] obtained the full-field strain distribution of C/C-SiC composites through DVC analysis and revealed the differences in local deformation under varying load conditions. These studies provide important experimental evidence for understanding the mechanical behavior of composites under complex stress environments. Additionally, similar studies on 2D and 3D woven CMCs using DVC technology have also been reported in the literature, further demonstrating the widespread application of DVC in composite deformation analysis [221].

Although DVC technology has opened a new dimension for studying 3D deformation or strain distribution, the segmentation of internal microcracks in CMCs still presents challenges. This is because these microcracks are often very small, with weak signals in μCT images, typically occupying only a few pixels in width, making segmentation more challenging [223]. However, with the rapid development of computer vision technology, the ability to extract image features has significantly improved, offering new techniques and methods to address this issue.

Inspired by the aforementioned studies, Zhu *et al.* [222] conducted an in-depth investigation into the microcrack evolution behavior of CMCs under high-temperature loading, with a particular focus on the quantitative tracking of microcracks. The research group introduced a microcrack segmentation method based on deep learning with a generative adversarial network (GAN) (see Figure 20a,b), enabling precise and reliable segmentation of microcracks, even when μCT images are degraded by

noise and artifacts. This technological breakthrough provides an important tool for studying internal damage in CMCs under high-temperature conditions. Additionally, Louis *et al.* [224] proposed a method for predicting the residual strength (RUS) of silicon carbide fiber-reinforced silicon carbide matrix composites (SiC_f/SiC) based on deep learning and acoustic emission (AE) signals (see Figure 20c). The study employed two machine learning techniques, random forest (RF) and convolutional neural network (CNN), to predict the RUS of the material based on AE signals. The results indicate that combining AE analysis with deep learning effectively monitors the degradation process of SiC_f/SiC materials and provides strong support for predicting material performance (see Figure 20d). In addressing the current research gap in quantitatively assessing internal damage and deformation of CMCs under load, Guo *et al.* [225] conducted a systematic study of the tensile damage evolution and mechanical behavior of SiC_f/SiC mini composites using 4D in-situ micro-CT tensile testing and data-driven modeling (see Figure 20e). The study utilized 4D in-situ X-ray CT technology, combined with deep learning image segmentation and DVC techniques, to quantitatively characterize the initiation and propagation of matrix cracks during tensile loading, identifying transverse cracks as the primary damage mode (see Figure 20f). This research not only revealed the key damage mechanisms of SiCf/SiC materials under tensile load but also provided valuable insights for future material design and performance optimization.

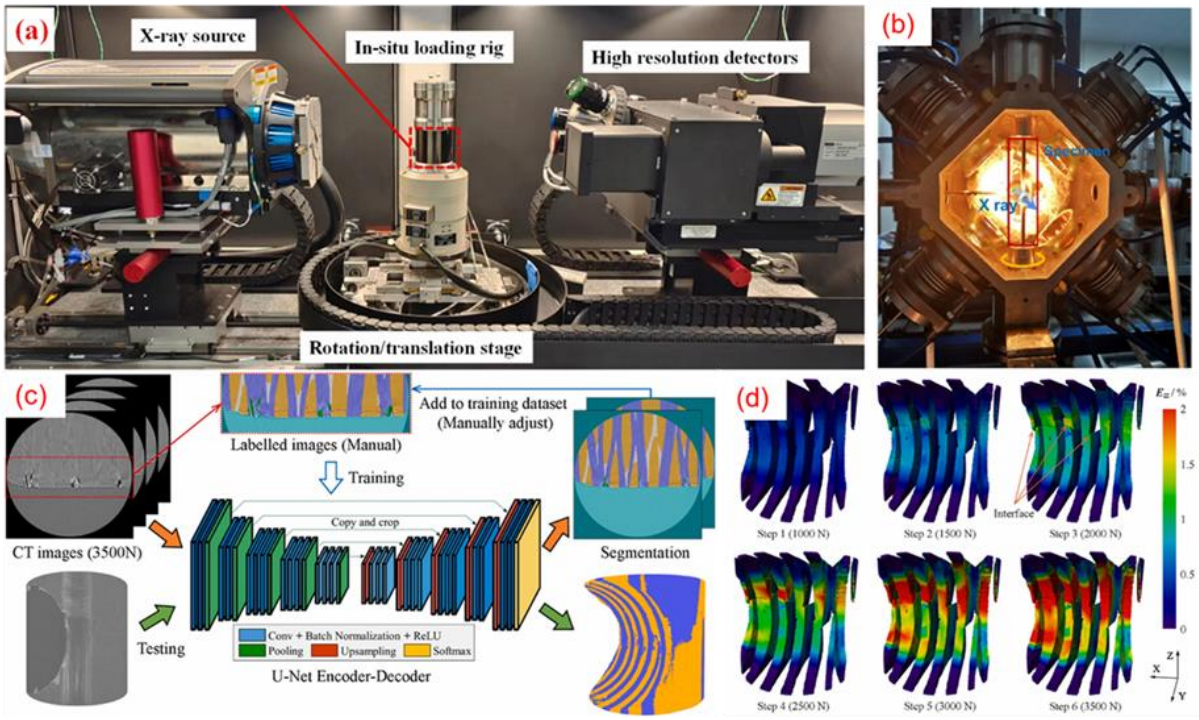

Figure 19. Imaging capture systems and U-net: (a) Zeiss Xradia 515 Versa testing system [212]; Reprinted with permission. Copyright 2024, Elsevier. (b) In-situ μCT system with a laboratory X-ray source under high temperature [222]; Reprinted with permission. Copyright 2023, Elsevier. (c) Detailed procedure for training and testing the U-Net deep learning segmentation model [212]; (d) 3D strain distribution of warp fiber tows along the loading direction at various loading steps [212].

In recent years, with the continuous advancement of detection methods and the rapid development of AI technologies, scholars have conducted a series of in-depth studies in the field of SiC composites,

particularly focusing on high-temperature material applications, and have achieved significant results [226–228]. Wu *et al.* [229] designed a combined radiative heating system and found that the thermomechanical properties of C/SiC composites significantly decrease with increasing temperature in extreme high-temperature (1000–1500 ℃) oxidation environments, providing data support for designing safer, more reliable high-temperature structural materials. Zhu *et al.* [230] significantly enhanced the creep and fatigue behavior of SiC/SiC composites at 1300 ℃ by adding a glass phase, providing a more reliable solution for the application of SiC composites in high-temperature environments. These studies have not only advanced materials science but also provided new solutions for industrial applications, especially in extreme environments. Nevertheless, in the promising field of SiC_f/SiC composites, particularly in the research of cladding tubes for nuclear reactors, studies integrating AI remain scarce and can even be considered an area in urgent need of exploration. From the perspective of nuclear reactor safety, SiC_f/SiC composites are considered one of the ideal candidate materials for next-generation ATF technology due to their excellent high-temperature resistance, irradiation tolerance, and corrosion resistance. However, the development and application of this technology face many complex challenges. First, the long-term stability and reliability of cladding tubes in extreme environments are critical to nuclear safety, which requires an in-depth understanding of the material's mechanical and thermal-physical properties under high temperatures, intense radiation, and chemical corrosion. Secondly, the current data on fundamental mechanical performance remains limited, posing challenges to the accuracy of new material designs and model parameters. Additionally, testing protocols and standards for extreme environments have not been fully established, adding uncertainty to the application of SiC_f/SiC composites in nuclear reactors.

In the future, in-depth research integrating AI technologies will become a key approach to addressing these challenges. By introducing AI technologies such as deep learning, machine learning, digital twin technology, high-throughput computation and screening, and big data analysis, the ability to predict the multiscale, multiphysical behavior of SiC_f/SiC composites can be significantly enhanced. Specifically, AI technologies can be used in high-throughput computation and screening of materials, generating large amounts of virtual experimental data across various conditions to analyze performance in extreme environments, accelerating the discovery and optimization of new materials—a technique successfully applied in superalloys [231], catalysts [232], and battery materials [233]. Additionally, using digital twin technology, researchers can simulate the long-term behavior of cladding tubes in complex environments, providing virtual experimental data to supplement critical information that is difficult to obtain under current experimental conditions. Moreover, AI can help address the shortage of experimental data. By applying deep learning and analysis to existing experimental data, it is possible to predict material performance under various operating conditions, further guiding experimental design and standard development. Currently, deep learning has successfully predicted fatigue life, crack resistance, and thermal stability in research on ceramic and metal materials [234–236]. This technology not only shortens the R&D cycle for new materials but also significantly reduces R&D costs, providing more reliable data support for the design and manufacturing of nuclear reactor cladding tubes.

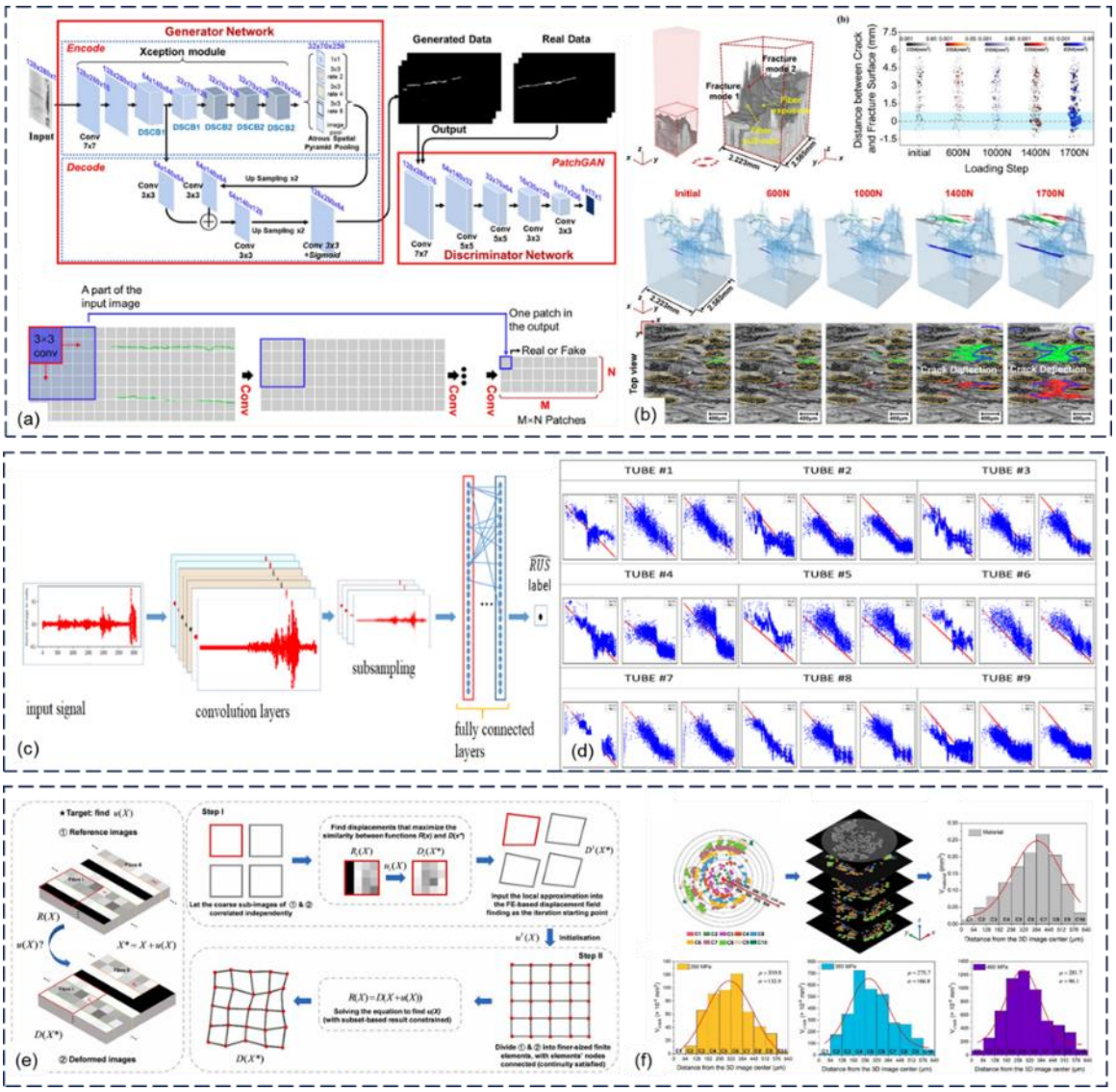

Figure 20. Further Applications of AI in CMCs: (a) Network architecture of the crack detection GAN [222]; (b) Fracture analysis using μCT [222]; (c) Workflow Schema of our CNN models [224]; (d) Stress *versus* RUS plots for each given tube [224]; (e) Workflow of subset-based DVC method and FE-based DVC method [225]; Reprinted with permission. Copyright 2024, Elsevier. (f) Image slices, material volume distribution, and the volume of transverse cracks as a function of the distance from the image center [225].

Looking ahead, as AI technology continues to permeate materials science, the application prospects of SiC_f/SiC composites in nuclear reactor cladding tubes will become even more promising. Researchers are expected to develop more intelligent and precise material design methods, enabling accurate control and prediction of material properties, which will promote the widespread application of SiC_f/SiC composites in the nuclear energy sector and enhance safety. Future research directions will include: (1) Developing AI-based multi-scale modeling and simulation technologies to enhance the accuracy of predicting SiC_f/SiC materials' behavior under extreme conditions; (2) Combining big data analysis with experimental validation to establish more comprehensive testing standards and safety evaluation systems; (3) Exploring the application of intelligent manufacturing technologies in cladding tube design and production to achieve efficient material production and quality control. Through these efforts,

SiC_f/SiC composites are expected to play a critical role in future nuclear energy systems, enhancing both reactor safety and efficiency while driving a new wave of technological innovation in materials science and nuclear engineering.

5. Application

SiC_f/SiC exhibits advantages such as high-temperature resistance, oxidation resistance, corrosion resistance, and radiation resistance, making it suitable for applications in harsh high-temperature and neutron radiation environments. In February 2015, GE's low-pressure turbine blades made significant advancements in aerospace engine applications, heralding the full-scale use of SiC_f/SiC composites in aircraft engines. Furthermore, these composites demonstrate low swelling rates under neutron irradiation and show insensitivity to neutron exposure, highlighting their potential in nuclear applications.

5.1. Aerospace field

SiC_f/SiC composites have attracted significant attention in the aerospace field due to their excellent high-temperature performance and lightweight properties. Over the years, countries around the world have invested significant effort and resources into the research and development of SiC_f/SiC composites. After decades of development, SiC_f/SiC composites have been widely applied in advanced technology and military fields, including spacecraft thermal protection systems, hot-end components of jet engines, high-temperature structural parts, and hypersonic vehicle shields.

(1) Spacecraft thermal protection systems: SiC_f/SiC composites are widely used in spacecraft thermal protection systems due to their high-temperature stability and oxidation resistance[237–239], especially during atmospheric re-entry when the spacecraft's outer surface must withstand extremely high temperatures. Figure 21a illustrates the thermal structure on the surface of the vehicle. SiC_f/SiC composites can maintain structural integrity at extreme high temperatures, preventing damage to the spacecraft during atmospheric re-entry. Compared to oxide ceramics, SiC_f/SiC can maintain greater structural integrity at extreme high temperatures, reducing thermal decomposition and oxidation rates to preserve structural integrity and prevent spacecraft damage during atmospheric re-entry.

(2) High-temperature structural components: Researchers have extensively validated the application of SiC_f/SiC composites in high-temperature structural components of aerospace engines and spacecraft [3,4], demonstrating their suitability in critical areas such as combustion chamber liners [240], turbine components[5], and blades [5]. SiC_f/SiC has significant advantages over nickel-based superalloys. While nickel-based superalloys exhibit good strength and creep resistance in high-temperature environments, their oxidation resistance weakens as temperatures rise further. In contrast, SiC_f/SiC can maintain oxidation and creep resistance even above 1200 °C. This not only helps to enhance the efficiency of the engine but also significantly extends its service life. In the 1980s, the French company SNECMA successfully developed the CERASEPR series of SiC_f/SiC composites, which were first applied to the nozzle of the M88-2 engine [241]. Additionally, SiC_f/SiC composites have been applied in high-temperature structural components of spacecraft, including missile nozzles[242], thermal insulation layers in jet engines [243], and rocket engine nozzles[244]. These components require materials to maintain stable performance under high temperatures and intense thermal shock, which SiC_f/SiC composites are well-equipped to meet, ensuring the reliability and safety of spacecraft in extreme environments.

(3) Thermal protection components: During the flight of a supersonic vehicle, its surface experiences extremely high temperatures due to friction with the air, necessitating materials with excellent high-temperature resistance and good thermal conductivity. Compared to traditional thermal barrier coating materials (such as oxide ceramics), SiC_f/SiC composites not only exhibit excellent ablation resistance but also offer superior thermal conductivity, facilitating rapid heat transfer and preventing local overheating. Additionally, the high strength and lightweight characteristics of SiC_f/SiC composites are unmatched by traditional materials, making them particularly suitable for thermal protection structural components in aerospace vehicles. For instance, Daimler Aerospace of Germany has implemented SiC_f/SiC composites in the thermal protection system of the Sanger spaceplane[245], as illustrated in Figure 21d (up). Similarly, the Japan Aerospace Exploration Agency has applied SiC_f/SiC composites to the leading-edge surface panels of the HOPE-X spacecraft [245], as shown in Figure 21d (down). These applications further demonstrate the reliability and superior performance of SiC_f/SiC composites in extreme environments.

5.2. The field of nuclear energy

The application prospects of SiC_f/SiC composites in the field of nuclear energy are promising, as their unique physical and chemical properties make them an ideal choice for next-generation nuclear reactor structural materials. Nuclear energy, as an efficient and low-carbon energy source, plays a crucial role in the global transition of energy structures and in addressing climate change. However, a primary challenge in the utilization of nuclear energy is the enhancement of reactor safety and efficiency, particularly in extreme environments where traditional materials, such as zirconium alloys, fail to meet the high standards required by modern nuclear systems. Consequently, SiC_f/SiC composites, with their outstanding properties, have emerged as important candidate materials for critical components in nuclear reactors. It demonstrates significant application potential in various fields, including nuclear fuel cladding tubes, reactor internal components, and nuclear waste management facilities. Each of these fields has its unique requirements, and SiC_f/SiC composites, with their exceptional high-temperature resistance, oxidation resistance, radiation resistance, and mechanical strength, are capable of meeting these needs, thereby significantly enhancing the overall safety and performance of nuclear energy systems.

(1) Nuclear fuel cladding tubes: Nuclear fuel cladding tubes are one of the core components of a nuclear reactor, responsible for encapsulating nuclear fuel and preventing the leakage of fission products, while also conducting heat generated within the reactor to the coolant [38]. While traditional zirconium alloy materials exhibit good performance at low temperatures, they are prone to oxidation and hydride formation in high-temperature environments, leading to embrittlement and fracture, which can result in severe safety incidents. In this context, SiC_f/SiC composites have emerged as ideal alternative materials due to their exceptional high-temperature resistance and oxidation resistance. SiC_f/SiC composites are capable of preserving structural integrity and mechanical performance in environments above 1200 ℃, a level that zirconium alloys cannot achieve. Additionally, the low neutron absorption cross-section of SiC_f/SiC composites contributes to safer use in high-irradiation environments, which is crucial for enhancing the safety margins and fault tolerance of nuclear reactors. By using SiC_f/SiC composites as nuclear fuel cladding tubes, nuclear power plants can better control fuel temperatures during severe accidents, extending emergency response times and thereby reducing accident risks and enhancing overall safety.

(2) Reactor internal components: Internal components of a nuclear reactor include control rod guide tubes, support structures, shielding components, and reflectors, which perform crucial functions such as load-bearing, heat conduction, and radiation protection within the reactor [49]. The selection of materials for these components is critical due to the high temperature, pressure, and radiation environments within the reactor. The high strength, corrosion resistance, and radiation resistance of SiC_f/SiC composites make them ideal materials for these critical components. Particularly in fourth-generation nuclear reactors, such as very high-temperature gas-cooled reactors and thorium molten salt reactors, SiC_f/SiC composites can maintain excellent performance at higher temperatures and radiation doses. Compared to traditional materials, SiC_f/SiC composites not only reduce expansion and deformation caused by neutron irradiation but also effectively mitigate thermal fatigue, thereby extending the operational lifespan and reliability of the reactor. Additionally, due to the low thermal expansion coefficient of SiC_f/SiC composites, their dimensional stability is enhanced in high-temperature and high-radiation environments, ensuring the long-term safe operation of the reactor.

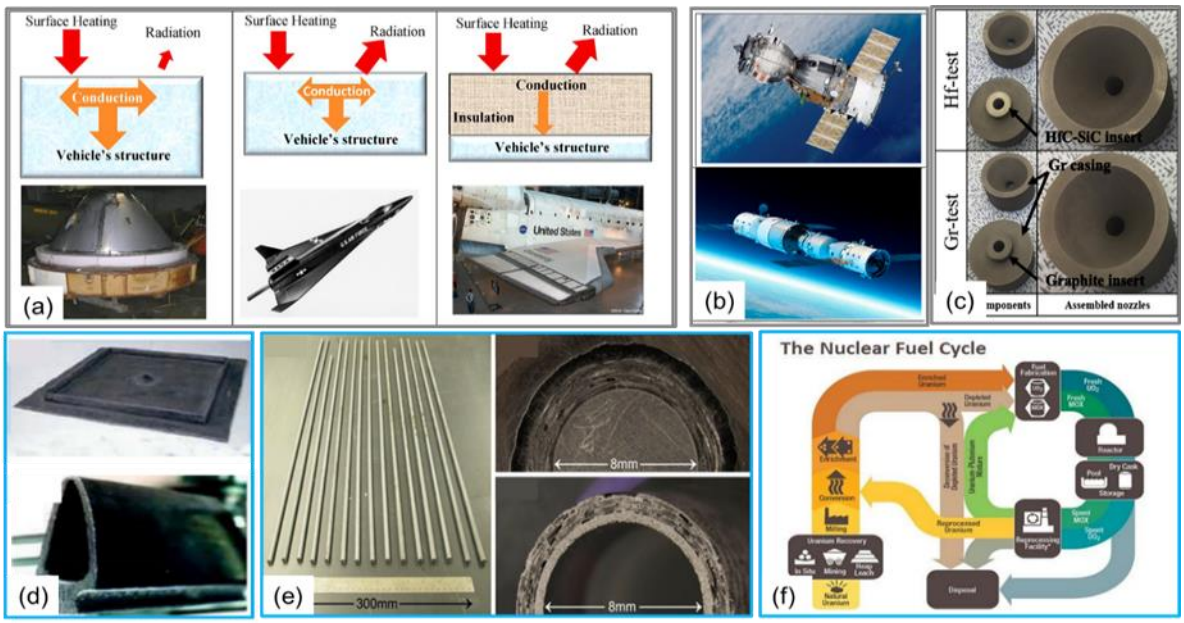

Figure 21. Applications in the aerospace and nuclear energy sectors: (a) Schematic diagram of thermal structure [246]; Reprinted with permission. Copyright 2020, Elsevier. (b) Soyuz spacecraft and Shenzhou spacecraft [246]; (c) Nozzle components [243]; Reprinted with permission. Copyright 2020, Elsevier. (d) SiC_f/SiC composite thermal protection parts[244]; (e) Nuclear fuel cladding tube [38]; (f) The Nuclear Fuel Cycle [245].

(3) Nuclear waste management facilities: Nuclear waste management presents a significant challenge in the utilization of nuclear energy, particularly concerning the high stability requirements of materials during the long-term storage of radioactive waste. SiC_f/SiC composites are considered an ideal choice for nuclear waste encapsulation materials due to their high strength, corrosion resistance, and radiation resistance. In high-level radioactive waste management facilities, SiC_f/SiC composites can effectively block the diffusion of radioactive substances, ensuring the safety of waste under geological storage conditions, as illustrated in Figure 21f. Compared to traditional materials, SiC_f/SiC composites not only resist material degradation caused by long-term irradiation but also maintain their structural

integrity in extreme environments, ensuring that nuclear waste remains leak-proof during storage periods of thousands of years. Additionally, the radiation-induced swelling resistance and low neutron absorption cross-section of SiC_f/SiC composites make them durable and reliable encapsulation materials in high-level radioactive waste management facilities, further enhancing the safety and stability of these facilities.

6. Summary and prospects

As a high-temperature ceramic matrix composite, SiC_f/SiC exhibits outstanding high-temperature resistance, excellent oxidation resistance, and radiation resistance, demonstrating significant application potential in aerospace and nuclear industries. Despite significant advancements in material preparation processes, microstructural optimization, and mechanical performance research in recent years, SiC_f/SiC composites still face multiple challenges in practical applications, including the complexity of preparation processes, high production costs, and performance stability in extreme environments. Currently, researchers have continuously optimized the density and microstructure of materials through various fabrication processes; however, each method still has shortcomings that make it difficult to fully meet the high density, high purity, and low-cost requirements of materials for nuclear applications. Consequently, future research efforts should prioritize integrating the strengths of multiple techniques to create more efficient and low-cost manufacturing methods, thereby achieving a balance between improved material performance and economic feasibility. In the study of the radiation resistance and corrosion resistance of SiC_f/SiC composites, existing experiments have revealed the mechanical behavior and microstructural changes of the material under high temperature and irradiation conditions; however, given the long-term usage demands in extreme environments like nuclear reactors, further in-depth exploration of the material's long-term stability, interface phase durability, and radiation damage resistance is still necessary. In the future, AI technology will become a key tool for addressing the challenges in the research of SiC_f/SiC composites. The application of techniques such as deep learning, machine learning, and big data analysis can significantly enhance the predictive accuracy of the material's multi-scale and multi-physics behavior. Specifically, AI can accelerate the discovery and optimization of new materials, reduce research and development cycles, and identify optimal material combinations through high-throughput computations. The introduction of digital twin technology enables researchers to simulate the long-term performance of encapsulation tubes in complex environments, generating virtual experimental data to address the limitations of experimental conditions. Additionally, AI can analyze existing data to predict material performance under various conditions, optimize experimental design and standardization, thereby reducing R&D costs and enhancing the reliability of design and manufacturing of nuclear reactor encapsulation tubes. Based on current research, future studies on the fabrication of SiC_f/SiC composites should be conducted in the following areas, which will be elaborated in detail:

(1) Optimization and innovation of fabrication processes

Current fabrication methods for SiC_f/SiC composites face several issues that need to be addressed in order to enhance the overall performance of these materials. During the optimization process, it is essential to ensure material density and mechanical properties while minimizing damage to the fibers. By integrating advanced manufacturing techniques and process control measures, the performance of the composites can be enhanced, leading to the development of more efficient and economically feasible

fabrication technologies that better meet the stringent application requirements in aerospace and nuclear energy fields. Additionally, building on existing technologies, the exploration of new fabrication techniques, such as integrating microwave sintering and spark plasma sintering, aims to enhance material density, reduce costs, and minimize fiber damage. The application of these new technologies could significantly shorten processing times while improving the mechanical properties and thermal stability of the composites.

(2) Modification of fiber and matrix materials

Although third-generation SiC fibers have demonstrated high crystallinity and radiation resistance, their high elastic modulus complicates weaving and winding processes. Future research should focus on developing more cost-effective high-performance SiC fibers, particularly those tailored for nuclear applications, which must balance mechanical properties and chemical stability to meet the demands of complex nuclear environments. In terms of the matrix, besides continuing to enhance the density and purity of SiC matrices, exploring the use of other refractory carbides (such as ZrC, TaC, HfC, *etc.*) for the modification or replacement of SiC matrices is an important direction for future research, aimed at improving the material's operating temperature and oxidation resistance.

(3) Large-scale industrial production

SiC_f/SiC composites are primarily produced at the laboratory scale; however, with the growing demand for high-performance materials, industrial production is becoming urgent. Future efforts should focus on developing scalable and cost-effective fabrication processes to achieve large-scale production of materials. Furthermore, the integration of smart manufacturing and automation technologies can enable precise control and optimization of SiC_f/SiC composite production, further advancing the industrial application of these materials.

(4) Application of AI technologies

By integrating AI technologies, the predictive accuracy of composite materials' performance in extreme environments can be further enhanced, leading to the development of more precise material design methods. As AI technologies continue to advance, the application prospects of SiC_f/SiC composites in fields such as nuclear energy and aerospace will become even broader. Through the deep integration of AI and materials science, researchers are expected to develop smarter and more efficient material design and production methods, facilitating the widespread application and further development of SiC_f/SiC composites in future technologies.

Acknowledgements

This work was supported by the National Natural Science Foundation of China [grant number 52075526]; the "Ningbo 3315 Plan Innovation Team" [grant number 2017A-28-C]; the National Natural Science Foundation of China [grant number 91860204]; the Fundamental Research Funds for the Central Universities [grant number DUT22LAB605].

Conflicts of interests

The authors declared that they have no conflicts of interests.

Authors' contribution

Conceptualization, L. S. and J. X.; methodology, X. F.; software, Y. Z.; validation, X. L., Y. Z. and H. L.; formal analysis, Z. Y.; investigation, X. F.; resources, X. F.; data curation, L. S.; writing—original draft preparation, X. L.; writing—review and editing, L. S.; visualization, J. X.; supervision, L. S.; project administration, Y. Z.; funding acquisition, J. X. All authors have read and agreed to the published version of the manuscript.

References

[1] Snead LL, Nozawa T, Katoh Y, Byun T-S, Kondo S, *et al.* Handbook of SiC properties for fuel performance modeling. *J. Nucl. Mater.* 2007, 371(1):329–377.
[2] Snead LL, Nozawa T, Ferraris M, Katoh Y, Shinavski R, *et al.* Silicon carbide composites as fusion power reactor structural materials. *J. Nucl. Mater.* 2011, 417(1):330–339.
[3] Zhu D. Aerospace Ceramic Materials: Thermal, Environmental Barrier Coatings and SiC/SiC Ceramic Matrix Composites for Turbine Engine Applications. 2018. Available: https://ntrs.nasa.gov/citations/20180002984 (accessed on 21 September 2024).
[4] Wang X, Gao X, Zhang Z, Cheng L, Ma H, *et al.* Advances in modifications and high-temperature applications of silicon carbide ceramic matrix composites in aerospace: A focused review. *J. Eur. Ceram. Soc.* 2021, 41(9):4671–4688.
[5] Zhou H, Wang Y, Liu G, Zhao L, Bao J. Development status of SIC fiber toughened SIC ceramic matrix composites and its application in aero engines. *Aeronaut. Manuf. Technol.* 2017, 60(15):76–84.
[6] Katoh Y, Snead LL. Silicon carbide and its composites for nuclear applications – Historical overview. *J. Nucl. Mater.* 2019, 526:151849.
[7] Koyanagi T, Katoh Y, Nozawa T. Design and strategy for next-generation silicon carbide composites for nuclear energy. *J. Nucl. Mater.* 2020, 540:152375.
[8] Yang Z, Li F, Chai G. Status and Perspective of China's Nuclear Safety Philosophy and Requirements in the Post-Fukushima Era. *Front. Energy Res.* 2022, 9:819634.
[9] Idris MI, Konishi H, Imai M, Yoshida K, Yano T. Neutron Irradiation Swelling of SiC and SiCf/SiC for Advanced Nuclear Applications. *Energy Procedia* 2015, 71:328–336.
[10] Ji S, Liang B, Yang B, Hu C, Jiang Y, *et al.* Long-term oxidation behaviors and strength retention properties of self-healing SiCf/SiC-SiBCN composites. *J. Eur. Ceram. Soc.* 2023, 43(5):1843–1852.
[11] Yang J, Ye F, Cheng L. In-situ formation of Ti3SiC2 interphase in SiCf/SiC composites by molten salt synthesis. *J. Eur. Ceram. Soc.* 2022, 42(4):1197–1207.
[12] Zhao S. Study on the structure, properties and irradiation behavior of SiC/SiC composites prepared by PIP process. 2013. (In Chinese)
[13] Dong S, Hu J, Zhang X. Preparation technology of SiC/SiC composites by MI process (In Chinese). *Aeronaut. Manuf. Technol.* 2014, 6:35–40.
[14] Jin L, Zhang K, Xu T, Zeng T, Cheng S. The fabrication and mechanical properties of SiC/SiC composites prepared by SLS combined with PIP. *Ceram. Int.* 2018, 44(17):20992–20999.
[15] Li G, Qin L, Cao X, Lu X, Tu Y, *et al.* Water vapor corrosion resistance and failure mechanism of SiCf/SiC composites completely coated with plasma sprayed tri-layer EBCs. *Ceram. Int.* 2022, 48(5):7082–7092.
[16] Quan H, Lianyi W, Huang J, Yang H, Yang X, *et al.* High-temperature oxidation behavior and mechanism of the Si-based thermal protective coating for SiCf/SiC composites under static oxidation and H2O/O2/Na2SO4 corrosion oxidation. *Compos. Part B Eng.* 2022, 238:109906.
[17] Wang P, Liu F, Wang H, Li H, Gou Y. A review of third generation SiC fibers and SiCf/SiC composites. *J. Mater. Sci. Technol.* 2019, 35(12):2743–2750.
[18] Iveković A, Novak S, Dražić G, Blagoeva D, de Vicente SG. Current status and prospects of SiCf/SiC for fusion structural applications. *J. Eur. Ceram. Soc.* 2013, 33(10):1577–1589.

[19] Liu Q, Xu J, Liu J. Research progress of matrix and coating modification of SIC ceramic matrix composites. *Journal of Ceramics* 2018, 46(12). (In Chinese)
[20] Li S, Sui Y, Miao K, Zhongliang L, Li D. Preparation and properties of continuous carbon fiber toughened silicon Carbide composites based on direct writing molding. *Aeronaut. Manuf. Technol.* 2021, 64(15):36–41,51.
[21] Yajima S, Okamura K, Hayashi J, Omori M. Synthesis of Continuous Sic Fibers with High Tensile Strength. *J. Am. Ceram. Soc.* 1976, 59(7–8):324–327.
[22] Ishikawa T. Recent developments of the SiC fiber Nicalon and its composites, including properties of the SiC fiber Hi-Nicalon for ultra-high temperature. *Compos. Sci. Technol.* 1994, 51(2):135–144.
[23] Vahlas C, Monthioux M. On the thermal degradation of lox-M tyranno® fibres. *J. Eur. Ceram. Soc.* 1995, 15(5):445–453.
[24] Chen D, Han W, Li S, Lu Z, Qiu H, *et al.* Preparation, structure, properties and application of continuous ceramic fibers: research status and development direction. *Modern Technologies of Ceramics* 2018, 39(3). (In Chinese)
[25] Wilson M, Opila E. A Review of SiC Fiber Oxidation with a New Study of Hi-Nicalon SiC Fiber Oxidation. *Adv. Eng. Mater.* 2016, 18(10):1698–1709.
[26] Nakayasu T, Sato M, Yamamura T, Okamura K, Katoh Y, *et al.* Recent Advancement of Tyranno/SiC Composites R&D. In *23rd Annual Conference on Composites, Advanced Ceramics, Materials, and Structures: B: Ceramic Engineering and Science Proceedings*. Hoboken: John Wiley & Sons, Inc., 1999, pp. 301–308.
[27] Zhang RJ, Yang YQ, Shen WT, Wang C, Luo X. Microstructure of SiC fiber fabricated by two-stage chemical vapor deposition on tungsten filament. *J. Cryst. Growth* 2010, 313(1):56–61.
[28] Dicarlo JA. Creep of chemically vapour deposited SiC fibres. *J. Mater. Sci.* 1986, 21(1):217–224.
[29] Bunsell AR, Joannès S, Thionnet A. *Fundamentals of fibre reinforced composite materials,* 2nd ed. Boca Raton: CRC Press, 2021.
[30] Crane RL, Krukonis VJ. Strength and fracture properties of silicon carbide filament. *Am. Ceram. Soc. Bull.* 1975, 54(2):184–188.
[31] Yun HM, Dicarlo JA. Comparison of the Tensile, Creep, and Rupture Strength Properties of Stoichiometric SiC Fibers. In *23rd Annual Conference on Composites, Advanced Ceramics, Materials, and Structures: A: Ceramic Engineering and Science Proceedings*. Hoboken: John Wiley & Sons, Inc., 1999, pp. 259–272.
[32] Chen M, Qiu H, Xie W, Zhang B, Liu S, *et al.* Research Progress of Continuous Fiber Reinforced Ceramic Matrix Composite in Hot Section Components of Aero engine. *IOP Conf. Ser. Mater. Sci. Eng.* 2019, 678(1):012043.
[33] Gosset D, Colin C, Jankowiak A, Vandenberghe T, Lochet N. X-ray Diffraction Study of the Effect of High-Temperature Heat Treatment on the Microstructural Stability of Third-Generation Fibers. *J. Am. Ceram. Soc.* 2013, 96(5):1622–1628.
[34] Karakoc O, Koyanagi T, Nozawa T, Katoh Y. Fiber/matrix debonding evaluation of SiCf/SiC composites using micropillar compression technique. *Compos. Part B Eng.* 2021, 224:109189.
[35] Flores O, Bordia RK, Nestler D, Krenkel W, Motz G. Ceramic Fibers Based on SiC and SiCN Systems: Current Research, Development, and Commercial Status. *Adv. Eng. Mater.* 2014, 16(6):621–636.
[36] Zhu D, Li Y, Gao M, Pan Y. Research progress on preparation technology and properties of SiCf/SiC ceramic matrix composites. *Mater. Guide* 2008, 22(3):5.
[37] Guérin Y, Was GS, Zinkle SJ. Materials Challenges for Advanced Nuclear Energy Systems. *MRS Bull.* 2009, 34(1):10–19.
[38] Deck CP, Jacobsen GM, Sheeder J, Gutierrez O, Zhang J, *et al.* Characterization of SiC–SiC composites for accident tolerant fuel cladding. *J. Nucl. Mater.* 2015, 466:667–681.
[39] Xu Y, Cheng L. Study on continuous fiber toughened SIC ceramic matrix composites. *J. Ceram.* 2002, 30(2):5.
[40] Guo N, Pei Y, Yuan W, Li Y, Zhao S, *et al.* Application of Methyl Trichlorosilane in SiC Growth.

In *2023 20th China International Forum on Solid State Lighting & 2023 9th International Forum on Wide Bandgap Semiconductors (SSLCHINA: IFWS)*, Xiamen, China, 27–30 November 2023, pp. 6–9.

[41] Liang J, Xiao H, Gao P, Guo W, Liu J. Microstructure and properties of 2D-Cf/SiC composite fabricated by combination of CVI and PIP process with SiC particle as inert fillers. *Ceram. Int.* 2017, 43(2):1788–1794.

[42] Kim WJ, Kang SM, Park JY, Ryu WS. Effect of a SiC whisker formation on the densification of Tyranno SA/SiC composites fabricated by the CVI process. *Fusion Eng. Des.* 2006, 81(8):931–936.

[43] Hua Y, Zhang L, Cheng L, Li Z, Du J. Microstructure and mechanical properties of SiCP/SiC and SiCW/SiC composites by CVI. *J. Mater. Sci.* 2010, 45(2):392–398.

[44] Tao P, Wang Y. Fabrication of highly dense three-layer SiC cladding tube by chemical vapor infiltration method. *J. Am. Ceram. Soc.* 2019, 102(11):6939–6945.

[45] Kang SM, Kim WJ, Yoon SG, Park JY. Effects of the PyC interface coating on SiC nanowires of SiCf/SiC composite. *J. Nucl. Mater.* 2011, 417(1):367–370.

[46] Liu Y, Chai N, Qin H, Li Z, Ye F, *et al.* Tensile fracture behavior and strength distribution of SiCf/SiC composites with different SiBN interface thicknesses. *Ceram. Int.* 2015, 41(1, Part B):1609–1616.

[47] Sun J, Liu W, Lv X, Jiao J. Characterization of BN interface and its effect on the mechanical behavior of SiCf/SiC composites. *Vacuum* 2023, 211:111918.

[48] Tang M, Liu Y, Liu L, Lin T, Liu X. Microstructure and mechanical properties of SiC/SiC joints reinforced by in-situ growth SiC nanowires. *Mater. Charact.* 2021, 179:111315.

[49] Deck CP, Khalifa HE, Sammuli B, Hilsabeck T, Back CA. Fabrication of SiC–SiC composites for fuel cladding in advanced reactor designs. *Progress Nucl. Energy* 2012, 57:38–45.

[50] Naslain R. Design, preparation and properties of non-oxide CMCs for application in engines and nuclear reactors: an overview. *Compos. Sci. Technol.* 2004, 64(2):155–170.

[51] Kohyama A, Kotani M, Katoh Y, Nakayasu T, Sato M, *et al.* High-performance SiC/SiC composites by improved PIP processing with new precursor polymers. *J. Nucl. Mater.* 2000, 283:565–569.

[52] Zhong H, Wang Z, Zhou H, Ni D, Kan Y, *et al.* Properties and microstructure evolution of Cf/SiC composites fabricated by polymer impregnation and pyrolysis (PIP) with liquid polycarbosilane. *Ceram. Int.* 2017, 43(10):7387–7392.

[53] Li X, Pei X, Zhong X, Mo G, He L, *et al.* Highly effective free-radical-catalyzed curing of hyperbranched polycarbosilane for near stoichiometric SiC ceramics. *J. Am. Ceram. Soc.* 2019, 102(3):1041–1048.

[54] Rahman A, Zunjarrao S, Singh R. Effect of degree of crystallinity on elastic properties of silicon carbide fabricated using polymer pyrolysis. *J. Eur. Ceram. Soc.* 2016, 36 (14):3285–3292.

[55] Dong SM, Katoh Y, Kohyama A, Schwab ST, Snead LL. Microstructural evolution and mechanical performances of SiC/SiC composites by polymer impregnation/microwave pyrolysis (PIMP) process. *Ceram. Int.* 2002, 28(8):899–905.

[56] Luo Z, Zhou X, Yu J, Wang F. High-performance 3D SiC/PyC/SiC composites fabricated by an optimized PIP process with a new precursor and a thermal molding method. *Ceram. Int.* 2014, 40(5):6525–6532.

[57] Li M, Yang D, Wang H, Zhou X. Fabrication of a 3D4d braided SiCf/SiC composite via PIP process assisted with an EPD method. *Ceram. Int.* 2019, 45(9):11668–11676.

[58] Yin J, Lee SH, Feng L, Zhu Y, Liu X, *et al.* Fabrication of SiCf/SiC composites by hybrid techniques of electrophoretic deposition and polymer impregnation and pyrolysis. *Ceram. Int.* 2016, 42(14):16431–16435.

[59] Iveković A, Dražić G, Novak S. Densification of a SiC-matrix by electrophoretic deposition and polymer infiltration and pyrolysis process. *J. Eur. Ceram. Soc.* 2011, 31(5):833–840.

[60] Besra L, Liu M. A review on fundamentals and applications of electrophoretic deposition (EPD). *Progress Mater. Sci.* 2007, 52(1):1–61.

[61] Sarkar P, Nicholson PS. Electrophoretic Deposition (EPD): Mechanisms, Kinetics, and

Application to Ceramics. *J. Am. Ceram. Soc.* 1996, 79(8):1987–2002.
[62] Zhang Q, Liu H, Qiao T, Withers PJ, Xiao P. Simple and efficient densification of SiCf/SiC composites by gradated concentration polymer infiltration and pyrolysis. *Mater. Sci. Eng. A* 2023, 874:145065.
[63] Wei Y, Ye F, Cheng L, Zhang L, Yang J. Effects of in-situ carbon layer and volume fraction of SiC fiber on the mechanical properties and fracture behaviors of SiCf/SiC composites fabricated by a modified PIP method. *J. Eur. Ceram. Soc.* 2023, 43(4):1397–1406.
[64] Kohyama A, Katoh Y. Advanced SiC/SiC ceramic composites: Developments and applications in energy systems. *Ceram. Trans.* 2002, 144:3–18.
[65] Gao Y, Jiao J. Research progress in the preparation of SiCf/SiC composites by NITE process. *J. Mater. Eng.* 2019, 047(008):33–39.
[66] Kohyama A, Dong S, Katoh Y. Development of SiC/SiC Composites by Nano-Infiltration and Transient Eutectoid (NITE) Process. In *26th Annual Conference on Composites, Advanced Ceramics, Materials, and Structures: A: Ceramic Engineering and Science Proceedings*. Hoboken: John Wiley & Sons, Inc., 2002, pp. 311–318.
[67] Konishi H, Idris MI, Imai M, Yoshida K, Yano T. Neutron Irradiation Effects of Oxide Sintering Additives for SiCf/SiC Composites. *Energy Procedia* 2015, 71:306–312.
[68] Parish CM, Terrani KA, Kim Y-J, Koyanagi T, Katoh Y. Microstructure and hydrothermal corrosion behavior of NITE-SiC with various sintering additives in LWR coolant environments. *J. Eur. Ceram. Soc.* 2017, 37(4):1261–1279.
[69] Chen H, Chen J, Yang J, Ahmad Z, Zhu M, *et al.* Microstructure and mechanical properties of multilayer SiC nanofiber paper-reinforced SiC composites by the NITE method. *J. Am. Ceram. Soc.* 2024, 107(9):6410–6421.
[70] Lee Y, Yoon H. Effect of Microstructure and Sintering Temperature on Fabrication of NITE-SiCf/SiC Composite. *Key Eng. Mater.* 2007, 345:1229–1232.
[71] Shimoda K, Hinoki T. Effects of fiber volume fraction on the densification and mechanical properties of unidirectional SiCf/SiC-matrix composites. *J. Eur. Ceram. Soc.* 2021, 41(2): 1163–1170.
[72] Eustathopoulos N, Nicholas MG, Drevet B. *Wettability at high temperatures.* St Louis: Elsevier, 1999.
[73] Ness JN, Page TF. Microstructural evolution in reaction-bonded silicon carbide. *J. Mater. Sci.* 1986, 21(4):1377–1397.
[74] Jepps NW, Page TF. Polytypic transformations in silicon carbide. *Prog. Cryst. Growth Charact.* 1983, 7(1):259–307.
[75] Caccia M, Amore S, Giuranno D, Novakovic R, Ricci E, *et al.* Towards optimization of SiC/CoSi2 composite material manufacture via reactive infiltration: Wetting study of Si–Co alloys on carbon materials. *J. Eur. Ceram. Soc.* 2015, 35(15):4099–4106.
[76] Caccia M, Narciso J. Key Parameters in the Manufacture of SiC-Based Composite Materials by Reactive Melt Infiltration. *Mater.* 2019, 12(15):2425.
[77] Sergi D, Camarano A, Molina JM, Ortona A, Narciso J. Surface growth for molten silicon infiltration into carbon millimeter-sized channels: Lattice–Boltzmann simulations, experiments and models. *Int. J. Mod. Phys. C* 2015, 27(06):1650062.
[78] Camarano A, Caccia M, Molina JM, Narciso J. Effects of Fe addition on the mechanical and thermo-mechanical properties of SiC/FeSi2/Si composites produced via reactive infiltration. *Ceram. Int.* 2016, 42(9):10726–10733.
[79] Margiotta JC, Zhang D, Nagle DC. Microstructural evolution during silicon carbide (SiC) formation by liquid silicon infiltration using optical microscopy. *Int. J. Refract. Metals Hard Mater.* 2010, 28(2):191–197.
[80] Jiao J, Yang J, Li B. Progress in Ceramic Matrix Composites Fabricated by Melt Infiltration Process (In Chinese). *Aeronaut. Manuf. Technol.* 2015, (S2):1–6,11.
[81] Hu J, Yang J, Zhang X, Ding Y, Zhou H, *et al.* Microstructure and properties of high density reaction sintered SiCf/SiC composites. *Aviation Manuf. Technol.* 2018, 61(14):6.
[82] Wang J, Zhang F, Liu Y, Li J, Dong N, *et al.* Y/YbB4-modified SiCf/SiC composites with enhanced water-oxygen corrosion resistance. *Ceram. Int.* 2023, 49(22): 37046–37050.

[83] Sun X, Chen X, Huang H, Jin X, Kan Y, *et al.* Microstructure and mechanical properties of SiCf/SiC–AlN composites prepared by low temperature reactive melt infiltration. *Ceram. Int.* 2024, 50(20, Part A):37844–37857.
[84] Zhang J, Chen X, Liao C, Guo F, Yang J, *et al.* Optimizing microstructure and properties of SiCf/SiC composites prepared by reactive melt infiltration. *J. Inorg. Mater.* 2021, 36(10):1103–1110.
[85] DiCarlo JA, Yun HM, Morscher GN, Bhatt RT. SiC/SiC Composites for 1200 °C and Above. In *Handbook of Ceramic Composites*. Boston: Springer, 2005, pp. 77–98.
[86] Liu R, Wang F, Zhang J, Chen J, Wan F, *et al.* Effects of CVI SiC amount and deposition rates on properties of SiCf/SiC composites fabricated by hybrid chemical vapor infiltration (CVI) and precursor infiltration and pyrolysis (PIP) routes. *Ceram. Int.* 2021, 47(19):26971–26977.
[87] Mu Y, Zhou W, Wang C, Luo F, Zhu D, *et al.* Mechanical and electromagnetic shielding properties of SiCf/SiC composites fabricated by combined CVI and PIP process. *Ceram. Int.* 2014, 40(7, Part A):10037–10041.
[88] Wei Y, Ye F, Cheng L, Guo G. Stress engineering of SiCf/SiC composites: Interfacial stress adjustment and its effects on tensile behaviors of UD SiCf/SiC composites fabricated by hybrid CVI and PIP methods. *Compos. Part B Eng.* 2024, 284:111711.
[89] Zhang J, Zhang Y, Wang Y, Wan F, Li J, *et al.* Long-term oxidation performance of SiCf/SiC composites at 1200°C in air atmosphere manufactured by PIP and hybrid CVI/PIP techniques. *Ceram. Int.* 2024, 50(7, Part A):10259–10267.
[90] Brennan JJ. Interfacial characterization of a slurry-cast melt-infiltrated SiC/SiC ceramic-matrix composite. *Acta Mater.* 2000, 48(18):4619–4628.
[91] Li M, Zhang R, He Z, Fu D, Li S. Study on Preparation Technology of Accident-resistant SiCf/SiC Composite Cladding Tube CVI+ Mouldless NITE. *Nuclear Power Engineering* 2020. (In Chinese)
[92] Raju K, Seong YH, Kim S, Han IS, Bang HJ, *et al.* Fabrication of SiCf/SiC composites through hybrid processing via chemical vapor infiltration, electrophoretic deposition, and liquid silicon infiltration. *J. Asian Ceram. Soc.* 2021, 9:1–7.
[93] Robb KR, Francis MW, Ott LJ. Insight from Fukushima Daiichi Unit 3 Investigations Using MELCOR. *Nucl. Technol.* 2014, 186(2):145–160.
[94] Uetsuka H, Furuta T, Kawasaki S. Failure-Bearing Capability of Oxidized Zircaloy-4 Cladding under Simulated Loss-of-Coolant Condition. *J. Nucl. Sci. Technol.* 1983, 20(11):941–950.
[95] Nagase F, Fuketa T. Fracture Behavior of Irradiated Zircaloy-4 Cladding under Simulated LOCA Conditions. *J. Nucl. Sci. Technol.* 2006, 43:1114–1119.
[96] Shapovalov K, Jacobsen GM, Shih C, Deck CP. C-ring testing of nuclear grade silicon carbide composites at temperatures up to 1900 °C. *J. Nucl. Mater.* 2019, 522:184–191.
[97] Lu Z, Yue J, Fu Z, Huang X, Yang H. Microstructure and mechanical performance of SiCf/BN/SiC mini-composites oxidized at elevated temperature from ambient temperature to 1500 °C in air. *J. Eur. Ceram. Soc.* 2020, 40(8): 2821—2827.
[98] Ma X, Yin X, Cao X, Chen L, Cheng L, *et al.* Effect of heat treatment on the mechanical properties of SiCf/BN/SiC fabricated by CVI. *Ceram. Int.* 2016, 42(2, Part B):3652–3658.
[99] Xu Q, Jin X, Liu L, Hou C, Hu N, *et al.* Thermal Shock and Residual Strength Testing of SiC/SiC Composite Braided Tubes. *Exp. Mech.* 2023, 63(5):955–964.
[100] Yuan G, Forna-Kreutzer JP, Xu P, Gonderman S, Deck C, *et al.* In situ high-temperature 3D imaging of the damage evolution in a SiC nuclear fuel cladding material. *Mater. Des.* 2023, 227:111784.
[101] Ben-Belgacem M, Richet V, Terrani KA, Katoh Y, Snead LL. Thermo-mechanical analysis of LWR SiC/SiC composite cladding. *J. Nucl. Mater.* 2014, 447(1):125–142.
[102] Jing X, Yang X, Shi D, Niu H. Tensile creep behavior of three-dimensional four-step braided SiC/SiC composite at elevated temperature. *Ceram. Int.* 2017, 43(9):6721–6729.
[103] Cluzel C, Baranger E, Ladevèze P, Mouret A. Mechanical behaviour and lifetime modelling of self-healing ceramic-matrix composites subjected to thermomechanical loading in air. *Compos. Part A Appl. Sci. Manuf.* 2009, 40(8):976–984.

[104] Ozawa K, Nozawa T, Katoh Y, Hinoki T, Kohyama A. Mechanical properties of advanced SiC/SiC composites after neutron irradiation. *J. Nucl. Mater.* 2007, 367: 713–718.
[105] Ozawa K, Katoh Y, Nozawa T, Snead LL. Effect of neutron irradiation on fracture resistance of advanced SiC/SiC composites. *J. Nucl. Mater.* 2011, 417(1):411–415.
[106] Ozawa K, Katoh Y, Nozawa T, Hinoki T, Snead LL. Evaluation of Damage Tolerance of Advanced SiC/SiC Composites after Neutron Irradiation. *IOP Conf. Ser. Mater. Sci. Eng.* 2011, 18(16):162005.
[107] Koyanagi T, Nozawa T, Katoh Y, Snead LL. Mechanical property degradation of high crystalline SiC fiber–reinforced SiC matrix composite neutron irradiated to ∼100 displacements per atom. *J. Eur. Ceram. Soc.* 2018, 38(4):1087–1094.
[108] Nogami S, Hasegawa A, Snead LL, Jones RH, Abe K. Effect of He pre-implantation and neutron irradiation on mechanical properties of SiC/SiC composite. *J. Nucl. Mater.* 2004, 329:577–581.
[109] Nozawa T, Katoh Y, Snead LL. The effects of neutron irradiation on shear properties of monolayered PyC and multilayered PyC/SiC interfaces of SiC/SiC composites. *J. Nucl. Mater.* 2007, 367:685–691.
[110] Katoh Y, Snead LL, Nozawa T, Kondo S, Busby JT. Thermophysical and mechanical properties of near-stoichiometric fiber CVI SiC/SiC composites after neutron irradiation at elevated temperatures. *J. Nucl. Mater.* 2010, 403(1):48–61.
[111] Katoh Y, Nozawa T, Shih C, Ozawa K, Koyanagi T, *et al.* High-dose neutron irradiation of Hi-Nicalon Type S silicon carbide composites. Part 2: Mechanical and physical properties. *J. Nucl. Mater.* 2015, 462:450–457.
[112] Perez-Bergquist AG, Nozawa T, Shih C, Leonard KJ, Snead LL, *et al.* High dose neutron irradiation of Hi-Nicalon Type S silicon carbide composites, Part 1: Microstructural evaluations. *J. Nucl. Mater.* 2015, 462:443–449.
[113] Chai Y, Zhang H, Zhou X, Zhang Y. Effects of silicon ion irradiation on the interface properties of SiCf/SiC composites. *Ceram. Int.* 2018, 44(2):2165–2169.
[114] Yang J, Ye F, Cheng L, Zhao K, Wei Y. Effects of hydrogen-helium ions irradiation on Ti3SiC2-containing interphase or coating in SiCf/SiC. *J. Eur. Ceram. Soc.* 2024, 44(11):6356–6366.
[115] Liu G, Ran G, He Z, Ye C, Li Y, *et al.* Microstructure characteristics of C+ and He+ irradiated SiCf/SiC composites before and after annealing. *Ceram. Int.* 2021, 47(6):8408–8415.
[116] Koyanagi T, Kondo S, Hinoki T. Internal residual stress analysis of SiC/SiC composites following ion irradiation. *IOP Conf. Ser. Mater. Sci. Eng.* 2011, 18(16):162008.
[117] Zhao Y, Li X, Liu C, Yang H, Chen B, *et al.* Irradiation effects on Amosic-3 silicon carbide composites by Si ions implantation. *J. Eur. Ceram. Soc.* 2019, 39(15):4501–4509.
[118] Xu S, Li X, Zhao Y, Liu C, Mao Q, *et al.* Micromechanical properties and microstructural evolution of Amosic-3 SiC/SiC composites irradiated by silicon ions. *J. Eur. Ceram. Soc.* 2020, 40(8):2811–2820.
[119] Taguchi T, Igawa N, Miwa S, Wakai E, Jitsukawa S, *et al.* Effect of displacement damage up to 50 dpa on microstructural development in SiC/SiC composites. *J. Nucl. Mater.* 2007, 367:698–702.
[120] Taguchi T, Wakai E, Igawa N, Nogami S, Snead LL, *et al.* Effect of simultaneous ion irradiation on microstructural change of SiC/SiC composites at high temperature. *J. Nucl. Mater.* 2002, 307:1135–1140.
[121] Li Q, Li X, Zhu Z, Ye L, Liu W, *et al.* Evolution of microstructure and mechanical properties of SiCf/SiC composites induced by He ions irradiation at various temperatures. *Ceram. Int.* 2023, 49(23, Part B):39449–39457.
[122] Ye C, Xue J, Liu T, Shu R, Yan Y, *et al.* The microstructure evolution in a SiCf/SiC composite under triple ion beam irradiation. *Ceram. Int.* 2020, 46(7):9901–9906.
[123] Nogami S, Hasegawa A, Abe K, Taguchi T, Yamada R. Effect of dual-beam-irradiation by helium and carbon ions on microstructure development of SiC/SiC composites. *J. Nucl. Mater.* 2000, 283:268–272.
[124] Xu S, Zheng C, Li X, Gao N, Huang Z, *et al.* The synergetic effect of He and Kr irradiation on helium bubble evolution in SiC/SiC composite: Combining in-situ TEM observation with MD

simulation. *J. Mater. Sci. Technol.* 2024, 197:238–246.
[125] Ye C, Xue J, Liu T, Shu R, Yan Y, *et al.* Evolution of microstructure and nanohardness of SiC fiber-reinforced SiC matrix composites under Au ion irradiation. *Ceram. Int.* 2020, 46(6):8165–8173.
[126] Katoh Y, Kotani M, Kishimoto H, Yang W, Kohyama A. Properties and radiation effects in high-temperature pyrolyzed PIP-SiC/SiC. *J. Nucl. Mater.* 2001, 289(1):42–47.
[127] Kishimoto H, Katoh Y, Kohyama A. Microstructural stability of SiC and SiC/SiC composites under high temperature irradiation environment. *J. Nucl. Mater.* 2002, 307:1130–1134.
[128] Kishimoto H, Ozawa K, Hashitomi O, Kohyama A. Microstructural evolution analysis of NITE SiC/SiC composite using TEM examination and dual-ion irradiation. *J. Nucl. Mater.* 2007, 367:748–752.
[129] Terrani KA, Yang Y, Kim YJ, Rebak R, Meyer HM, *et al.* Hydrothermal corrosion of SiC in LWR coolant environments in the absence of irradiation. *J. Nucl. Mater.* 2015, 465:488–498.
[130] Yang H, Li X, Liu C, Zhao Y, Chen B, *et al.* Hydrothermal corrosion behavior of SiCf/SiC composites candidate for PWR accident tolerant fuel cladding. *Ceram. Int.* 2018, 44(18):22865–22873.
[131] Park JS, Kim JI, Nakazato N, Kishimoto H, Makimura S. Oxidation resistance of NITE-SiC/SiC composites with/without CVD-SiC environmental barrier coating. *Ceram. Int.* 2018, 44(14):17319–17325.
[132] Qin Y, Li X, Liu C, Zheng C, Mao Q, *et al.* Effect of deposition temperature on the corrosion behavior of CVD SiC coatings on SiCf/SiC composites under simulated PWR conditions. *Corros. Sci.* 2021, 181:109233.
[133] Berdoyes I, Plaisantin H, Danet J, Lepetitcorps Y, Roger J. The corrosion behavior of various CVD SiC coatings in molten silicon. *Ceram. Int.* 2024, 50(2, Part B):3877–3886.
[134] Nasiri NA, Patra N, Ni N, Jayaseelan DD, Lee WE. Oxidation behaviour of SiC/SiC ceramic matrix composites in air. *J. Eur. Ceram. Soc.* 2016, 36(14):3293–3302.
[135] Zok FW, Maxwell PT, Kawanishi K, Callaway EB. Degradation of a SiC-SiC composite in water vapor environments. *J. Am. Ceram. Soc.* 2020, 103(3):1927–1941.
[136] Guo F, Chen X, Yang J, Zhang X, Hu J, *et al.* Stress-corrosion behavior of SiCf/SiC under CMAS-wet-oxygen environments. *Corros. Sci.* 2024, 228:111844.
[137] Cui GY, Luo RY, Wang LY, Huang P, Song JQ, *et al.* Mechanical properties evolution of SiCf/SiC composites with a BN/SiC multilayer interface oxidized at elevated temperature. *Appl. Surf. Sci.* 2021, 570:151065.
[138] Wang LY, Luo RY, Cui GY, Chen ZF. Oxidation resistance of SiCf/SiC composites with a PyC/SiC multilayer interface at 500 °C to 1100 °C. *Corros. Sci.* 2020, 167:108522.
[139] Zhang J, Liu R, Jian Y, Wan F, Wang Y. Degradation mechanism of SiCf/SiC composites after long-time water vapor and oxygen corrosion at 1300 °C. *Corros. Sci.* 2022, 197:110099.
[140] Koyanagi T, Karakoc O, Hawkins C, Lara-Curzio E, Deck C, *et al.* Stress rupture of SiC/SiC composite tubes under high-temperature steam. *Int. J. Appl. Ceram. Technol.* 2023, 20(3):1658–1666.
[141] Luan Xg, Xu X, Zou Y, Wang L, Cheng L, *et al.* Wet oxidation behavior of SiC/(SiC-SiBCN)x composites prepared by CVI combined with PIOP process. *J. Am. Ceram. Soc.* 2019, 102(10):6239–6255.
[142] Hallstadius L, Johnson S, Lahoda E. Cladding for high performance fuel. *Prog. Nucl. Energy* 2012, 57:71–76.
[143] Koyanagi T, Hawkins C, Lamm B, Lara-Curzio E, Deck C, *et al.* Mechanical degradation of duplex SiC-fiber reinforced SiC matrix composite tubes under a controlled high-temperature steam environment. *Ceram. Int.* 2024, 50(14):25558–25567.
[144] Kim D, Lee HJ, Jang C, Lee H-G, Park JY, *et al.* Influence of microstructure on hydrothermal corrosion of chemically vapor processed SiC composite tubes. *J. Nucl. Mater.* 2017, 492:6–13.
[145] Tan X, Liu W, Cao L, Dai S. Oxidation behavior of a 2D-SiCf/BN/SiBCN composite at 1350–1650 °C in air. *Mater. Corros.* 2018, 69(9):1227–1236.
[146] Camarano AD, Giuranno D, Narciso J. New advanced SiC-based composite materials for use in highly oxidizing environments: Synthesis of SiC/IrSi3. *J. Eur. Ceram. Soc.* 2020, 40(3):603–611.
[147] Li G, Li J, Lu X, Lü K, Huang J, *et al.* Oxidation behavior and interface evolution of tri-layer

Si/Yb2SiO5/LaMgAl11O19 thermal and environmental barrier coatings under isothermal heat treatment at 1300 °C. *Surf. Coat. Technol.* 2023, 464:129554.
[148] Li G, Li J, Chen W, Lu X, Lü K, *et al.* Cyclic oxidation and water vapor corrosion behaviors of multi-layer environmental barrier coatings with HfO2-Si bond coat for SiCf/SiC. *Mater. Chem. Phys.* 2022, 292:126768.
[149] Garcia E, Sotelo-Mazon O, Poblano-Salas CA, Trapaga G, Sampath S. Characterization of Yb2Si2O7–Yb2SiO5 composite environmental barrier coatings resultant from *in situ* plasma spray processing. *Ceram. Int.* 2020, 46(13):21328–21335.
[150] Mainzer B, Jemmali R, Watermeyer P, Kelm K, Frieß M, *et al.* Development of damage-tolerant ceramic matrix composites (SiC/SiC) using Si-BN/SiC/pyC fiber coatings and LSI processing. *J. Ceram. Sci. Technol.* 2017, 8:113–120.
[151] Hu Q, Wang Y, Guo X, Huang Z, Tu Y, *et al.* Oxidation resistance of SiCf/SiC composites with three-layer environmental barrier coatings up to 1360 °C in air atmosphere. *Ceram. Int.* 2022, 48(7):9610–9620.
[152] Seshadri A, Shirvan K. Development of hydrothermal corrosion model and BWR metal coating for CVD SiC in light water reactors. *J. Nucl. Mater.* 2023, 576:154252.
[153] Zhong X, Niu Y, Li H, Zhou H, Dong S, *et al.* Thermal shock resistance of tri-layer Yb2SiO5/Yb2Si2O7/Si coating for SiC and SiC-matrix composites. *J. Am. Ceram. Soc.* 2018, 101(10):4743–4752.
[154] Wang Z, Cao X, Hong Z, Li J, Han G, *et al.* Failure behavior of SiC/SiC with BSAS-based EBC in gas combustion environment. *Ceram. Int.* 2024, 50(14):25041–25051.
[155] Liu T. Research progress of interfacial phases of SiCf/SiC composites. *Mater. Guide* 2010, (1):6.
[156] Li LB, Song YD, Sun YC. Modeling the Tensile Behavior of Unidirectional C/SiC Ceramic-Matrix Composites. *Mech. Compos. Mater.* 2014, 49(6):659–672.
[157] Meyer P, Waas AM. FEM predictions of damage in continuous fiber ceramic matrix composites under transverse tension using the crack band method. *Acta Mater.* 2016, 102:292–303.
[158] Wang L, Wang Z, Dong SM, Zhang W, Wang Y. Finite element simulation of stress distribution and development of Cf/SiC ceramic–matrix composite coated with single layer SiC coating during thermal shock. *Compos. Part B Eng.* 2013, 51:204–214.
[159] Zhang C, Curiel-Sosa JL, Bui TQ. A novel interface constitutive model for prediction of stiffness and strength in 3D braided composites. *Compos. Struct.* 2017, 163:32–43.
[160] Zhang Y, Li H, Gao Y, Lou R, Ge L, *et al.* Multi-scale modeling and elastic properties prediction of 3D four-directional tubular braided composites. *Compos. Struct.* 2022, 292:115632.
[161] Wang J, Chen Y, Feng Y, Zhao G, Jian X, *et al.* Influence of porosity on anisotropic thermal conductivity of SiC fiber reinforced SiC matrix composite: A microscopic modeling study. *Ceram. Int.* 2020, 46(18, Part A):28693–28700.
[162] Tang J, Zhao G, Wang J, Ding Y, Feng Y, *et al.* Computational Geometry-Based 3D Yarn Path Modeling of Wound SiCf/SiC-Cladding Tubes and Its Application to Meso-Scale Finite Element Model. *Front. Mater.* 2021, 8:701205.
[163] Feng Y, Wang J, Shang N, Zhao G, Zhang C, *et al.* Multiscale Modeling of SiCf/SiC Nuclear Fuel Cladding Based on FE-Simulation of Braiding Process. *Front. Mater.* 2021, 7:634112.
[164] Ashouri Vajari D, González C, Llorca J, Legarth BN. A numerical study of the influence of microvoids in the transverse mechanical response of unidirectional composites. *Compos. Sci. Technol.* 2014, 97:46–54.
[165] Shen L, Yan W, Zhu T, Li H, Xiao C, *et al.* Analysis of multi-scale failure behavior of SiCf/SiC composite clad tube under flexible clamping damage. *J. Eur. Ceram. Soc.* 2024, 44(11):6269–6285.
[166] He C, Ge J, Qi D, Gao J, Chen Y, *et al.* A multiscale elasto-plastic damage model for the nonlinear behavior of 3D braided composites. *Compos. Sci. Technol.* 2019, 171:21–33.
[167] Dong J, Huo N. A two-scale method for predicting the mechanical properties of 3D braided composites with internal defects. *Compos. Struct.* 2016, 152:1–10.
[168] Ge L, Li H, Liu B, Fang D. Multi-scale elastic property prediction of 3D five-directional braided

composites considering pore defects. *Compos. Struct.* 2020, 244:112287.
[169] Gao J, Bai Y, Fan H, Song G, Zou X, *et al.* Phase-field simulation of microscale crack propagation/deflection in SiCf/SiC composites with weak interphase. *J. Am. Ceram. Soc.* 2023, 106:4877–4890.
[170] Wang B, Zhao J, Guo Z, Wang B. Failure envelope prediction of 2D SiCf/SiC composites based on XGBoost model. *Compos. Part A Appl. Sci. Manuf.* 2024, 185:108287.
[171] Shi D, Wang Z, Marrow J, Liu C, Wan F, *et al.* Piecewise damage model for SiC/SiC composites with multilevel experimental validation. *Compos. Part A Appl. Sci. Manuf.* 2024, 178:107952.
[172] Zhang S, Qin H, Li Z, Wei C, Zhang C, *et al.* In-situ observation of damage evolution in Mo-SiCf/SiC heterogeneous composite. *Compos. Part B Eng.* 2023, 264:110901.
[173] Mital SK, Bednarcyk BA, Arnold SM, Lang J. Modeling of Melt-Infiltrated SiC/SiC Composite Properties. 2009. Available: https://ntrs.nasa.gov/citations/20090041359 (accessed on 21 September 2024).
[174] Wu Z, Shi L, Cheng X, Liu Y, Hu X. Meso-Level Finite Element Modeling Method for Mechanical Response of Braided Composite Tube with Gradient Structure in Axial Direction. *Appl. Compos. Mater.* 2019, 26:1101–1119.
[175] Zhang Y, Li H, Liu X, Gao Y, Guan C. Trans-scale elastic–plastic damage analysis of 3D tubular braided composites with void defects. *Int. J. Solids Struct.* 2023, 274: 112288.
[176] Zhang S, Liu C, Zhang X, Du J, Chen Q, *et al.* Simulation of failure behavior of 2.5D SiC/SiC variable thickness dovetail joint structures based on mesoscale model. *Compos. Struct.* 2024, 327:117716.
[177] Pu J, Wang J, Tang J, Shen L, Huang Q, *et al.* Multi-scale Progressive Damage and Failure Behavior Analysis of Three-Dimensional Winding SiC Fiber-Reinforced SiC Matrix Composite Tube. *Appl. Compos. Mater.* 2023, 30(5): 1605–1626.
[178] Yan W, Ren Z, Fan X, Yan Z, Shen L, *et al.* Multi-scale pore model construction and damage behavior analysis of SiCf/SiC composite tubes. *Mater. Charact.* 2024, 214:114083.
[179] Chen Y, Gélébart L, Chateau C, Bornert M, Sauder C, *et al.* Analysis of the damage initiation in a SiC/SiC composite tube from a direct comparison between large-scale numerical simulation and synchrotron X-ray micro-computed tomography. *Int. J. Solids Struct.* 2019, 161:111–126.
[180] Mazars V, Caty O, Couégnat G, Bouterf A, Roux S, *et al.* Damage investigation and modeling of 3D woven ceramic matrix composites from X-ray tomography in-situ tensile tests. *Acta Mater.* 2017, 140:130–139.
[181] Naslain RR. The design of the fibre-matrix interfacial zone in ceramic matrix composites. *J. Ceram. Process. Eng.* 1998, 29(9–10):1145–1155.
[182] A JB, A HP, A KK, B RW. A new fibre-bundle pull-out test to determine interface properties of a 2D-woven carbon/carbon composite. *J. Compos. Sci. Technol.* 2003, 63(5):653–660.
[183] Sauder C, Brusson A, Lamon J. Influence of Interface Characteristics on the Mechanical Properties of Hi-Nicalon type-S or Tyranno-SA3 Fiber-Reinforced SiC/SiC Minicomposites. *J. Am. Ceram. Soc.* 2010, 7(3):291–303.
[184] Buet E, Sauder C, Sornin D, Poissonnet S, Rouzaud J, *et al.* Influence of surface fibre properties and textural organization of a pyrocarbon interphase on the interfacial shear stress of SiC/SiC minicomposites reinforced with Hi-Nicalon S and Tyranno SA3 fibres. *Compos. Sci. Technol.* 2014, 34(2):179–188.
[185] Mueller WM, Moosburger-Will J, Sause M, Horn SJ. Microscopic analysis of single-fiber push-out tests on ceramic matrix composites performed with Berkovich and flat-end indenter and evaluation of interfacial fracture toughness. *J. Electrochem. Soc.* 2013, 33(2):441–451.
[186] Wang JY, Liu HT, Jiang R, Cheng HF. Sol-gel temperature dependent ductile-to-brittle transition of aluminosilicate fiber reinforced silica matrix composite. *J. Compos. Mater. Eng.* 2017, 119:79–89.
[187] Liu HT, Yang LW, Sun X, Cheng HF, Wang CY, *et al.* Enhancing the fracture resistance of carbon fiber reinforced SiC matrix composites by interface modification through a simple fiber heat-treatment process. *Carbon* 2016, 109:435–443.

[188] Liu HT, Yang LW, Han S, Cheng HF, Mao WG, *et al.* Interface controlled micro- and macro-mechanical properties of aluminosilicate fiber reinforced SiC matrix composites. *J. Eur. Ceram. Soc.* 2017, 37(3):883–890.
[189] Jin E, Du S, Li M, Liu C, He S, *et al.* Influence of helium atoms on the shear behavior of the fiber/matrix interphase of SiC/SiC composite. *J. Mater. Sci.* 2016, 479:504.
[190] Zhan JM, Yao XH, Li WH, Zhang XQ. Tensile mechanical properties study of SiC/graphene composites based on molecular dynamics. *J. Ceram. Mater. Sci.* 2017, 131:266–274.
[191] Wang Y, Ma Y, Zheng R, Li L, Chen Y, *et al.* Microstructure of PyC dominates interfacial shear failure in SiCf/SiC composites: From localized sliding to uniform plasticity. *Compos. Part A Appl. Sci. Manuf.* 2023, 174:107742.
[192] Niu X, Bian J, Chen X, Ding J, Sun Z, *et al.* Molecular dynamics simulation on PyC interfacial failure mechanism and shear strength of SiC/SiC composites. *Model. Simul. Mater. Sci. Eng.* 2021, 29(8):085008.
[193] Wang R, Han J, Mao J, Hu D, Liu X, *et al.* A molecular dynamics based cohesive zone model for interface failure under monotonic tension of 3D four direction SiC_f/SiC composites. *Compos. Struct.* 2021, 274:114397.
[194] Almutairi B, Jaradat S, Kumar D, Goodwin CS, Usman S, *et al.* Weight loss and burst testing investigations of sintered silicon carbide under oxidizing environments for next generation accident tolerant fuels for SMR applications. *Mater. Today Commun.* 2022, 30:102958.
[195] Cheng ZQ, Liu H, Tan W. Advanced computational modelling of composite materials. *Eng. Fract. Mech.* 2024, 305:110120.
[196] Mirkhalaf M, Rocha I. Micromechanics-based deep-learning for composites: Challenges and future perspectives. *Eur. J. Mech. A/Solids* 2024, 105:105242.
[197] Liu Z, Wu CT. Exploring the 3D architectures of deep material network in data-driven multiscale mechanics. *J. Mech. Phys. Solids* 2019, 127:20–46.
[198] Liu X, Tang T, Yu W, Pipes RB. Multiscale modeling of viscoelastic behaviors of textile composites. *Int. J. Eng. Sci.* 2018, 130:175–186.
[199] Agarwal M, Pasupathy P, Wu X, Recchia SS, Pelegri AA. Multiscale Computational and Artificial Intelligence Models of Linear and Nonlinear Composites: A Review. *Small Sci.* 2024, 4(5):2300185.
[200] Li M, Wang B, Hu J, Li G, Ding P, *et al.* Artificial neural network-based homogenization model for predicting multiscale thermo-mechanical properties of woven composites. *Int. J. Solids Struct.* 2024, 301:112965.
[201] Fotouhi S, Pashmforoush F, Bodaghi M, Fotouhi M. Autonomous damage recognition in visual inspection of laminated composite structures using deep learning. *Compos. Struct.* 2021, 268:113960.
[202] Zhang D, Liu Y, Liu H, Feng Y, Guo H, *et al.* Characterisation of damage evolution in plain weave SiC/SiC composites using *in situ* X-ray micro-computed tomography. *Compos. Struct.* 2021, 275:114447.
[203] Zhang S, Feng Y, Gao X, Song Y, Wang F, *et al.* Modeling of fatigue failure for SiC/SiC ceramic matrix composites at elevated temperatures and multi-scale experimental validation. *J. Eur. Ceram. Soc.* 2022, 42(8):3395–3403.
[204] Ai S, Song W, Chen Y. Stress field and damage evolution in C/SiC woven composites: Image-based finite element analysis and *in situ* X-ray computed tomography tests. *J. Eur. Ceram. Soc.* 2021, 41(4):2323–2334.
[205] Du Z, Liu Z, Chen C, Wang X. Stab resistance mechanism of lightweight PLA/CFRP hybrid composite structures. *Eng. Fail. Anal.* 2024, 156:107795.
[206] Shi D, Zhang B, Liu C, Wang L, Yang X, *et al.* In-situ study on compressive behaviors of different types of 3D SiC/SiC composites using X-ray computed tomography and digital image correlation. *J. Mater. Res. Technol.* 2023, 22:3475–3488.
[207] Qu J, Xu C, Meng S. Experimental investigation on interlaminar and in-plane shear damage evolution of 2D C/SiC composites using acoustic emission and X-ray computed

microtomography. *Ceram. Int.* 2023, 49(7):11711–11717.
[208] Xu X, Takeda SI, Wisnom MR. Investigation of fracture process zone development in quasi-isotropic carbon/epoxy laminates using *in situ* and ex situ X-ray Computed Tomography. *Compos. Part A Appl. Sci. Manuf.* 2023, 166:107395.
[209] Wang Y, Luo Q, Xie H, Li Q, Sun G. Digital image correlation (DIC) based damage detection for CFRP laminates by using machine learning based image semantic segmentation. *Int. J. Mech. Sci.* 2022, 230:107529.
[210] Helwing R, Hülsbusch D, Walther F. Deep learning method for analysis and segmentation of fatigue damage in X-ray computed tomography data for fiber-reinforced polymers. *Compos. Sci. Technol.* 2022, 230:109781.
[211] Ali MA, Guan Q, Umer R, Cantwell WJ, Zhang T. Deep learning based semantic segmentation of μCT images for creating digital material twins of fibrous reinforcements. *Compos. Part A Appl. Sci. Manuf.* 2020, 139:106131.
[212] Wang Y, Chen Q, Luo Q, Li Q, Sun G. Characterizing damage evolution in fiber reinforced composites using in-situ X-ray computed tomography, deep machine learning and digital volume correlation (DVC). *Compos. Sci. Technol.* 2024, 254:110650.
[213] Gao Y, Wang Y, Yang X, Liu M, Xia H, *et al.* Synchrotron X-ray tomographic characterization of CVI engineered 2D-woven and 3D-braided SiCf/SiC composites. *Ceram. Int.* 2016, 42:17137–17147.
[214] Larson NM, Zok FW. In-situ 3D visualization of composite microstructure during polymer-to-ceramic conversion. *Acta Mater.* 2018, 144:579–589.
[215] Wang L, Yuan K, Luan X, Li Z, Feng G, *et al.* 3D Characterizations of Pores and Damages in C/SiC Composites by Using X-Ray Computed Tomography. *Appl. Compos. Mater.* 2019, 26(2):493–505.
[216] Quiney Z, Weston E, Ian Nicholson P, Pattison SJ, Bache MR. Volumetric assessment of fatigue damage in a SiCf/SiC ceramic matrix composite via *in situ* X-ray computed tomography. *J. Eur. Ceram. Soc.* 2020, 40(11):3788–3794.
[217] Wan F, Liu R, Wang Y, Cao Y, Zhang C, *et al.* Damage development during flexural loading of a 5-directional braided C/C-SiC composite, characterized by X-ray tomography and digital volume correlation. *Ceram. Int.* 2019, 45(5):5601–5612.
[218] Mazars V, Caty O, Couégnat G, Bouterf A, Roux S, *et al.* Damage investigation and modeling of 3D woven ceramic matrix composites from X-ray tomography in-situ tensile tests. *Acta Mater.* 2017, 140:130–139.
[219] Forna-Kreutzer JP, Ell J, Barnard H, Pirzada TJ, Ritchie RO, *et al.* Full-field characterisation of oxide-oxide ceramic-matrix composites using X-ray computed micro-tomography and digital volume correlation under load at high temperatures. *Mater. Des.* 2021, 208:109899.
[220] Chen Y, Shi Y, Chateau C, Marrow J. In situ X-ray tomography characterisation of 3D deformation of C/C-SiC composites loaded under tension. *Compos. Part A Appl. Sci. Manuf.* 2021, 145:106390.
[221] Liu C, Chen Y, Shi D, Marrow J, Jing X, *et al.* In situ investigation of failure in 3D braided SiCf/SiC composites under flexural loading. *Compos. Struct.* 2021, 270:114067.
[222] Zhu R, Niu G, Qu Z, Wang P, Zhang R, *et al.* In-Situ Quantitative Tracking of Micro-Crack Evolution Behavior Inside CMCs Under Load at High Temperature: A Deep Learning Method. *Acta Mater.* 2023, 255:119073.
[223] Creveling PJ, Fisher JH, LeBaron N, Czabaj MW. 4D Imaging of ceramic matrix composites during polymer infiltration and pyrolysis. *Acta Mater.* 2020, 201:547–560.
[224] Louis SYM, Nasiri A, Bao J, Cui Y, Zhao Y, *et al.* Remaining Useful Strength (RUS) Prediction of SiCf-SiCm Composite Materials Using Deep Learning and Acoustic Emission. *Appl. Sci.* 2020, 10(8):2680.
[225] Guo W, Zhang D, Zhang Y, Du Y, Chen C. Tensile damage evolution and mechanical behaviour of SiCf/SiC mini-composites through 4D in-situ micro-CT and data-driven modelling. *Compos. Part B Eng.* 2024, 279:111439.

[226] Guo S, Liu T, Ping DH, Nishimura T. Enhanced high-temperature strength of HfB2–SiC composite up to 1600 °C. *J. Eur. Ceram. Soc.* 2018, 38(4):1152–1157.
[227] Shi Y, Kessel F, Friess M, Jain N, Tushtev K. Characterization and modeling of tensile properties of continuous fiber reinforced C/C-SiC composite at high temperatures. *J. Eur. Ceram. Soc.* 2021, 41(5):3061–3071.
[228] Li H, Zhang L, Cheng L, Wang Y. Fabrication of 2D C/ZrC–SiC composite and its structural evolution under high-temperature treatment up to 1800 °C. *Ceram. Int.* 2009, 35(7):2831–2836.
[229] Wu D, Wang Y, Shang L, Pu Y, Gao Z. Thermo-mechanical properties of C/SiC composite structure under extremely high temperature environment up to 1500 °C. *Compos. Part B Eng.* 2016, 90:424–431.
[230] Zhu S, Mizuno M, Nagano Y, Cao J, Kagawa Y, *et al.* Creep and Fatigue Behavior in an Enhanced SiC/SiC Composite at High Temperature. *J. Am. Ceram. Soc.* 1998, 81(9):2269–2277.
[231] Liu F, Wang Z, Wang Z, Zhong J, Zhao L, *et al.* High-Throughput Method–Accelerated Design of Ni-Based Superalloys. *Adv. Funct. Mater.* 2022, 32(28):2109367.
[232] Yeo BC, Nam H, Nam H, Kim MC, Lee HW, *et al.* High-throughput computational-experimental screening protocol for the discovery of bimetallic catalysts. *npj Comput. Mater.* 2021, 7(1):137.
[233] Kirklin S, Meredig B, Wolverton C. High-Throughput Computational Screening of New Li-Ion Battery Anode Materials. *Adv. Energy Mater.* 2013, 3(2):252–262.
[234] Qu N, Liu Y, Liao M, Lai Z, Zhou F, *et al.* Ultra-high temperature ceramics melting temperature prediction via machine learning. *Ceram. Int.* 2019, 45(15):18551–18555.
[235] Evsevleev S, Paciornik S, Bruno G. Advanced Deep Learning-Based 3D Microstructural Characterization of Multiphase Metal Matrix Composites. *Adv. Eng. Mater.* 2020, 22(4):1901197.
[236] Su YF, Li XG, Wang J, Zhang PF, Su MM, *et al.* Transverse indentation response and residual axial compressive characteristics of metal-composites hybrid tubes by deep learning-based acoustic emission and micro-CT. *Thin-Walled Struct.* 2023,185:110651.
[237] Gogu C, Bapanapalli SK, Haftka RT, Sankar BV. Comparison of Materials for an Integrated Thermal Protection System for Spacecraft Reentry. *J. Spacecraft Rockets* 2009, 46(3):501–513.
[238] Shen L, Zhu T, Shi S, Xu J, Wang J, *et al.* Cross-scale static/dynamic shear damage evolution mechanism of 2D C/SiC ceramic matrix composite with transient hysteresis effect. *Ceram. Int.* 2024, 50(10):17898–17912.
[239] Biamino S, Antonini A, Eisenmenger-Sittner C, Fuso L, Pavese M, *et al.* Multilayer SiC for thermal protection system of space vehicles with decreased thermal conductivity through the thickness. *J. Eur. Ceram. Soc.* 2010, 30(8):1833–1840.
[240] Kurth G, Bauer C, Meyer T, Ramsel J, Thumann A. Development and Testing of a C/SiC Combustion Chamber for High Speed Throttleable Ducted Rocket Applications. In *51st AIAA/SAE/ASEE Joint Propulsion Conference*, Orlando, USA, 27–29 July 2015, pp. 4232.
[241] Desaulty M, Devaux C. The SNECMA M88 engine family. In *36th AIAA/ASME/SAE/ASEE Joint Propulsion Conference and Exhibit*, Las Vegas, USA, 24–28 July 2000, pp. 3462.
[242] DiCarlo JA, van Roode M. Ceramic Composite Development for Gas Turbine Engine Hot Section Components. In *Turbo Expo: Power for Land, Sea, and Air*, Barcelona, Spain, 8–11 May 2006, pp. 221–231.
[243] Kim KS, Lee SH, Nguyen VQ, Yun Y, Kwon S. Ablation characteristics of rocket nozzle using HfC-SiC refractory ceramic composite. *Acta Astronaut.* 2020, 173:31–44.
[244] Wang H. Preparation and properties of continuous fiber reinforced SiC matrix composites by reactive impregnation. 2012. (In Chinese)
[245] Zhao Y. Geomechanical aspects of Sintered Silicon Carbide (SSiC) waste canisters for dis posal of high level radioactive waste. 2021. Available: https://tubaf.qucosa.de/landing-page/?tx_dlf[id]=https%3A%2F%2Ftubaf.qucosa.de%2Fapi%2Fqucosa%253A74150%2Fmets (accessed on 21 September 2024).
[246] Uyanna O, Najafi H. Thermal protection systems for space vehicles: A review on technology development, current challenges and future prospects. *Acta Astronaut.* 2020, 176:341–356.